STUDIES ON THE CATALYTIC REACTION OF *STREPTOMYCES* PHOSPHOLIPASE D

YOSHIKO UESUGI

2005

CONTENTS

LIST OF ABBREVIATIONS

Am	ampicillin
CD	circular dichroism
CHAPS	3-[(3-cholamidopropyl)dimethylammonio]-1-propanesulfonic acid
Cm	chloramphenicol
E. coli	*Escherichia coli*
EtOH	ethanol
Kan	kanamycin
LUV	large unilamellar vesicle
MLV	multilamellar vesicle
PA	phosphatidic acid
PC	phosphatidylcholine
PCR	polymerase chain reaction
PEtOH	phosphatidylethanol
PG	phosphatidylglycerol
PLD	phospholipase D
POPC	1-palmitoyl-2-oleoyl-*sn*-glycero-3-phosphocholine
POPG	1-palmitoyl-2-oleoyl-*sn*-glycero-3-[phospho-*rac*-(1-glycerol)]
POPS	1-palmitoyl-2-oleoyl-*sn*-glycero-3-[phospho-L-serine]
PpNP	phosphatidyl-*p*-nitrophenol
PS	phosphatidylserine
RIBS	repeat-length independent and broad spectrum
RU	resonance unit
SDS-PAGE	sodium dodecyl sulfate-polyacrylamide gel electrophoresis
Sm	streptomycin
SPR	surface plasmon resonance
SUV	small unilamellar vesicle
TLC	thin-layer chromatography

GENERAL INTRODUCTION

Phospholipase D (PLD, EC 3.1.4.4) is a ubiquitous enzyme found in bacteria, fungi, plants, and mammals (Exton, 1998). PLD catalyzes two reactions: one is hydrolysis of phospholipids to produce phosphatidic acids (PA) and a free alcohol, and the other is transphosphatidylation of phosphatidyl groups to various phosphatidylalcohols (Fig. 1). The transphosphatidylation is a very useful reaction synthesizing rare natural phospholipids, such as phosphatidylserine (PS) and phosphatidylglycerol (PG), and novel artificial phospholipids (Juneja *et al*., 1987; Juneja *et al*., 1989; Takami *et al*., 1994). These phospholipids have been used for pharmaceuticals, foods, cosmetics, and other industries. The transphosphatidylation reaction is usually carried out in a biphasic system consisting of water and water-insoluble organic solvents. The reaction usually accompanied with various amounts of the hydrolysis product PA. The economical point of the phospholipid synthesis depends on the selectivity of the product and byproduct, therefore minimizing the byproduct formation is very important for utilizing PLD.

All of the PLD superfamily members contain one or two copies of the conserved HxKxxxxD (HKD) motif (Ponting & Kerr, 1996; Waite, 1999). The complete conservation of the HKD motifs among PLDs and their relatives means a vital role of the HKD motifs catalytic reaction, which was verified by mutational studies. Substitution of amino acid residues in either HKD motif in mammalian PLD1 leads the enzyme to inactive, and these findings were the same as extensive studies using mammalian PLD2 and SPO14 yeast PLD (Sung *et al*., 1997, 1999a, 1999b; Hughes & Parker, 2001).

More than 30 years ago, Stanacev & Stuhne-Sekalec proposed that the catalytic mechanism of PLD involved a two-step reaction, in which formation of a covalent

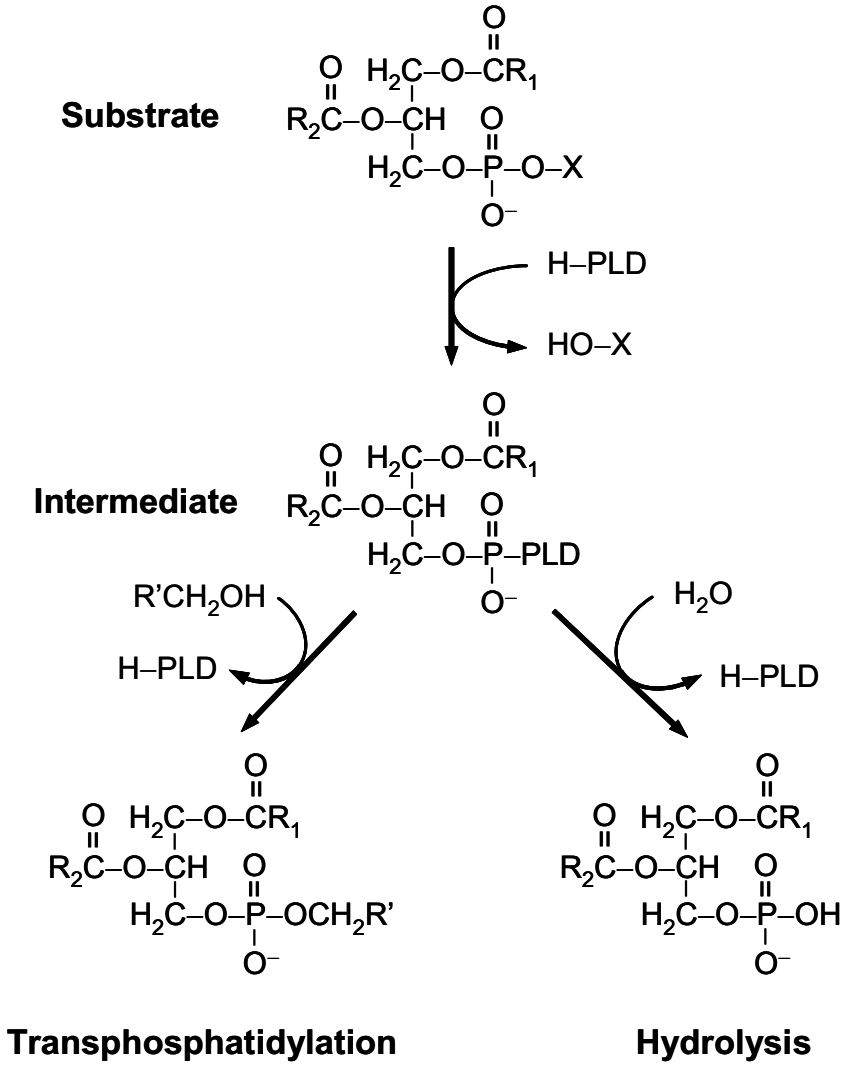

Figure 1. Reactions catalyzed by PLD.

phosphatidyl-enzyme intermediate was shown by radiolabel exchange experiments using plant PLD (Stanacev & Stuhne-Sekalec, 1970) (Fig. 2). *Salmonella typhimurium* endonuclease, Nuc, possesses only one HKD motif, dimerizes to perform catalysis, and each monomer lies adjacent to each other forming an active site, held together by a series of hydrogen bonds (Stuckey & Dixon, 1999). It was revealed that the structure of *Streptomyces* sp. PMF PLD (PMFPLD) resembles to that of the Nuc, and the two catalytic motifs of the enzyme come together to form a single active site (Leiros *et al*., 2000). For Nuc enzyme, it is suggested that the histidine residue of the HKD motif acts as a nucleophile in catalytic reaction (Gottlin *et al*., 1998). These studies show that the histidine residue of one HKD motif acts as nucleophile, which attacks the phosphate of the phosphodiester bond to form a phosphor-enzyme intermediate, and the histidine residue of another motif acts as a general acid that makes protonation of the leaving group. Recently, Iwasaki *et al.* showed that the C-terminal fragment containing a HKD motif was bound to the artificial phospholipid, and therefore speculated that the C-terminal HKD motif acts as the initial catalytic nucleophile that attacks the phosphatidyl group of substrate phospholipids (Iwasaki *et al*., 1999). In contrast, the tertiary structure of PMFPLD in the presence of short-chain substrate revealed that the histidine residue of the N-terminal HKD motif was more close to the phosphate atom of the substrate than that of the C-terminus (Leiros *et al*., 2004). In spite of these results, it has been discussed which HKD motif act as an initial catalytic nucleophile. Furthermore, there has been unclear for the other residues in PLDs, which is related to PLD-catalyzed reaction.

To elucidate the mechanism of PLD-catalyzed reaction in detail should be useful for creating a novel high-performance PLD that has a superior transphosphatidylation activity and low hydrolysis activity. This thesis is devoted to determining the residues relating PLD-catalyzed reaction and to elucidating the catalytic mechanism of PLD.

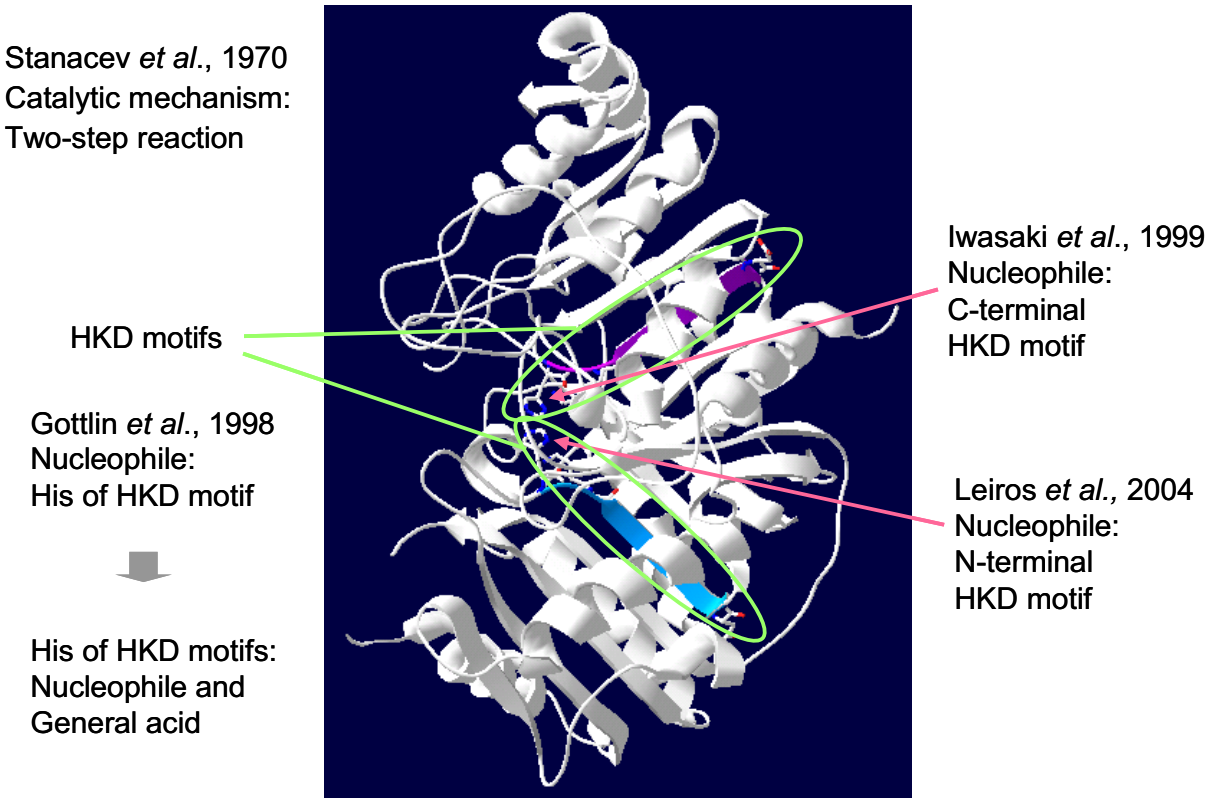

Figure 2. Proposed mechanism of PLD-catalyzed reaction.

The genes coding PLD have been cloned from various sources, which are from mammals to bacteria (Waksman *et al*., 1996; Iwasaki *et al*., 1994; Hammond *et al*., 1995). The linear structures of PLDs are shown in Fig. 3 (Exton, 2002, Morris *et al*., 1996). They all show two conserved sequences designated I and IV, both which contain one catalytic HKD motif, and some of them have the additional conserved sequences (II and III). *Streptomyces* PLDs have three regions essential for the PLD activities, and shows most compact structure among many sources. *Streptomyces* PLDs have been hoped for industrial use because of its higher transphosphatidylation activity than those of many other documented sources (Juneja *et al*., 1988; Hagishita *et al*., 1999). Moreover, the amount of PLD secreted from the cells is even higher than that from other sources. Therefore, *Streptomyces* PLDs are thought to be the most suitable PLD for the catalytic reaction study among those from other documented sources.

Streptomyces PLDs are categorized into two groups; one is an iron-containing enzyme including that from *Streptomyces chromofuscus*, in which catalytic activities depend on Ca^{2+} (Yang *et al*., 2002), and the other is a member of a PLD superfamily. All of PLD superfamily members contain one or two copies of the conserved HKD motif. On the other hand, the *Streptomyces chromofuscus* PLD contains no typical HKD motif (Yang *et al*., 2002), but instead has a tightly bound iron that is necessary for the catalytic activity (Zambonelli *et al*., 2003). *Streptomyces chromofuscus* PLD has significantly low transphosphatidylation activity compared to its hydrolysis activity (Juneja *et al*., 1988; Hagishita *et al*., 1999; Shimbo *et al*., 1989). For instance, *Streptomyces* sp. PLD can produce large amounts of PS, although *Streptomyces chromofuscus* PLD produces no PS, but only PA (Comfurius *et al*., 1990).

The crystal structure of PLD was elucidated only one of PLDs, the PLD from *Streptomyces* sp. PMF (Leiros *et al*., 2000, 2004). As shown in Fig. 4, PMFPLD is a monomer consisted of two domains with similar topology and PMFPLD includes 35 secondary structure

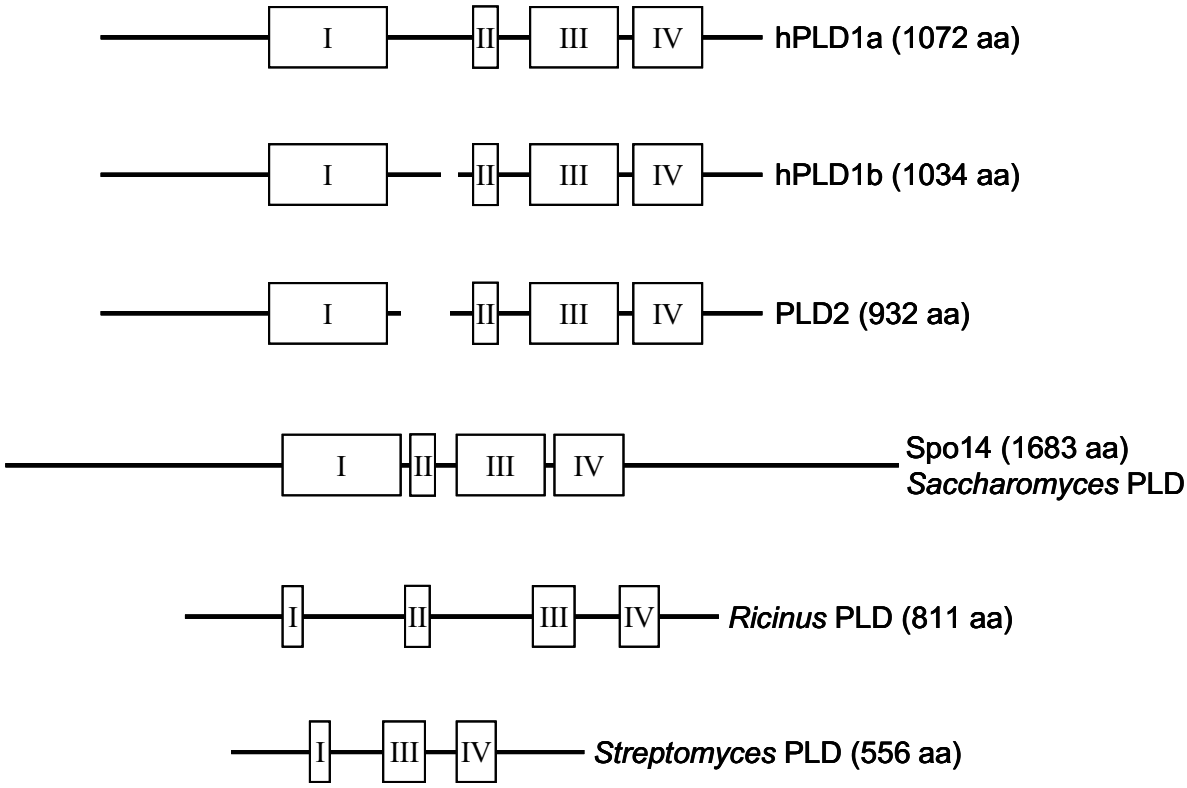

Figure 3. Conserved regions (I-IV) in PLDs obtained from various sources.

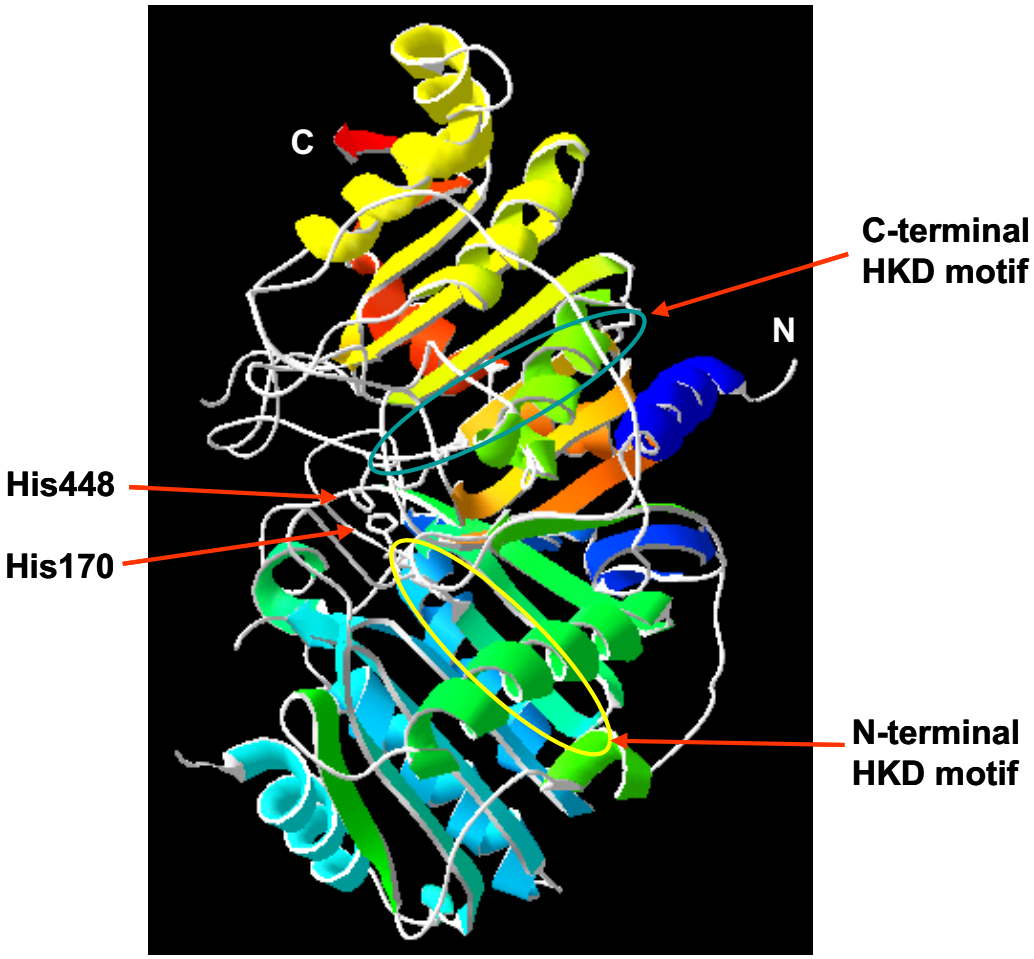

Figure 4. Tertiary structure of PLD from *Streptomyces* sp. strain PMF.

elements arranged as an α-β-α-β-α-sandwich structure. Nine and eight β strands form two β sheets which are flanked by 18 α helices. Moreover, several extended loop regions are shown. One of these loop regions (residues 382-389), which is conserved in most *Streptomyces* species, and therefore it is considered as interfacial binding region. The active site region is also located in the interface of the two domains. The active-site entrance (entrance of the substrate-binding pocket) is cone-shaped with a width across the top of about 30 Å.

Recently, PLD-producing *Actinomycetes* have been screened for their PLD activities. The PLD from *Streptomyces septatus* TH-2 (TH-2PLD) showed the highest specific activity and the highest ratio of the transphosphatidylation activity to the hydrolytic activity among these PLDs (Hagishita *et al*., 2000). Although the primary sequences have high homology (about 70%) among known *Streptomyces* PLDs, which contain two HKD motifs, these PLDs exhibit different specific activity (7.1 – 90 unit/mg) in transphosphatidylation, and different ratios (5.9 – 12.9) of the transphosphatidylation activity to the hydrolytic activity (Hagishita *et al*., 2000). Moreover, the composition of phosphatidic acids produced by the side-reaction during the transphosphatidylation reaction of *Streptomyces* PLDs were significantly different (Sato *et al*., 2004).

On the bases of these findings, I assumed that other residues different from the two HKD motifs are involved in the recognition of phospholipids, and effect on the selectivity of transphosphatidylation reaction (Fig. 5).

Moreover, PLD belongs to the enzymes which react water-insoluble substrates. As valid for most of these enzymes, also PLDs are generally more active toward aggregated substrates than free substrates. Previous studies show that activities of PLD depend on the substrate form. It is reported that PLD was activated at the interface with micelle-forming substrates

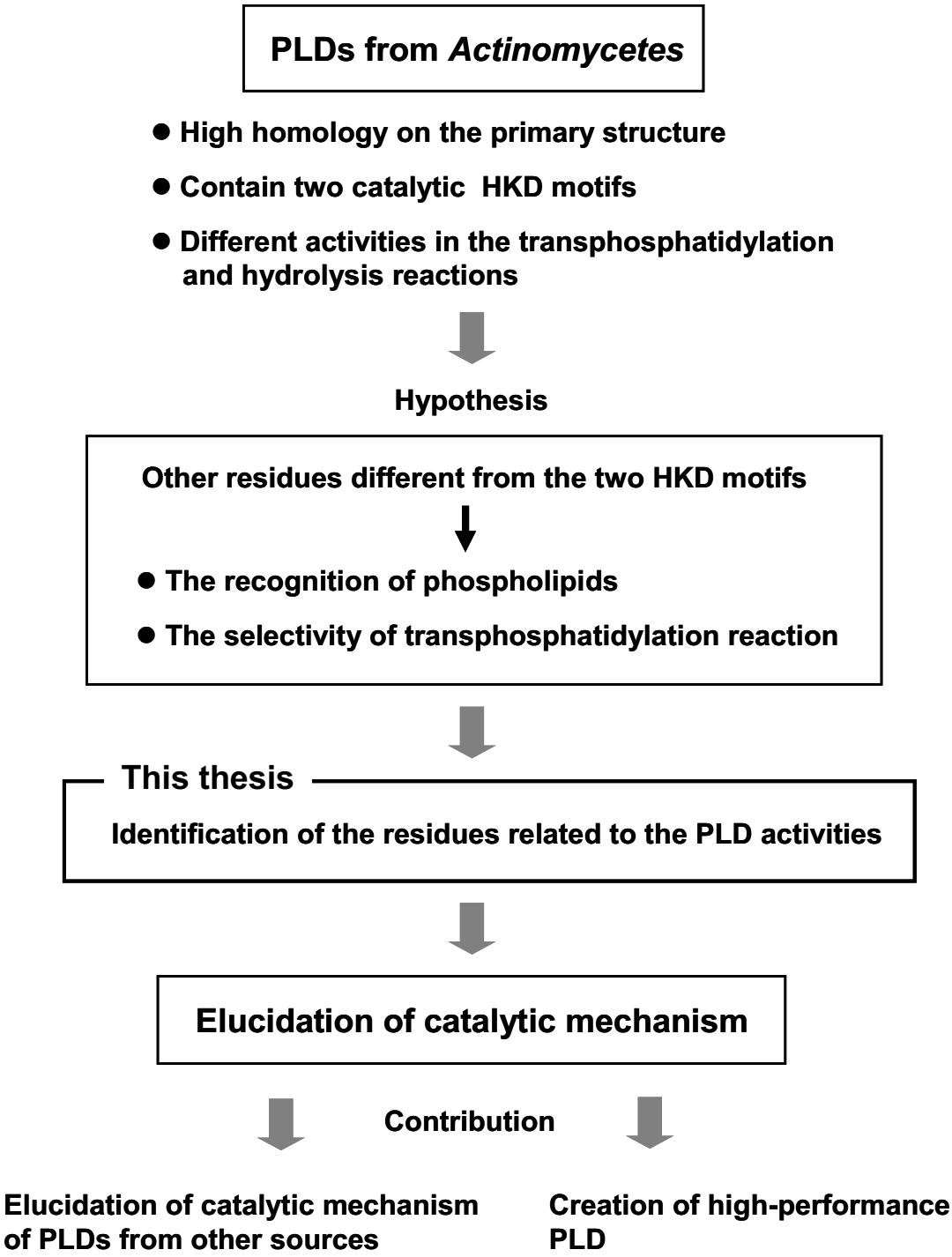

Figure 5. Overview of this thesis

(Lambrecht &Ulbrich-Hofmann, 1992). In contrast, the activity of PLD drastically reduced toward phospholipids vesicles in comparison with both micelle-forming and monomer substrate (Yang *et al.*, 2003). The geometry of the aggregated substrates plays an important role in the reactions, nevertheless the recognition mechanism of PLD toward the substrate form is still unclear.

The general purpose of this thesis is an elucidation of catalytic mechanism of *Streptomyces* PLD. To investigate the contribution of amino acid residues to the enzyme reaction of *Streptomyces* PLD, I have constructed chimeras between two parental PLDs, which have highly homology but indicate different activity in transphosphatidylation reaction, using RIBS (repeat-length independent and broad spectrum) *in vivo* DNA shuffling (Mori *et al*., 2005).

Techniques for the randomization and recombination used as manipulating and tailoring of biocatalysts are listed in Table 1. The most widely used methods for the randomization of protein are the oligonucleotide-directed randomization (Hughes *et al*., 2003; Chopra & Ranganathan, 2003) and the error-prone PCR (Chen & Arnold, 1993; You & Arnold, 1996;Wong *et al*., 2004). However, these methods have several disadvantages, such as a small library size and an amplification bias, and critical problems, in which the mutation frequencies need to be carefully tuned: generally, beneficial mutations are rare, while deleterious mutations are common. The most dramatic results in the field of directed evolution are obtained by *in vitro* DNA shuffling (Stemmer, 1994; Crameri *et al*., 1998; Arnold & Moore, 1997). In 1994, the *in vitro* DNA shuffling method developed by Stemmer for random DNA recombination, and has been used for evolution of proteins. It enables the combination of multiple mutation alleles in the target protein. However, *in vitro* DNA shuffling is hard to apply to targets that are difficult to express or screen, such as cytotoxic

Table 1 Summary of techniques for generating molecular diversity

Methodology	Target	Outcome	Advantage	Disadvantage	Ref.
Oligonucleotide-directed randomization					
MAX randomization	Zinc-finger protein	More uniform codon distibution; bias from genetic code removed	Removal of codon bias; Unbiased libraries	Small library sizes	Hughes et al., 2003
Whole gene randomization					
Error-prone PCR	Subtilisin E	Activity in organic solvents was increased	Controllable mutation spectrum	Amplification bias; Rare beneficial mutation	Chen & Arnold, 1993
Homology-dependent recombination					
in vitro DNA shuffling	β-Lactamase	Total activity was increased 3200-fold and substrate specificity altered	High frequency of recombination	Amplification error by PCR; Hard applicable of cytotoxic proteins	Stemmer, 1994
in vivo DNA shuffling	G-protein-coupled receptors	Region relating affinity was identified	Selection of chimeras independent of target gene expression	Limitation in number and variability of recombination	Kim & Devreotes, 1994
Homology-independent recombination					
Sequence-independent site-directed chimera genesis (SISDC)	TEM-1 and PSE-4β-lactamases	Of 256 possible variants, 14 retain up to 30% WT activity	Recombination with little or no homology	Number and locations of crossovers specified	Hiraga & Arnold, 2003
Structure-based combinatorial protein engineering (SCOPE)	DNA polymerases β and X	Hybrids with up to five crossovers complement auxotroph	Some variability in linkers between specified subdomain building blocks	Only applicable to proteins with known three-dimensional structures	O'Maille et al., 2002

proteins, because it requires the functional screening of chimeric genes to isolate chimeric proteins with altered specificities. On the contrary, the conventional *in vivo* DNA shuffling (Kim *et al.*, 1994; Satoh *et al.*, 1999) has potential advantages for cytotoxic targets, whereas the variation of chimeras is limited.

RIBS *in vivo* DNA shuffling is a novel method of random chimeragenesis based on the combination of highly frequent deletion formation in the *Escherichia coli ssb-3* strain (Mukaihara *et al*., 1997) with the *rpsL*-based chimera selection system (Mori *et al*., 2005). This system overcomes the disadvantages of *in vitro* and *in vivo* DNA shuffling methods mentioned above. Therefore, I selected this system for constructing chimeric PLD library.

By comparing the transphosphatidylation and hydrolysis activities of chimeras, I determined the residues related to these activities. Furthermore, I suggested which motif contains the catalytic nucleophile using inactive mutants from the surface plasmon resonance study. From these results and previous evidence, I proposed the PLD-catalyzed reaction mechanism.

The elucidation of catalytic mechanism of *Streptomyces* PLD could be applicable to elucidation of those of PLDs from other sources, because *Streptomyces* PLD has conserved catalytic regions within the most compact structure. Furthermore, based on this catalytic mechanism, I showed the guideline for the creation of a high-performance PLD, which has superior transphosphatidylation activity with low hydrolysis activity and is very useful for the synthesis of phospholipids used in the pharmaceuticals, foods, cosmetics and other industries. PS is a particularly unique phospholipid among those, because PS can depress brain energy metabolism, as measured by rise in brain glucose (Bigon *et al*., 1979). PS is also a potent anticoagulant with respect to its ability to overcome the strong procoagulant effect of brain thromboplastin both *in vivo* and *in vitro* (Turner *et al*., 1970). Moreover, clinical studies

revealed that PS could support brain functionality that tended to decline with age (Amaducci, 1988). Therefore, the creation of a high-performance PLD also contributes to the prevention and treatment of nervous diseases.

In Chapter 1, I focused catalytic HKD motifs. To determine which motif contains the initial catalytic nucleophile that attacks the phosphatidyl group of the substrates, I investigated recognition of phospholipids by *Streptomyces* PLD mutants using surface plasmon resonance.

In Chapter 2, to investigate amino acid residues involved in PLD-catalyzed reactions other than those in the two HKD motifs, I constructed chimeras between TH-2PLD and PLDP from a distinct *Streptomyces* sp., which has been used extensively in transphosphatidylation reactions (Juneja *et al*., 1987; Juneja *et al*., 1989; Takami *et al*., 1994; Hatanaka *et al*., 2002a), using RIBS *in vivo* DNA shuffling, and compared the activities of the obtained chimeras. By comparing the activities of chimeras, two candidate regions, residues 188-203 and 425-442 of TH-2PLD, was shown to relate to transphosphatidylation activity.

In Chapter 3, I first focused on the N-terminal region (residues 188-203 of TH-2PLD) of the two candidate regions, and identified the key residues related to transphosphatidylation activity. Second, the effect of the identified amino acid residues on the recognition of phospholipids was analyzed by surface plasmon spectroscopy. Finally, I studied on the other residues in the C-terminal region, residues 425-442 of TH-2PLD, related to the transphosphatidylation reaction. Moreover, I estimated the decrease of formed byproduct, PA, during transphosphatidylation from phosphatidylcholine to phosphatidylglycerol.

In General Conclusion, the contents of each chapter were briefly summarized to discuss the PLD-catalyzed reaction mechanism. Future perspectives on the creation of a high-performance PLD are also commented.

CHAPTER 1

LOCATION OF THE CATALYTIC NUCLEOPHILE OF PHOSPHOLIPASE D

1. Introduction

The general findings of the PLD catalyzed reactions lead to postulate formation of a phosphatidyl-enzyme intermediate. Early evidence showing retention of configuration at the substrate phosphorous atom in the reactions catalyzed by cabbage PLD and *Escherichia coli* phosphatidylserine synthase suggested a "ping-pong" type reaction through the formation of covalent phosphatidyl-enzyme intermediate (Stanacev & Stuhne-Sekalec, 1970; Raetz *et al*., 1987; Bruzik & Tsai, 1984). Gottlin *et al*. substantiated this two-step reaction and demonstrated that the highly conserved histidine residue of the HKD motif acts as a catalytic nucleophile in the reaction of an endonuclease (Nuc) from *Salmonella typhimurium* (Gottlin *et al*., 1998). Nuc is a PLD homologue and act as a homodimetric protein consisting of two identical subunits, each containing a single copy of the HKD motif. The crystal structure of Nuc supported the importance of the histidines and lysines of HKD motif in the each subunit, and revealed that all four residues are clustered together in the active center of the dimeric enzyme (Stuckey & Dixon, 1999; Leiros, 2000). Stuckey and Dixon proposed a catalytic mechanism that a histidine residue of the HKD motif in one subunit acts as the nucleophile and another histidine residue in the other HKD motif functions as a general acid. A similar mechanism has also been proposed for *Yersinia pestis* murine toxin (Ymt), another PLD superfamily member (Rudolph *et al*., 1999). However, it was unclear which of the two HKD motifs in PLD possesses the nucleophilic histidine residue, because the subunits of Nuc are not distinguishable from each other because of its symmetric structure.

Recently, Iwasaki *et al*. have indicated that the histidine residue in the C-terminal HKD

motif of PLD from *Streptomyces antibioticus* included the catalytic nucleophile that bound directly to the phosphatidyl group of the substrate on the basis of the binding assay of the N- or C-terminal halves of PLD to the fluorescent-labelled substrate (Iwasaki *et al.*, 1999). On the other hand, Leiros *et al.* showed that His170 in the N-terminal HKD motif of PLD from *Streptomyces* sp. PMF (PMFPLD) acts as the initial nucleophile that attacks the phosphorus atom of the substrate based on the crystal structures of PMFPLD interacting with short-chain phospholipids and PLD products (Leiros *et al.*, 2004). Thus, it has been discussed which HKD motif contains the initial catalytic nucleophile attacking the phosphatidyl group of the substrate phospholipids.

In this chapter, first of all, to identify which HKD motif contains the initial catalytic nucleophile in *Streptomyces* PLD, I constructed two mutants in which the His170 or His443 of the N- or C-terminal HKD motifs of the PLD from *Streptomyces septatus* TH-2 (TH-2PLD) was substituted with Ala, respectively. Using these two mutants, I analyzed the association of these mutants and substrate retaining a covalent phosphatidyl-enzyme intermediate (General Introduction, Fig. 1) by surface plasmon resonance (SPR). By comparing the affinities of these mutants with natural substrates, I revealed the location of the nucleophile. Furthermore, I examined the effect of these histidine residues on the recognition of several phospholipids.

2. Experimental procedures

2.1. Materials

Plasmid pETKmS2 (Mishima *et al*., 1997) was kindly provided by Dr. Tsuneo Yamane, Nagoya University, Japan. 1-Palmitoyl-2-oleoyl-*sn*-glycero-3-phosphocholine (POPC), 1-palmitoyl-2-oleoyl-*sn*-glycero-3-[phospho-*rac*-(1-glycerol)] (POPG) and 1-palmitoyl-2-oleoyl-*sn*-glycero-3-[phospho-L-serine] (POPS) were obtained from Avanti Polar Lipids and used without further purification. All the other chemicals were of the highest purity available.

2.2. Preparation of PLDs

The recombinant TH-2PLD was expressed with a C-terminal His6 tag, and purified by nickel affinity chromatography as detailed previously (Mori *et al*., 2005). The mutants, in which the His170 or His443 of the N- or C-terminal HKD motifs of TH-2PLD was substituted with Ala, were prepared as follows. To construct the mutant TH-2(H170A), the mutagenic anti-sense primer, where the *Bst*XI site (underlined) was substituted with a silent mutation, was synthesized, 5'-CACGAC(G→C)AGGAGCTTGGAG(TG→GC, His→Ala)GTTCC-3' (corresponding to the *th-2pld* gene, 503-528, *TH-2(H170A)*). The target mutation was introduced with the primer set of 5'-CGACCGCTGCTGCTGGTCTGC-3' (a sense primer, corresponding to part of the *pelB* signal sequence) and the above mutagenic primer using the GC-RICH PCR system (Roche). The partial *th-2pld* gene was amplified by PCR with a combination of a sense primer (5'-GGAAC(CA→GC, His→Ala)CTCCAAGCTCCT(G→C)GTCGTG-3' for the silent mutation of the *Bst*XI site (underlined), corresponding to the *th-2pld* gene, 503-528, *TH-2(BstXI)*) and an anti-sense primer 5’-AGGCCCACGACGCACTTGGTG-3’ (corresponding to the *th-2pld* gene, 885-905). The amplified DNA fragments were cloned into the T-vector pGEM-TEasy (Promega), and

sequenced. The plasmid containing *TH-2(H170A)* was digested with *Nco*I and *Bst*XI. The plasmid containing *TH-2(BstXI)* was digested with *Bst*XI and *Pst*I. The fragments were ligated into the *Nco*I-*Pst*I gap of vector pETKmS2TH-2 to construct the expression vector.

To construct the other mutant TH-2(H443A), the mutagenic gene was amplified by PCR with a combination of a sense primer 5'-CCCTGCGCGCGCTCGTCGGCA-3' (corresponding to the *th-2pld* gene, 962-982) and an anti-sense primer 5'-ACCAGCTTGTGG(TG→GC, His →Ala)CTGCGCGTACG-3' (corresponding to the *th-2pld* gene, 1316-1340, *TH-2(H443A)*). Then, the amplified DNA fragment was cloned, sequenced and digested with *Bgl*II and *Van*91I. The plasmid (pUC19(*TH-2*) (Mori *et al*., 2005)) was digested with *Bgl*II and *Van*91I. The fragment was exchanged for the homologous region of the subcloned *th-2pld* gene. The resultant mutant gene was digested with *Nco*I and *Bam*HI and the fragment was ligated into the *Nco*I-*Bam*HI gap of vector pETKmS2.

The preparation of mutant enzymes was similar to that of wild-type TH-2PLD.

2.3. Gel electrophoresis of proteins

SDS-PAGE was performed by the method of Laemmli (Laemmli, 1970) using a 15% acrylamide gel. The molecular weight standards (BIO-RAD) included phosphorylase b (111 kDa), bovine serum albumin (93 kDa), ovalbumin (53.5 kDa), carbonic anhydrase (36.1 kDa), soybean trypsin inhibitor (29.5 kDa) and lysozyme (21.3 kDa). Proteins on the gels were stained with Coomassie brilliant blue R-250 (Bio-RAD) and destained with water.

2.4. Circular dichroism (*CD) spectroscopy*

The folding of PLDs was confirmed by CD spectroscopy using a J-720WI spectrometer (Jasco). Proteins were dissolved to a final concentration of 0.1 mg/ml in 10 mM potassium phosphate buffer (pH 7.0). Spectra were acquired at 25°C using a 2-mm cuvette. Molar

ellipticities (per residue) were calculated using the equation $[\theta] = 100(\theta) / (lcN)$, where $[\theta]$ is the molar ellipticity per residue, (θ) is the observed ellipticity in degrees, l is the optical path length in centimeters, c is the molar concentration of the protein, and N is the number of residues in the protein.

2.5. Preparation of vesicles

An appropriate aliquot of phospholipid dissolved in chloroform was evaporated and further dried under a vacuum for at least 3 h. The lipid was hydrated at a concentration of 10 mM in phosphate-buffered saline. Then, the lipid suspensions were vortexed vigorously and frozen and thawed 10 times in liquid nitrogen. To obtain small unilamellar vesicles (SUVs), the suspension was passed 30 times through polycarbonate membranes (50 nm pore diameter) using a Lipofast extruder (Avestin) (MacDonald *et al*., 1991).

2.6. Surface plasmon resonance (Biacore)

Real time interactions between PLD molecules and phospholipids were measured using a Biacore instrument (BIAcore 2000, Biacore AB, Uppsala, Sweden). Liposomes were captured onto the surface of a Sensor Chip L1 (Biacore AB, Uppsala, Sweden). The surface of the L1 sensor chip was first cleaned with 20 mM CHAPS at a flow rate of 5 μl/min followed by the injection of SUVs (60 μl, 0.5 mM lipid concentration) at a flow rate of 2 μl/min in buffer A (10 mM sodium acetate, pH 5.5, 4 mM $CaCl_2$) which resulted in the deposition of approximately 7000-9000 resonance units. To measure the association of PLDs with lipids, purified mutant of TH-2PLD (140-709 nM diluted in buffer A) was applied to the captured SUVs at a flow rate of 20 μl/min. After binding of PLDs to phospholipids, the dissociation process was observed at the same flow rate for 10 min. The evaluation of the kinetic parameters for PLD binding to lipids was performed by nonlinear fitting of binding data using

the BIA evaluation 4.1 analysis software. The apparent association (k_a) and dissociation (k_d) rate constants were evaluated from the differential binding curves (sample-control (Fig. 1)) as shown in Fig. 4 assuming an A + B = AB association type for the protein-lipid interaction. The affinity constant K_D was calculated from the equation $K_D = k_d / k_a$.

2.7. Statistical analysis

All statistical evaluations were performed by an unpaired *t*-test or analysis of variance (ANOVA). All data are presented as means ± standard deviations of at least three determinations.

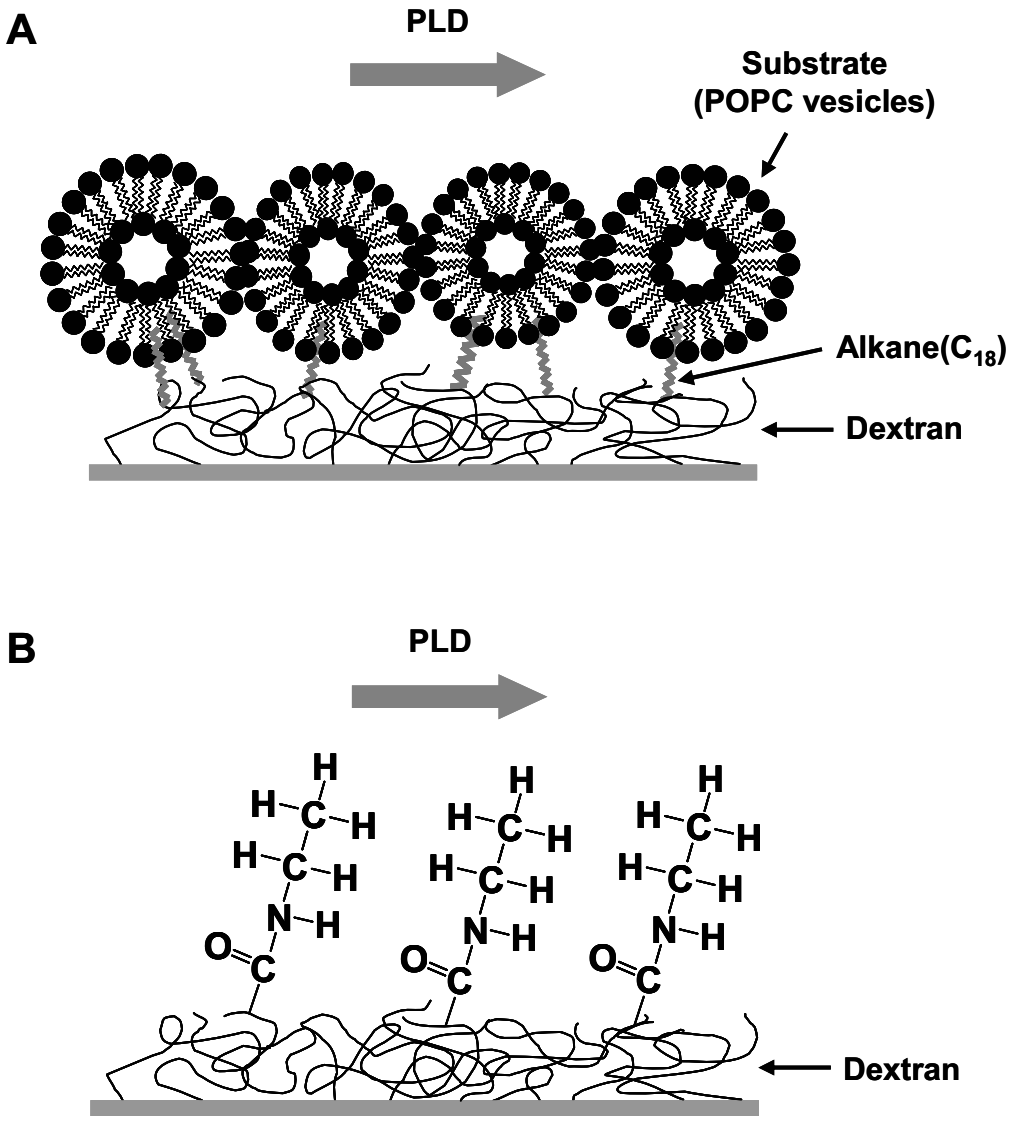

Figure 1. Surface plasmon resonance (Biacore). (A) Sample (B) control.

3. Results

3.1. Preparation of wild-type TH-2PLD and its mutants

To determine the location of the catalytic nucleophilic residue, in addition to wild-type TH-2PLD two mutants in which His170 or His443 of the N- or C-terminal HKD motif of TH-2PLD is substituted with Ala were constructed (Fig. 2A), and the expressed protein products were purified. The purified mutants showed a single band at the same molecular weight (approximately 57 kDa) position as wild-type TH-2PLD on SDS-PAGE (Fig. 2B). Furthermore, upon Western blot analysis using two anti-wild-type TH-2PLD antibodies and an anti-His6 tag antibody, these mutants and the wild-type TH-2PLD demonstrated similar results. The wild-type TH-2PLD had high activities (transphosphatidylation activity: 174 μmol/min/mg, hydrolytic activity: 59 μmol/min/mg; Chapter 2, Fig. 8), while each mutant enzyme had no detectable activity.

3.2. The folding of PLDs

To confirm the folding of wild-type TH-2PLD and the inactive mutants, their CD spectra were measured. As shown in Fig. 3, the CD spectra showed that two inactive mutants were folded with a secondary structure similar to that of wild-type TH-2PLD. These results suggest that two inactive mutant enzymes were successfully prepared, and therefore a surface plasmon resonance (SPR) analysis were carried out using these PLDs.

3.3. Association of inactive mutants with POPC vesicles

To clarify the difference in the interactions between TH-2(H170A) and TH-2(H443A) toward natural substrates, the binding profiles of TH-2(H170A) and TH-2(H443A) on POPC vesicles were analyzed using surface plasmon spectroscopy (Biacore). Overlaid sensorgrams (Fig. 4A, B) were obtained when different concentrations of TH-2(H170A) and TH-2(H443A)

(from 210 nM to 709 nM) were passed over the captured POPC vesicles at a flow rate of 20 μl/min. The associations of inactive mutants with POPC vesicles are summarized in Fig. 4C. For both TH-2(H170A) and TH-2(H443A), the association increased in a dose-dependent manner. TH-2(H443A) showed a significantly higher interaction rate than that of TH-2(H170A) at all concentrations (ANOVA; $P < 0.0001 – 0.05$). The values of k_a, k_d, and the affinity constant K_D were calculated from each sensorgram, and the averages of each parameter representing the kinetic parameters of TH-2(H170A) and TH-2(H443A) are shown in Table 1. The association rate constants (k_a) were 1.71×10^4 M^{-1} s^{-1} and 6.10×10^4 M^{-1} s^{-1} for TH-2(H170A) and TH-2(H443A), respectively. The dissociation rate constants (k_d) were 6.32×10^{-4} s^{-1} and 2.24×10^{-4} s^{-1} for TH-2(H170A) and TH-2(H443A), leading to affinity constants (K_D values) of 3.82×10^{-8} and 4.71×10^{-9} M, respectively. The affinity constant of TH-2(H443A) was lower than that of TH-2(H170A) by 1 order of magnitude. Hence, TH-2(H443A) bound to POPC with 8-fold higher affinity compared to that of TH-2(H170A). This suggests that the histidine residue in the N-terminal HKD motif of TH-2PLD functions as the initial catalytic nucleophile which attacks the phosphorus atom of the substrate phospholipids.

3.4. Comparison of interaction of PLDs with several phospholipid vesicles

To confirm that the difference in affinities between TH-2(H170A) and TH-2(H443A) for POPC could also be observed for other phospholipids (Fig. 5), affinities to POPG and POPS vesicles were determined (Fig. 6). The maximal responses measured for inactive mutant associations with phospholipid vesicles are shown in Fig. 6D. For POPS vesicles, the injection of 473 nM TH-2(H443A) resulted in a binding signal of 607 RU, whereas the association of TH-2(H170A) was significantly (*t*-test; $P < 0.001$) lower (208 RU). This result shows that there is a greater difference in the affinities between the two inactive mutants for

POPS vesicles than POPC vesicles, and supports the proposal that the histidine residue in the N-terminal HKD motif of PLD is the catalytic nucleophile. However, for POPG vesicles, TH-2(H170A) (368 RU) showed slightly higher affinity when compared with TH-2(H443A) (248 RU, $P < 0.05$). As shown in Fig. 6A, the sensorgram of TH-2(H170A) rose more sharply in the association phase when the POPG vesicles were used than when POPC vesicles were used, indicating that POPG vesicles have more rapid association kinetics with TH-2(H170A) than POPC vesicles. In contrast, TH-2(H443A) bound to POPG vesicles slowly, and the binding response to POPG vesicles was 2.5-fold lower than that with other phospholipid vesicles. Interestingly, the interaction of wild-type TH-2PLD with POPG vesicles increased similarly to that with POPS vesicles (Fig. 6C), although TH-2(H443A) showed a low degree of interaction with POPG vesicles. This result suggests that the histidine residue in the C-terminal HKD motif of PLD significantly effects on the association with POPG vesicles.

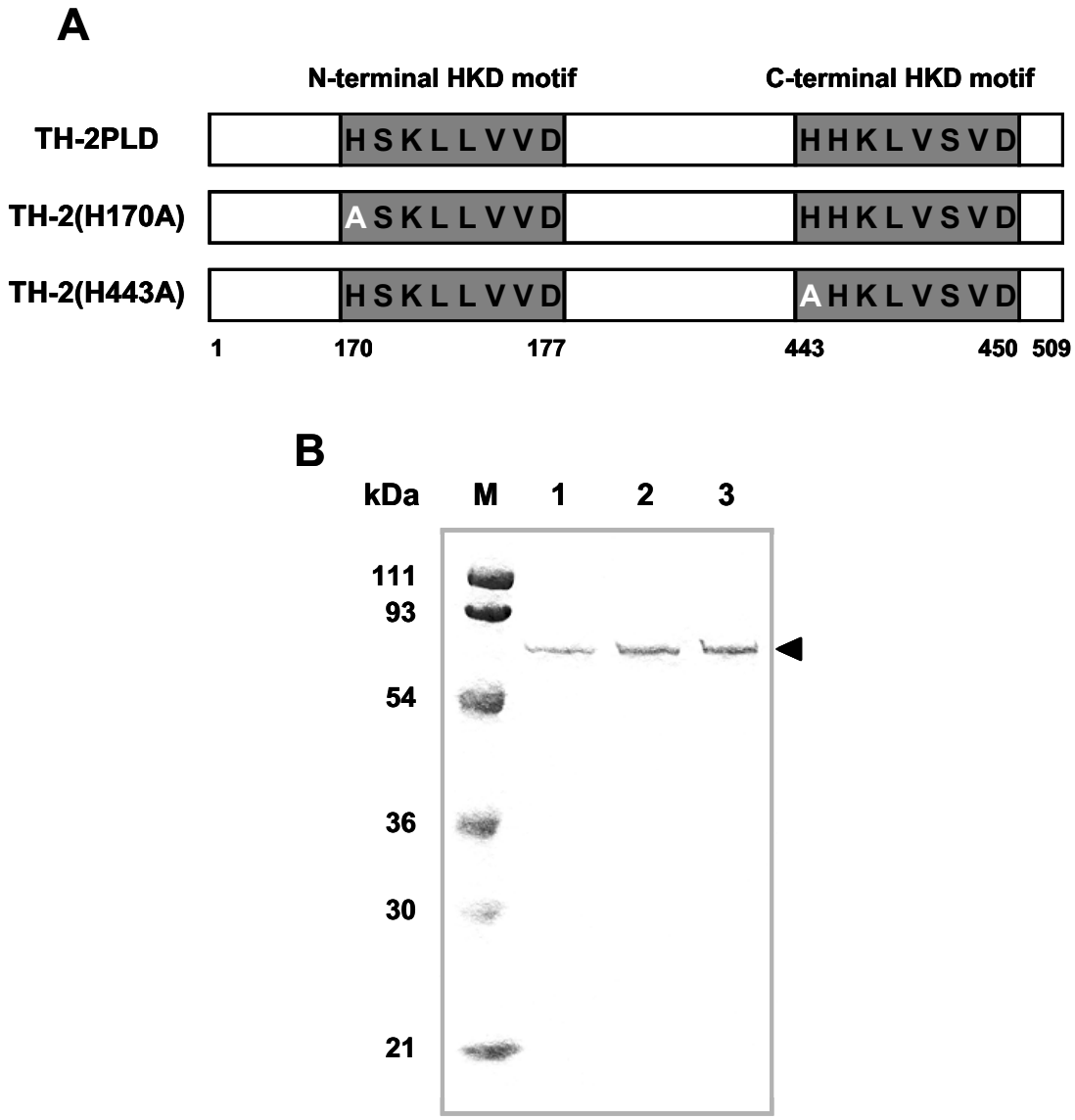

Figure 2. Preparation of wild-type TH-2PLD and its mutants. (A) Schematic structure of PLDs. White characters indicate His residues mutated to Ala. The numbers below the schematic structure indicate those of amino acid residues of TH-2PLD. (B) SDS-PAGE of purified PLDs. Lanes 1-3 contained 1.5 μg of TH-2PLD, TH-2(H170A) and TH-2(H443A), respectively. Lane M indicates SDS-PAGE standard proteins (molecular weights, 111,000, 93,000, 53,500, 36,100, 29,500 and 21,300). Samples were loaded on a 15% acrylamide gel. Arrow indicates the position of purified PLDs.

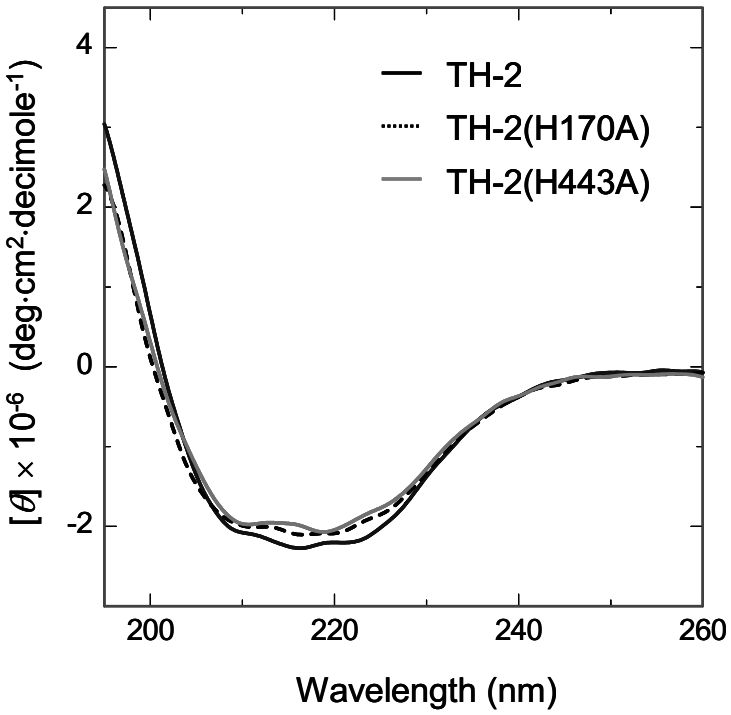

Figure 3. Circular dichroism spectra of PLDs. The spectrum of protein (0.1 mg/ml) in 10 mM potassium phosphate buffer (pH 7.0) was measured at 25°C.

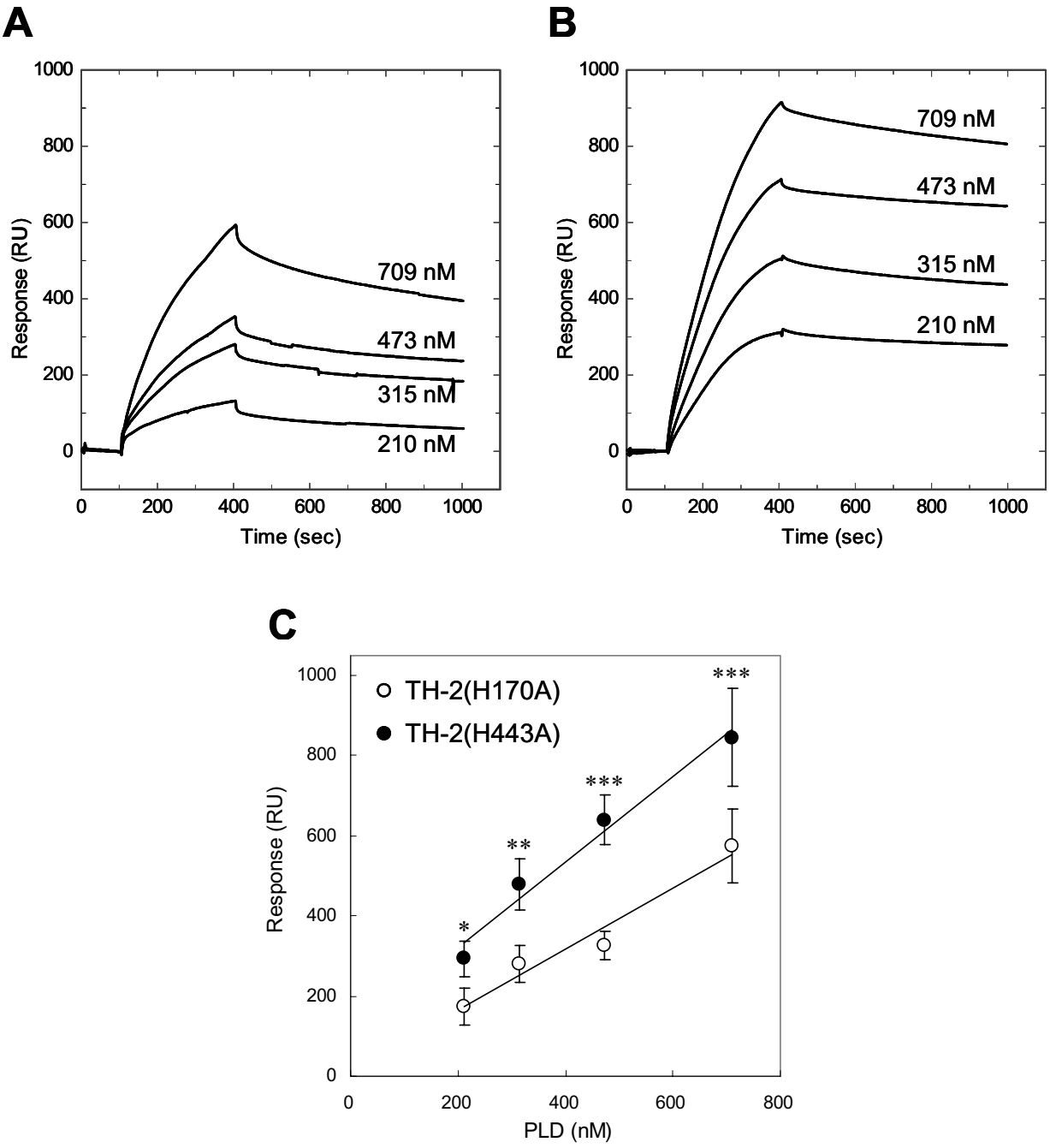

Figure 4. Sensorgrams with different concentrations of inactive mutants of TH-2PLD. SPR sensorgrams obtained when TH-2(H170A) (A) and TH-2(H443A) (B) at 709, 473, 315 and 210 nM, (from top to bottom) were passed over the POPC vesicles immobilized on a sensor chip L1 at a flow rate of 20 μl/min. (C) The values of maximal responses measured for PLD interactions with POPC vesicles were obtained from sensorgrams of mutants (A, B). Each value represents the mean ± SD from three independent experiments. TH-2(H443A) induced significant interaction with POPC vesicles when compared with TH-2(H170A) (*: $P < 0.05$, **: $P < 0.01$, ***: $P < 0.0001$, calculated by ANOVA).

Table 1 Kinetic parameters for interactions of inactive mutants of TH-2PLD with POPC vesicles

	k_a (1/Ms)	k_d (1/s)	K_D (M) [a]	Fold increase in K_D [b]
TH-2(H170A)	1.71×10^4	6.32×10^{-4}	3.82×10^{-8}	8.11
TH-2(H443A)	6.10×10^4	2.24×10^{-4}	4.71×10^{-9}	1

[a] Apparent affinity constants K_D were calculated from k_d/k_a.
[b] Fold increase in K_D relative to the binding of TH-2(H443) to POPC vesicles.

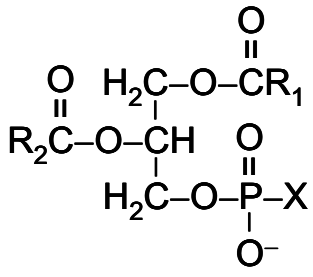

X=

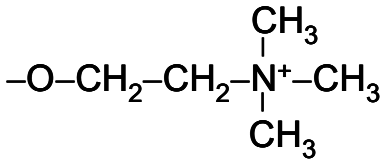

phosphatidylcholine (PC)

phosphatidylglycerol (PG)

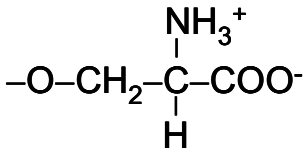

phosphatidylserine (PS)

Figure 5. The structure of phospholipid substrates. R represents an alkyl chain, and X represents a polar head groups.

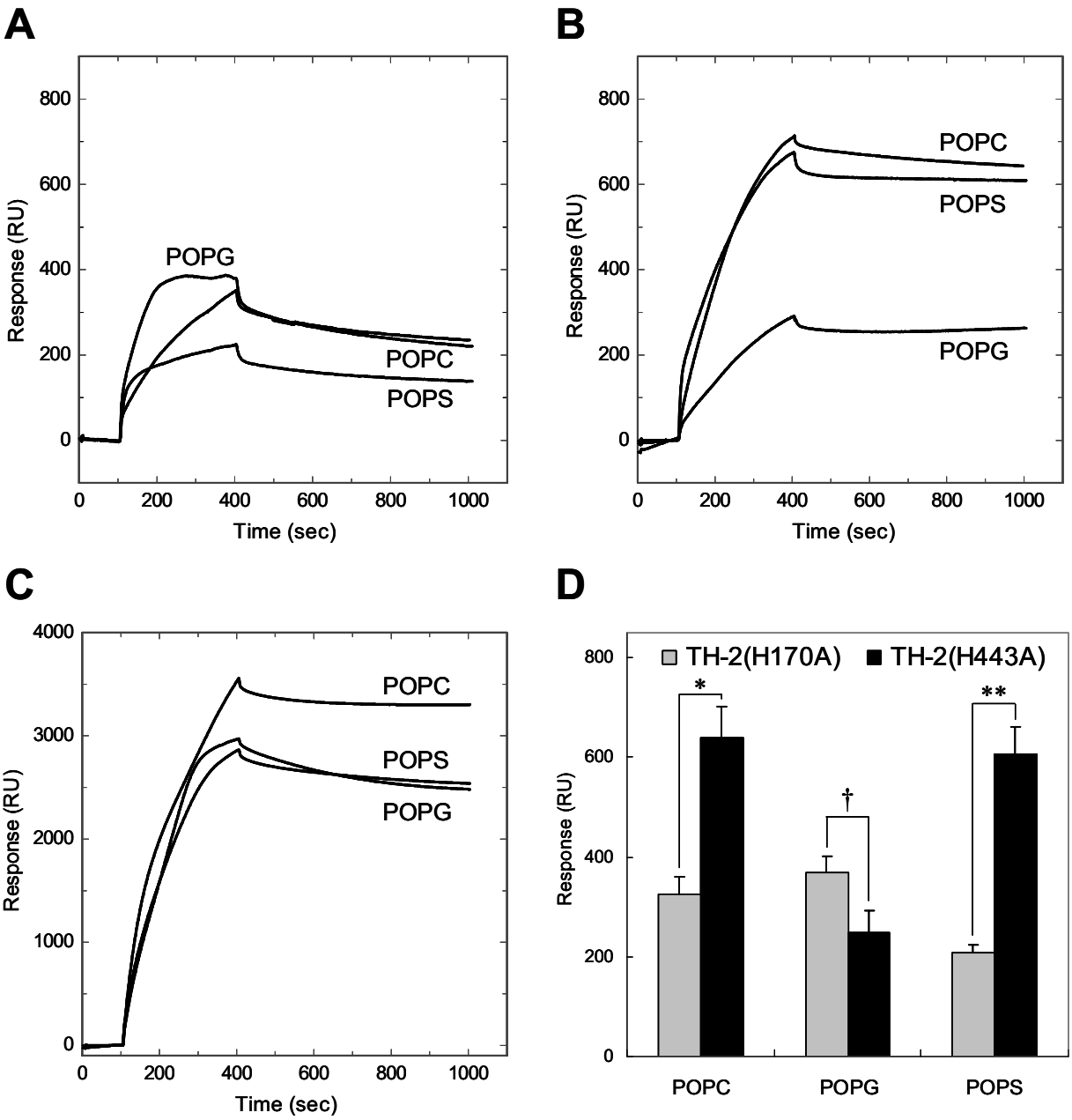

Figure 6. Interaction of PLDs and phospholipid vesicles. Overlay plots of TH-2(H170A) (A), TH-2(H443A) (B) and TH-2 (C) with POPC, POPG and POPS vesicles are shown. Each PLD (473 nM) was injected at a flow rate of 20 μl/min. (D) The *bar graph* represents the maximal responses measured for specific PLD associations with phospholipids. Each value represents the mean ± SD from three independent experiments. TH-2(H443A) induced significant interaction with POPC and POPS vesicles when compared with TH-2(H170A) (∗: $P < 0.01$, ∗∗: $P < 0.001$, calculated by *t*-test). In contrast, TH-2(H170A) induced significant interaction with POPG vesicles when compared with TH-2(H443A) (†: $P < 0.05$, calculated by *t*-test).

4. Discussion

Previous kinetic studies in PLDs proposed that PLD-catalyzed reactions proceed via a two-step mechanism (Stanacev & Stuhne-Sekalec, 1970; Raetz *et al*., 1987; Bruzik & Tsai, 1984; Gottlin *et al*., 1998; Rudolph *et al*., 1999; Xie *et al*., 2000). The first step is formation of a covalently linked phosphatidyl-enzyme intermediate through nucleophilic attack on the phosphorus atom by a residue in the enzyme. The second step involves hydrolysis or transphosphatidylation of the intermediate by a water molecule or an alcohol. This two-step mechanism offers an attractive explanation for essential catalytic amino acid residues on PLD. Sung *et al*. reported that Ser911 of hPLD1 is an enzyme-intrinsic nucleophile, which transfers a proton to the histidine residue in the C-terminal HKD motif (Sung *et al*., 1997). Gottlin *et al*. demonstrated that the substitution of conserved histidine with asparagines of Nuc endonuclease, which has a single copy of the HKD motif, lead to be unable to form an intermediate with an artificial substrate (Gottlin *et al*., 1998). The result showed the histidine residue in the HKD motif of the Nuc is actually the first nucleophile in the catalytic reaction via a covalent phosphohistidine intermediate. This suggests that the histidine residue from one HKD motif acts as a nucleophile attacking the phosphate of the phosphodiester bond, while histidine residue of the other HKD motif acts as a general acid protonating the leaving group.

Iwasaki *et al*. proposed that a histidine residue (His442) in the C-terminal HKD motif of PLD from *Streptomyces antibioticus* is the residue involved in the formation of covalent enzyme-substrate intermediate in the catalytic reaction (Iwasaki *et al*., 1999). On the contrary, Leiros *et al.* showed that His170 in the N-terminal HKD motif of PMFPLD acts as the initial nucleophile that attacks the phosphorus atom of the substrate based on the crystal structures of PMFPLD interacting with short-chain phospholipids and PLD products (Leiros *et al*., 2004). Therefore, it has been discussed which of the histidine residues in the HKD motifs contains the catalytic nucleophile.

In this chapter, to identify which HKD motif contains the catalytic nucleophile, I analyzed the associations of phospholipids and two mutants (Fig. 2A). One mutant, TH-2(H170A), in which His170 of the N-terminal HKD motif of the TH-2PLD was substituted with Ala. The other mutant, TH-2(H443A), was constructed by substituting a histidine residue in the C-terminal HKD motif with Ala. By SPR analysis, retaining of a covalent phosphatidyl-enzyme intermediate (General Introduction, Fig. 1) was evaluated.

Based on these results, it is speculated that two primary factors contributed to association toward substrate. One of these factors is a formation of covalent phosphatidyl-enzyme intermediate, and the other is the recognition of the substrate by the enzyme. The latter comprises non-covalent interactions, such as hydrogen bonds and hydrophobic bonds. It has been considered that the histidine residue from one HKD motif acts as a nucleophile, and a histidine residue of the other HKD motif acts as a general acid. Based on this hypothesis, it is expected that the substituting a histidine residue containing a general acid with Ala would lead increase of interaction rate toward substrate, because intermediate could be formed and no more reaction should be proceeded. Moreover, it is also expected that the substituting histidine residue containing a nucleophile with Ala would cause significantly decrease interaction rate, because intermediate could not be formed (General Introduction, Fig. 1). In fact, the results in this study showed that the inactive mutant, in which the His170 of the N-terminal HKD motif was substituted with Ala (TH-2(H170A)), exhibited substantially lower affinity toward POPC and POPS than those of the mutant of the C-terminal HKD motif (TH-2(H443A)) (Figs. 4, 6D). TH-2(H170A) bound to POPC with 8-fold lower affinity (K_D = 4.71×10^{-9} M) compared to that of TH-2(H443A) ($K_D = 3.82 \times 10^{-8}$ M) (Table 1). From above discussion, it is suggested that His170 in the N-terminal HKD motif has a role of the catalytic nucleophile, which attacks the phosphatidyl group of substrate phospholipids, and His443 in the C-terminal HKD motif should act as the general acid.

TH-2(H170A), which is lacking the nucleophile, showed higher affinity toward POPG than TH-2(H443A) (Fig. 6D), the contents of TH-2(H170A) bound to POPG were comparable in those to POPC and POPS. I speculate that these phenomena reveal the non-covalent binding by the substrate recognition of the enzyme. That is to say, these interactions show that there is the binding ability toward the substrate, which is independent of the catalytic nucleophile.

Furthermore, TH-2(H443A), which possesses the nucleophile, showed much lower affinity to POPG compared with POPC and POPS. This result suggests that the residues relating the recognition of PG existed in C-terminal region of *Streptomyces* PLDs, and the substitution of His443 with Ala affected on this recognition site. By computer analysis using the automated docking program, 'AutoDock', Aikens *et al*. demonstrated that the glycerol group of PG was bound to a well composed of Ser453, Lys454, Asn455, Tyr457, Ser459 and Leu461 of PMFPLD (Aikens *et al.*, 2004). The above residues correspond to Ser458, Lys459, Asn460, Tyr462, Ser464 and Leu466 in the C-terminal region of TH-2PLD. PMFPLD and TH-2PLD are 85% homologous in primary structure. Hence, the residues in the C-terminal region may act for the recognition of PG. As shown in Fig. 5, the structure of head group of PG is different from those of PC and PS. I speculate that the substitution of His443 with Ala leads to change the C-terminal recognition site toward PG. The decrease of the binding ability would be caused by the change of the chemical and physical state of the recognition site, which binds to the head group of PG with hydrogen bonds and hydrophobic bonds despite of the existence of the nucleophile. However, contribution of the recognition sites, which would be located in the N-terminal region, toward POPC and POPS are negligible because of similar affinities of TH-2(H170A) toward POPC, POPS and POPG. Therefore, it is difficult to explain the results that TH-2(H170A) expressed lower affinities than those of TH-2 (H443A) toward POPC and POPS due to the change of the recognition site of PC and PS. Thus, these results

agree with the opinion that His170 act as the catalytic nucleophile.

In conclusion, previous evidence and the results in this chapter lead to the suggestion for the PLD-catalyzed reaction mechanism as follows (Fig. 7): (i) nucleophilic attack by His170 in the N-terminal HKD motif on the phosphodiester, then (ii) PLD and phospholipids form a phosphatidylhistidine intermediate and a base is released, (iii) an alcohol or water attack on the phosphatidyl intermediate, followed by (iv) dissociation of PLD from the intermediate and synthesis of a new phospholipid or PA.

Interestingly, the wild-type TH-2PLD interacted similarly with POPG and POPS vesicles (Fig. 6C), despite the mutant, in which His443 was mutated to Ala, expressed lower affinity toward POPG vesicles (Fig. 6D). Recently, Yang and Roberts showed activity of *Streptomyces chromofuscus* PLD, which does not contain the HKD motif, toward a variety of phospholipids (Yang *et al.*, 2003). It utilizes a direct attack of water or alcohol molecules on the phosphorus atom to generate PA or new phospholipid products. They demonstrated that zwitterionic phospholipid vesicles, for example POPC (11.7 $\mu mol \cdot min^{-1} \cdot mg^{-1}$) and POPE (3.7 $\mu mol \cdot min^{-1} \cdot mg^{-1}$), were much better substrates than anionic phospholipids vesicles, for example POPS (0.002 $\mu mol \cdot min^{-1} \cdot mg^{-1}$) and POPG (0.013 $\mu mol \cdot min^{-1} \cdot mg^{-1}$), for *Streptomyces chromofuscus* PLD. These results suggest that these PLDs have not only quite different mechanisms for the catalytic reaction but also recognize phospholipids differently. These different mechanisms embedded in the amino acid sequences on PLDs will be elucidated in the future.

5. Conclusions

From SPR analysis using inactive mutants of TH-2PLD and phospholipids, it was revealed that the histidine residues in the HKD motifs indeed have different roles during catalysis. That is to say, it was suggested that His170 in the N-terminal HKD motif of

TH-2PLD has a role of the initial catalytic nucleophile, which attacks the phosphorus atom of the substrate phospholipids. On the other hand, it was also demonstrated that His443 in the C-terminal HKD motif of TH-2PLD should act as a general acid. Furthermore, it was also suggested that His443 significantly effects on the interaction with the phosphatidylglycerol vesicles.

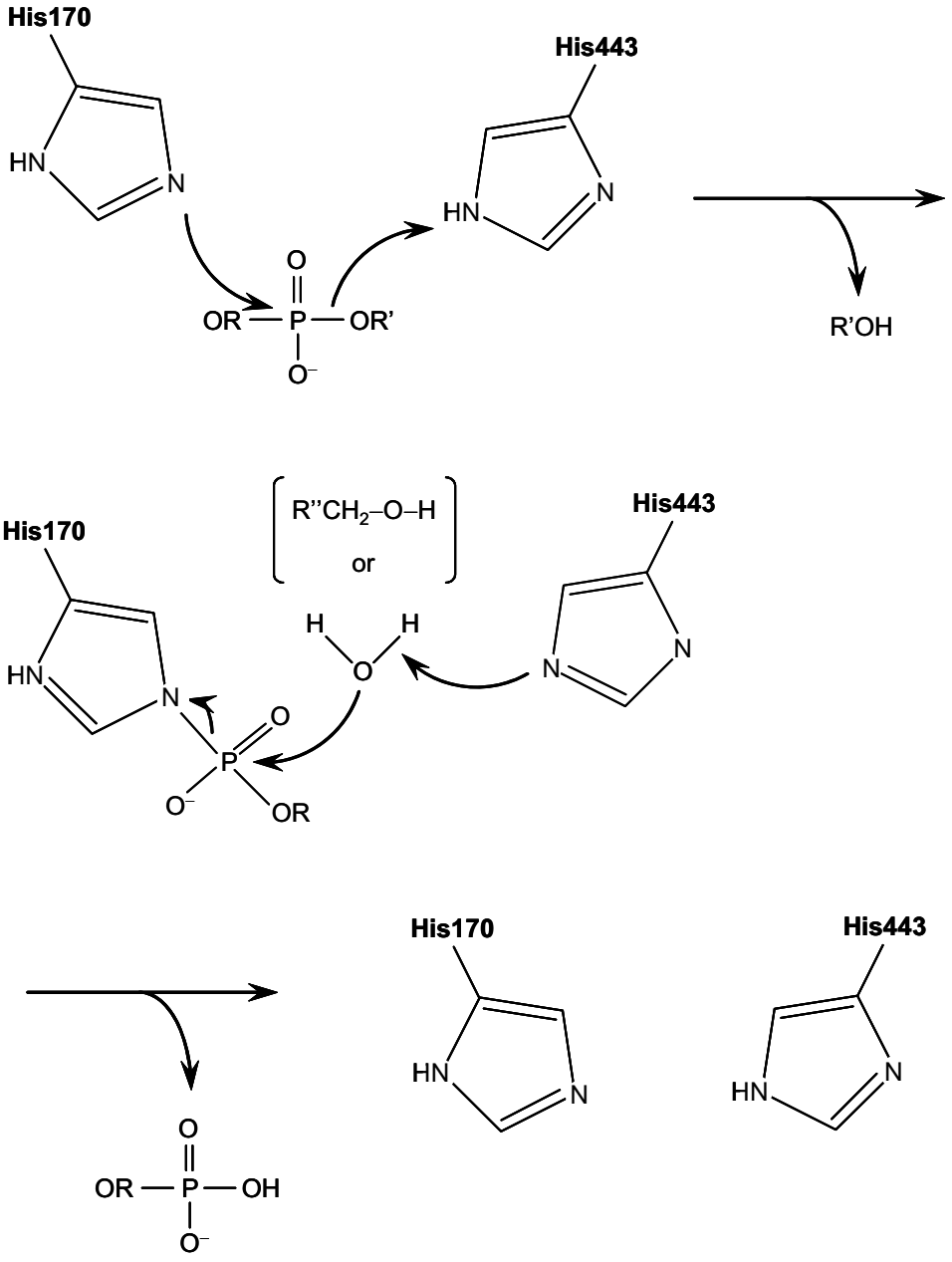

Figure 7. Suggested catalytic mechanism of PLD.

CHAPTER 2

INVESTIGATION OF THE REGIONS RELATED TO THE ENZYME REACTION OF PHOSPHOLIPASE D USING RIBS *IN VIVO* DNA SHUFFLING

1. Introduction

In the reaction mechanism of PLD, the role of the HKD motifs has been studied extensively. However, amino acid residues other than those in the HKD motifs, which are related to PLD-catalyzed activities, have not yet been identified experimentally.

Sequence homology-dependent methods for recombining genes, such as DNA shuffling, opened a new field of protein engineering, and these methods have been successful in evolving proteins with improvement of enzyme activity (Crameri *et al*., 1998; Arnold & Moore, 1997), stability (Giver *et al*., 1998; Negishi *et al*., 2005; Mori *et al*., 2005), and substrate specificity (Zhang *et al*., 1997). DNA shuffling is performed using two distinct methods, *in vitro* (Stemmer, 1994; Crameri *et al.*, 1998) and *in vivo* (Kim *et al.*, 1994; Satoh *et al.*, 1999). The *in vitro* DNA shuffling method using polymerase chain reaction (PCR) is very powerful tool for studies of molecular evolution. When this method is applied to improve protein functions, the establishment of a suitable selection procedure for the isolation of proteins on demand is an issue. However, it is impossible to apply the *in vitro* DNA shuffling method to toxic proteins, such as PLD (Mishima *et al.*, 1997), because of its lethality to the host bacterial strains. On the other hand, *in vivo* DNA shuffling using a linear plasmid was performed by RecA-dependent recombination and the resulting chimeric proteins were limited in number and variability (Kim *et al.*, 1994; Satoh *et al.*, 1999).

Recently, Mori *et al*. have described a novel method of random chimeragenesis, RIBS (repeat-length independent and broad spectrum) *in vivo* DNA shuffling, which overcome the

disadvantages of *in vitro* and *in vivo* DNA shuffling methods mentioned above (Mori *et al*., 2005). This method is based on highly frequent deletion formation of the introduced plasmids in the *Escherichia coli ssb-3* strain (Mukaihara *et al*., 1997) and a deletion-directed chimera selection system that uses the *rpsL*$^{+}$ gene as a reporter. By using this system, Gly188, Ala426 and Lys433 of PLD from *Streptomyces septatus* TH-2 were identified as thermostability-related amino acid residues (Negishi *et al*., 2005; Mori *et al*., 2005).

In this chapter, to investigate amino acid residues related to the PLD-catalyzed reaction other than the HKD motifs, I constructed chimeras between TH-2PLD and PLDP from a distinct *Streptomyces* sp., which has been studied extensively in transphosphatidylation reactions (Juneja *et al*., 1987; Juneja *et al*., 1989; Takami *et al*., 1994; Hatanaka *et al*., 2002a), using RIBS *in vivo* DNA shuffling. Although these parental PLDs exhibit high homology (Fig. 1), the activity in transphosphatidylation reaction is quite different. By comparing the activities of chimeras, the amino acid regions relating to the reactions other than the HKD motifs will be discussed.

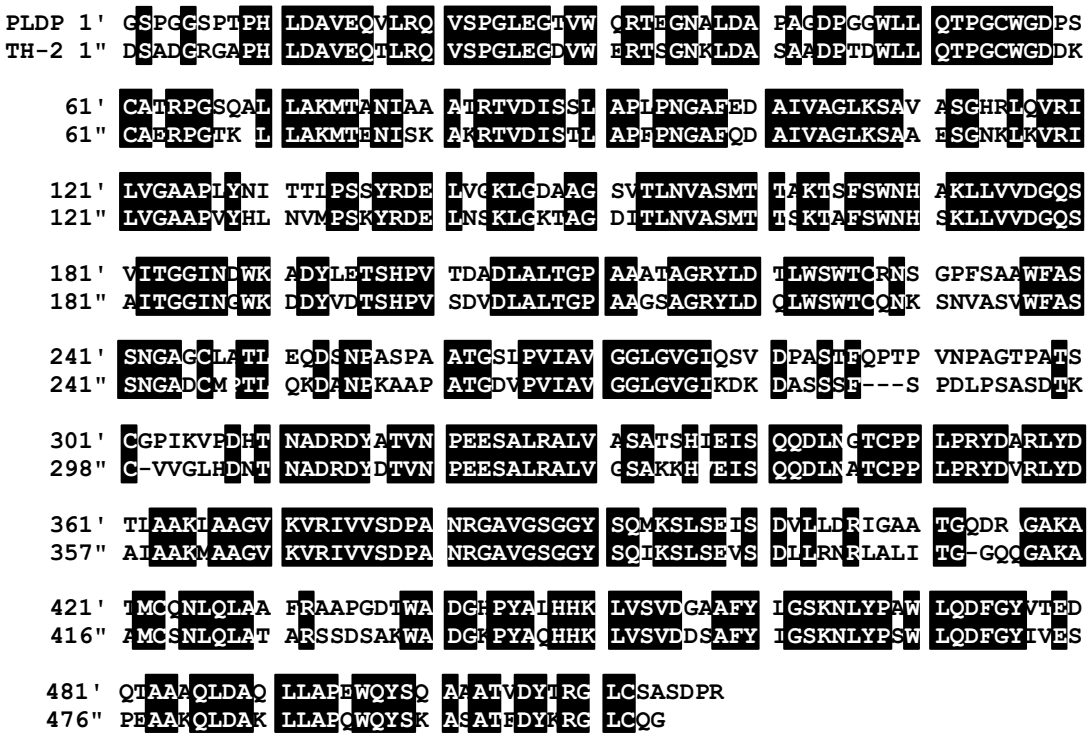

Figure 1. Comparison of primary structures of *Streptomyces* sp. PLDP and *Streptomyces septatus* TH-2. Conserved sequences in the parental PLDs are indicated by shade.

2. Experimental procedures

2.1. Materials

Plasmid pETKmS2 (Mishima *et al*., 1997) was kindly provided by Dr. Tsuneo Yamane, Nagoya University, Japan. Phosphatidyl-*p*-nitrophenol (PpNP) was prepared from soybean phosphatidic acid and *p*-nitrophenol according to the procedure of D'Arrigo *et al*. (D'Arrigo *et al*., 1995). All the other chemicals were of the highest purity available.

2.2. Strains

E. coli MK1019 was *rpsL* (Sm^r) mutant derivative of *E. coli* EJ2885 (*lacI3* Δ*lacZ* $lacY^+$ Δ*fliC ssb*-3). *E. coli* EJ2885 was a tetracycline-sensitive derivative of *E. coli* EJ2882 (*lacI3* Δ*lacZ* $lacY^+$ Δ*fliC ssb*-3 *zjc*::Tn*10*) (Mukaihara *et al*., 1997).

2.3. The pldp gene synthesis

I requested Hokkaido System Science to synthesize the artificial *pldp* gene on the basis of the sequence described in Ref. Takahara *et al*., 1993. I altered the gene by a silent mutation to facilitate its expression in *Escherichia coli*. Firstly, I altered several codons for Pro, Ser and Arg at the third nucleotide to cytosine because the expression of the *th-2pld* gene including a codon for Ser with adenine or thymine at the third nucleotide in *E. coli* was unsuccessful (personal data). I then added an *Eco*RI site and an *Nco*I site to the 5' end of the gene, and added a *Bam*HI site to the 3' end to construct a vector for RIBS shuffling. Finally, the *Bam*HI site in the wild-type *pldp* gene was deleted by silent mutation to construct the vector. The *pldp* fragment was cloned into the *Eco*RI-*Bam*HI gap of pUC19 or pETKmS2, and the resulting plasmid pUC19(*pldp*) or pETKmS2(*pldp*) was obtained.

2.4. Construction of plasmids for RIBS in vivo DNA shuffling

The plasmids for RIBS *in vivo* DNA shuffling was constructed as detailed previously (Mori *et al.*, 2005). For RIBS *in vivo* DNA shuffling, a plasmid that contained the *pldp* and *th-2pld* genes cloned in tandem was constructed as follows. The *pldp* gene in plasmid pUC19 was digested with *Nco*I and *Bam*HI, then the *pldp* gene was ligated into the *Nco*I-*Bgl*II gap of plasmid pACTIS4b (Mori *et al.*, 2005) to obtain pACTIS4b(*pldp*). Next, the *th-2pld* gene in pBluescript was digested with *Eco*RV and *Bam*HI, and the gene was ligated into the *Pma*CI-*Bam*HI gap of plasmid pACTIS4b(*pldp*), yielding pACTIS4b(*pldp/th-2pld*). Then, the Gm^r-$rpsL^+$ cassette from pNC124 (Mori *et al.*, 2005) was digested with *Kpn*I, and the cassette was inserted into the *Kpn*I site between the two *pld* genes in pACTIS4b(*pldp/th-2pld*) to construct pACTIS4b(*pldp/*Gm^r-$rpsL^+$/*th-2pld*) (Fig. 2). The resulting vector was used for RIBS *in vivo* DNA shuffling.

2.5. Random chimeragenesis of PLD genes

Straregy of random chimeragenesis is as follows (Fig. 2). Two homologous genes (*pldp* and *th-2pld*) were placed in the same direction, and a cassette containing the Gm^r and *E. coli* $rpsL^+$ genes was inserted between them. $rpsL^+$ encodes the ribosomal protein S12 (Mori *et al.*, 2005), the target of Sm. *E. coli* MK1019 (*ssb-3 rpsL*(Sm^r)) was prepared as a host for chimeragenesis. A certain mutation in the genomic *rpsL* gene led this strain to Sm^r. The transformation of MK1019 with pACTIS4b(*pldp/*Gm^r-$rpsL^+$/*th-2pld*) altered the phenotype of cells from Sm^r to Sm^s (and also Gm^s to Gm^r), because the Sm^s ribosome was reconstituted with the wild-type RpsL protein encoded by the plasmid. When recombination occurs between two homologous genes, the Gm^r-$rpsL^+$ cassette is simultaneously deleted from the plasmid and the cells reverse their phenotype from Sm^s/Gm^r to Sm^r/Gm^s. The Gm^r gene excludes the accidental deletion of the Gm^r-$rpsL^+$ cassette. In strain MK1019, the expression levels of chimeric *pld* genes in

resulting plasmids are negligible, since these genes are controlled by the T7-*lac* promoter; however, this strain does not have T7 RNA polymerase. Moreover, leaky expression must be repressed by LacI encoded by the plasmid. Thus, the intact form of the chimeric gene is selectable without expression.

E.coli MK1019 was transformed with pACTIS4b(*pldp*/Gm^r-*rpsL*$^+$/*th-2pld*) by electroporation, and transformants were selected on LB plates containing chloramphenicol and gentamicin. The sensitivities of Cm^r/Gm^r transformants to streptomycin (Sm^s) were confirmed on LB plates containing chloramphenicol, gentamicin and streptomycin. Sm^s transformants from each host were cultivated in the LB medium containing chloramphenicol. Cultures were spread on LB plates containing chloramphenicol with streptomycin. Plasmids isolated from 48 selected Sm^r revertants from each host were analyzed by agarose gel electrophoresis. The 1.6-kb DNA fragment containing the *PLD* gene on isolated plasmids was amplified by PCR using a GC-Rich PCR system (Roche) with primers corresponding to the coding regions of the pelB signal (5'-CGACCGCTGCTGCTGGTCTGC-3') and His6 tag (5'-TGGTGGTGGTGCTCGAGTGCGGC-3'). Recombination sites were mapped on the basis of the change in the pattern of the digestion of these fragments with several restriction endonucleases and determined in detail by DNA sequencing.

2.6. Expression and purification of PLDs

E. coli BL21-Gold(DE3) (Invitrogen) was transformed with PLD expression plasmids. Expression was carried out according to a method described previously (Hatanaka *et al.*, 2002b) in the presence of appropriate antibiotics (chloramphenicol (50 μg/ml) and kanamycin (50 μg/ml) for strains harboring plasmids obtained from the random chimeragenesis and plasmids derived from pETKmS2, respectively) except for the addition of premixed protease inhibitor tablet Complete^{TM}, Mini, EDTA-free (Roche) at the induction period (one tablet per

culture). Cultures were centrifuged for 60 min at 3,500 × g. The culture broth was concentrated with an ultrafiltration device using Amicon Ultra (Millipore, 30 kD cut), and dialyzed against 20 mM Tris-HCl (pH 8.0). His-tagged PLDs were purified using Magextractor-His Tag (TOYOBO). The purified PLDs were dialyzed against 10 mM acetate buffer (pH 5.5).

2.7. Gel electrophoresis of proteins

SDS-PAGE was performed by the method of Laemmli (Laemmli, 1970) using a 15% acrylamide gel. The molecular weight markers (Amersham Biosciences) included phosphorylase b, albumin, ovalbumin, carbonic anhydrase, trypsin inhibitor and α-lactalbumin. Proteins on the gels were stained with Coomassie brilliant blue R-250 (Bio-RAD) and destained with water.

2.8. Circular dichroism (CD) spectroscopy

The secondary structures of PLDs were determined by CD spectroscopy using a J-720WI spectrometer (Jasco). Proteins were dissolved to a final concentration of 0.1 mg/ml in 10 mM potassium phosphate buffer (pH 7.0). Spectra were acquired at 25°C using a 2-mm cuvette. Molar ellipticities (per residue) were calculated using the equation $[\theta] = 100(\theta) / (lcN)$, where $[\theta]$ is the molar ellipticity per residue, (θ) is the observed ellipticity in degrees, l is the optical path length in centimeters, c is the molar concentration of the protein, and N is the number of residues in the protein.

2.9. Assay for PLD activities using PpNP

Hydrolytic activity was determined based on the hydrolytic activity of PpNP. The procedure was similar to the method described previously (Hatanaka *et al*, 2002a).

PLD-catalyzed transphosphatidylation activity was determined by measuring the production of *p*-nitro-phenol from PpNP and ethanol according to the method that used a biphasic system consisting of benzene and water as described previously (Hatanaka *et al*, 2002a). One unit of PLD was defined as the amount of the enzyme that released 1 μmol of *p*-nitro-phenol per minute under the assay conditions. PLDs used in this thesis showed both hydrolysis and transphosphatidylation activities in the absence of Ca^{2+}. The kinetic assays for both activities were carried out as described previously (Hatanaka *et al*, 2002a). In the assay of hydrolytic activity, the reactions were carried out in 1.5-ml cuvettes; the 1-ml reaction mixture consisted of PpNP at final concentrations ranging from 0.11 to 2 mM in 0.1 M acetate buffer (pH 5.5) and the purified PLDs. In the assay for transphosphatidylation activity, the reactions were performed for 10 min in 1.5-ml sample tubes; the 400-μl reaction mixture consisted of PpNP at a final concentrations ranging from 1.8 mM to 20 mM, and ethanol at final concentration of 800 mM, in an emulsion containing benzene and acetate buffer (pH 5.5). The purified PLDs (200 ng) were used in the assay.

2.10. Statistical analysis

All statistical evaluations were performed by an unpaired Student's *t* test or analysis of variance (ANOVA). All data are presented as means ± standard deviations of at least three determinations.

3. Results

3.1. Construction of chimeric pld genes

The chimeric *pld* genes were obtained when the plasmid pACTIS4b for RIBS *in vivo* DNA shuffling (Fig. 2) was transformed into the *ssb-3* mutant. To identify recombination sites, restriction mapping was applied to 51 chimeric *pld* genes (Fig. 3A). The recombination sites were widely distributed over the entire chimeric *pld* genes accumulating mainly in the region corresponding to the *pldp* gene 792-1038. On the other hand, no chimeras were obtaind in the N-terminal region (1-172). To confirm these recombination sites, the complete sequences of the resulting chimeric *pld* genes were determined (Fig. 3B). The recombination occurred in the homologous regions from 4 to 29 nucleotides. Variations of chimeric genes were 21 kinds.

3.2. Preparation of chimeric PLDs

I chose eight typical chimeras having a recombination site in each restriction mapping region for the expression of genes. Fig. 4A shows the recombination positions of the primary structures of the eight chimeras. Chimeric PLDs were expressed according to a previous study (Mori *et al.*, 2005). All of the chimeric PLDs were obtained from the extracellular fraction. Chimeric PLDs were purified by nickel affinity chromatography. The molecular weight of purified PLDs analyzed by SDS-PAGE was approximately 57 kDa which coincided with the calculated value (56.5 kDa) (Fig. 4B).

3.3. The folding of PLDs

To confirm the folding of wild-type TH-2PLD, PLDP and chimeric PLDs, their CD spectra were measured. As shown in Fig. 5, a large change might not be expected in secondary structure.

3.4. Comparison of activities of chimeric PLDs

PLD activities were determined on the basis of transphosphatidylation and hydrolysis of phosphatidyl-*p*-nitrophenol as described by Hatanaka *et al*. (Hatanaka *et al*, 2002a) with several modifications (Figs. 6, 7). To determine the region related to hydrolysis and transphosphatidylation reactions, I first analyzed the specific activities of two parental and eight chimeric PLDs (Fig. 8A, B). Although chimeras A, B, C and H had high transphosphatidylation activities similar to that of TH-2PLD, those of chimeras D to G had much lower activities than that of TH-2PLD (Fig. 8B upper). Among the chimeric PLDs examined, chimera C had the highest transphosphatidylation activity. Interestingly, the transphosphatidylation activity of chimera C was significantly different from that of chimera D (*t* test; $P < 0.01$), despite these two chimeras exhibiting equivalent hydrolytic activity (*t* test; $P > 0.05$). A similar significant difference in activity was observed between chimera G and H. Furthermore, I constructed chimera I (recombination site: corresponding to the *th-2pld* gene, nucleotide 1326-1340) using the *Van*91I site (corresponding to the *th-2pld* gene, nucleotide 1329-1339), which are adjacent C-terminal HKD motif, and analyzed its specific activities. The transphosphatidylation activity of chimera I was higher than those of chimeras G and H (231 μmol/min/mg), and significantly different from that of chimera G, while hydrolytic activity of chimera I was somewhat higher than those of chimeras G and H (81 μmol/min/mg). From these results, I assumed that two regions, residues 188-203 and 425-442 of TH-2PLD, are related to the transphosphatidyl activity.

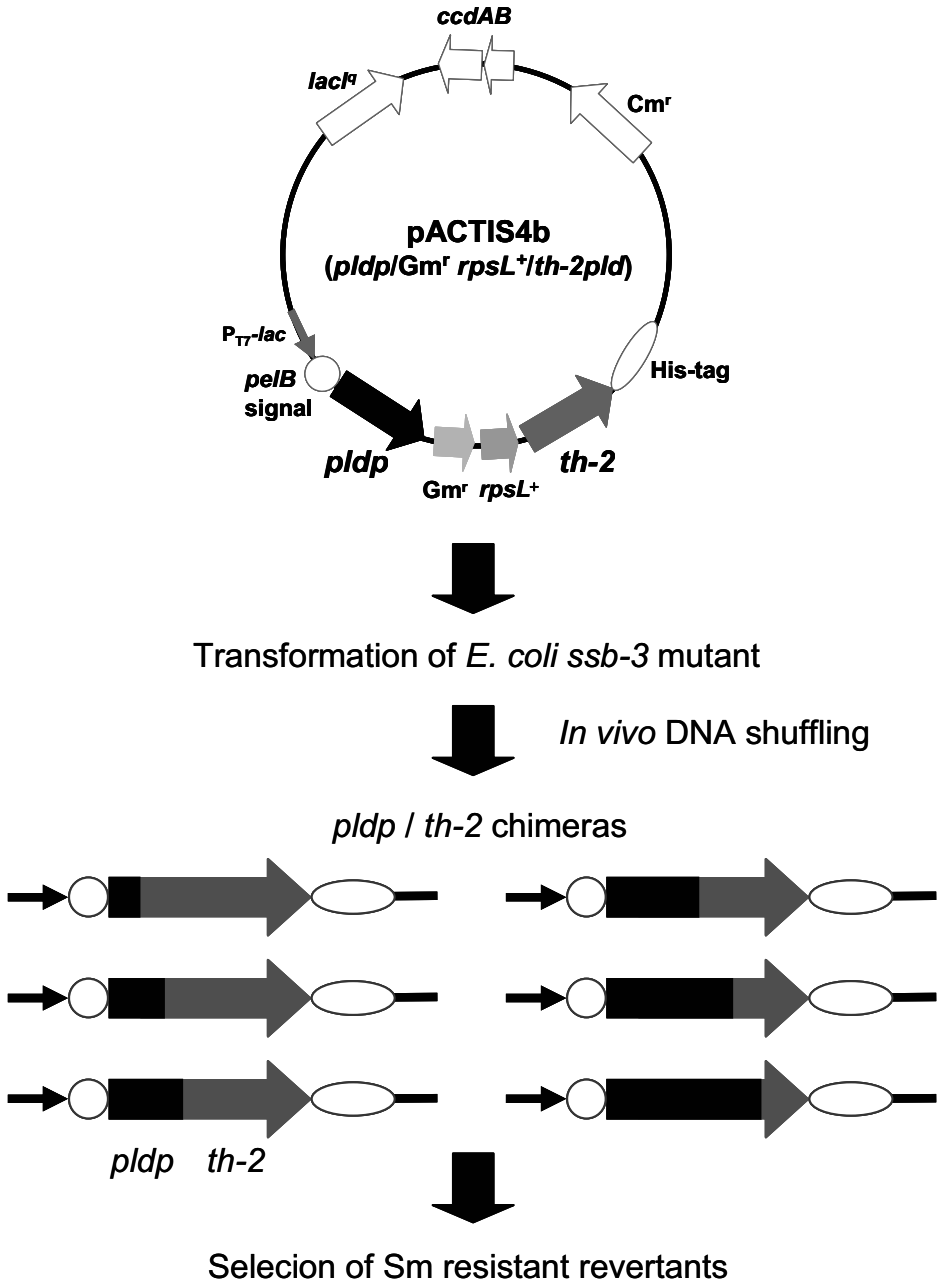

Figure 2. Strategy of random chimeragenesis. The transformation of *E. coli* strain MK1019 (*ssb-3 rpsL*[Sm^r]) with plasmid pACTIS4b(*pldp*/Gm^r-*rpsL*$^+$/*th-2*) altered the phenotype of this host from Sm^r to Sm^s by the wild-type RpsL protein expressed from the plasmid (*rpsL*$^+$ and *rpsL*(Sm^r) represent genes for Sm^s wild-type and Sm^r mutant of ribosomal protein S12 of *E. coli*, respectively). Then, Sm^s-transformants were cultivated overnight at 37 ˚C in medium containing Cm. When an in-frame deletion between two *pld* genes (*pldp* and *th-2*), i.e., the formation of a chimeric *pld* gene (*pldp/th-2*) concomitant with the deletion of the Gm^r-*rpsL*$^+$ cassette occurs, the phenotype of the cells is reversed from Sm^s to Sm^r. Therefore, strains carrying chimeric *pld* genes are selectable on Sm/Cm plates. The resulting chimera can be expressed in an appropriate *E.* coli strain for the T7 expression system and purified with C-terminal His6 tag by nickel-affinity chromatography. *pelB* and *lacI*^{q} encode a secretion signal peptide of *Erwinia carotovorai* pectate lyase and repressor protein of *E. coli lac* operon, respectively. *ccdA* and *ccdB* compose the stabilizing system of the *E. coli* F plasmid.

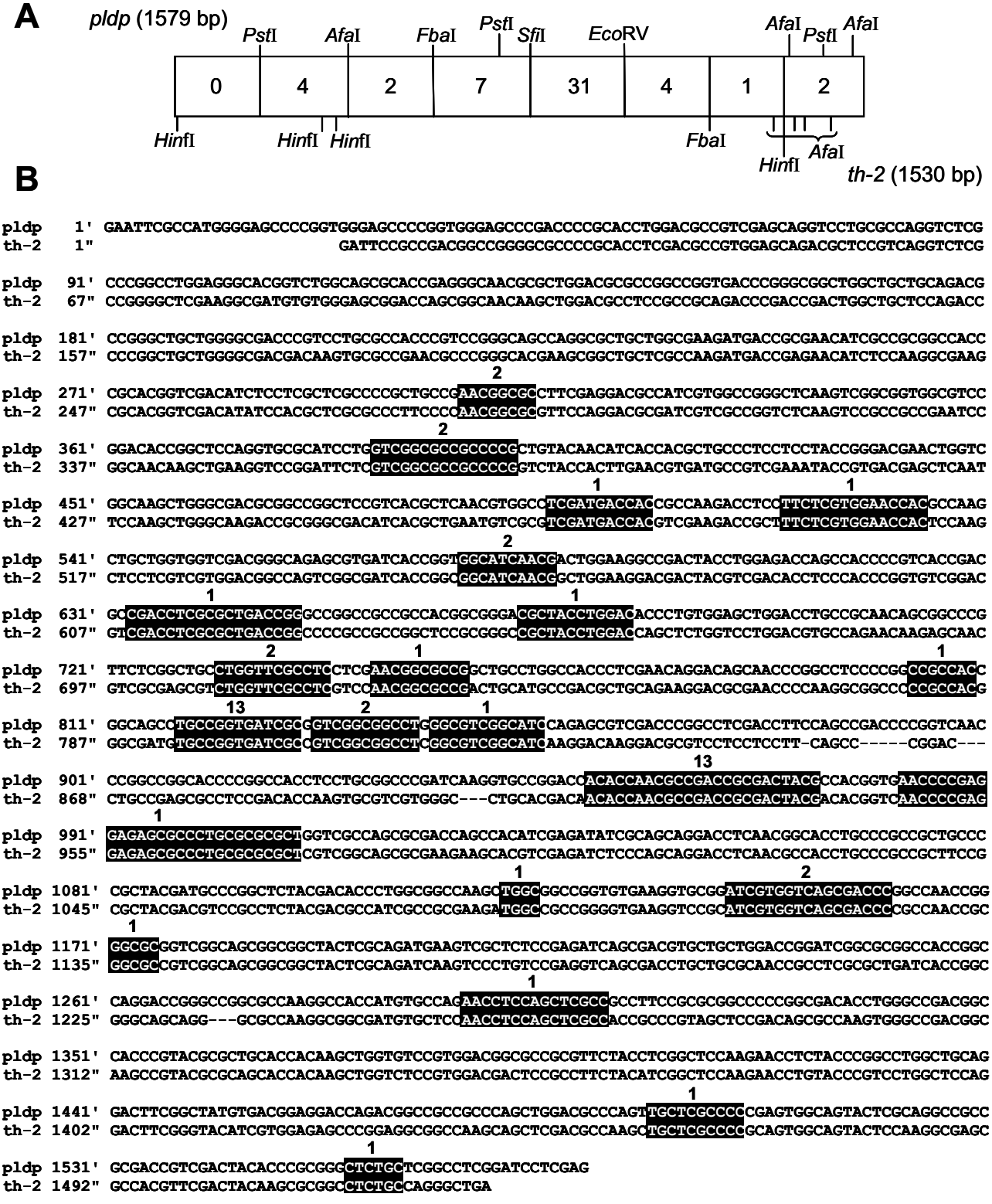

Figure 3. Distribution of recombination sites. (A) Restriction mapping of chimeric *pld* genes. Open bar indicates the DNA region subjected to RIBS *in vivo* DNA shuffling. The restriction sites are indicated on the top (corresponding to *pldp*) and bottom (corresponding to *th-2*) of the open bar, respectively. The numbers in open bar indicate the number of obtained chimeric *plds* in each region. (B) Distribution of nucleotide-based recombination sites. The numbers of nucleotide are indicated on the left. Recombination sites observed are indicated by shade. The numbers of chimeras are indicated by bold capital letters.

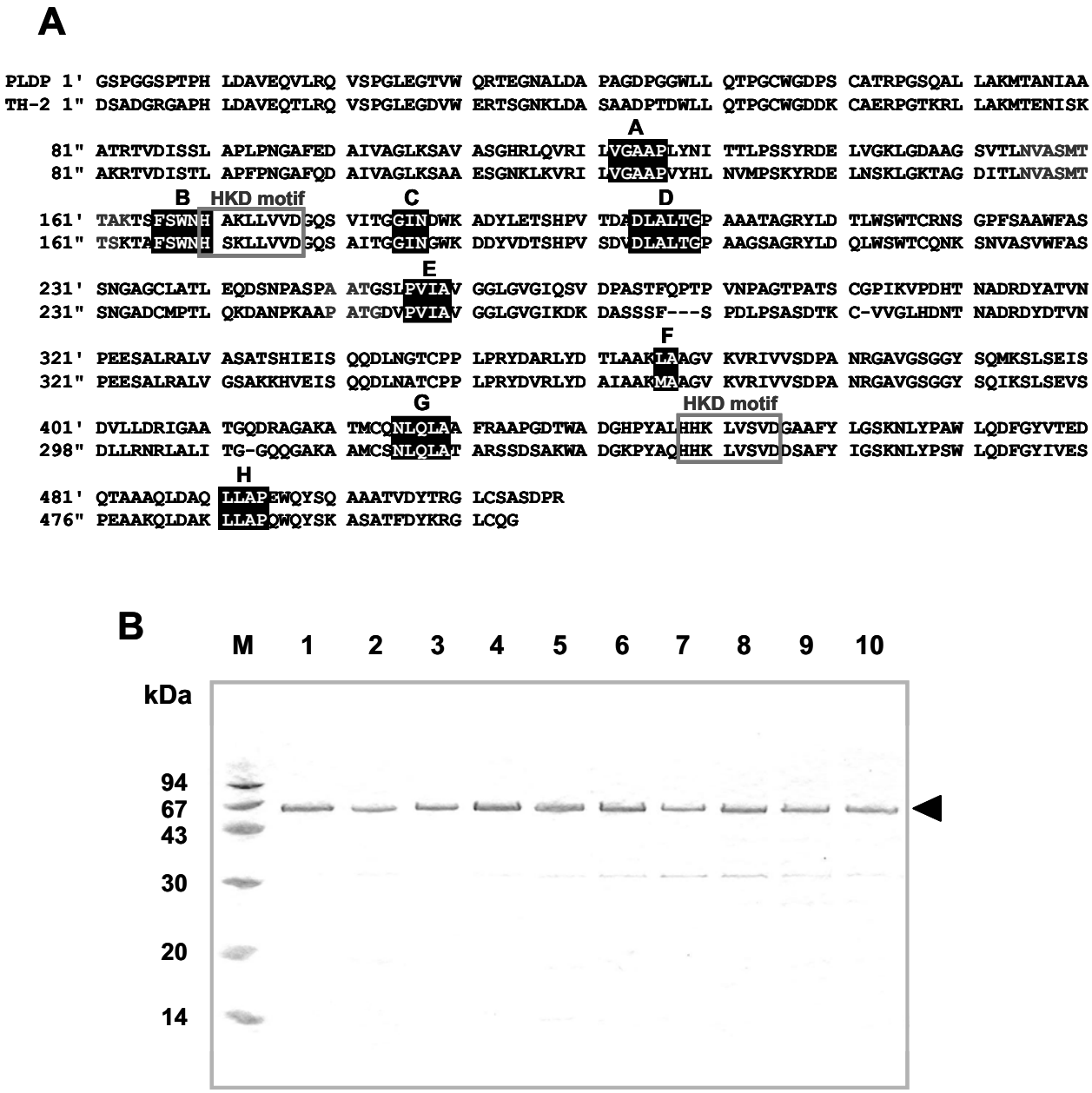

Figure 4. (A) Recombination sites of eight chimeric PLDs used in this study. The primary structures of PLDP (upper) and TH-2PLD (lower) are shown. The numbers of amino acid residues are indicated on the left. The recombination sites of the eight chimeras are boxed. The names of chimeras are indicated by bold capital letters. (B) SDS-PAGE of purified TH-2, PLDP and chimeric PLDs. Lane 1 contained 1.5 μg of TH-2PLD. Lanes 2-9 contained 1.5 μg of chimeric PLDs (A-H), respectively. Lane 10 contained 1.5 μg of PLDP. Lane M indicates low-molecular-weight marker proteins (molecular weights, 94,000, 67,000, 43,000, 30,000, 20,100 and 14,400). Samples were loaded on a 15% acrylamide gel. Arrow indicates the position of purified PLDs.

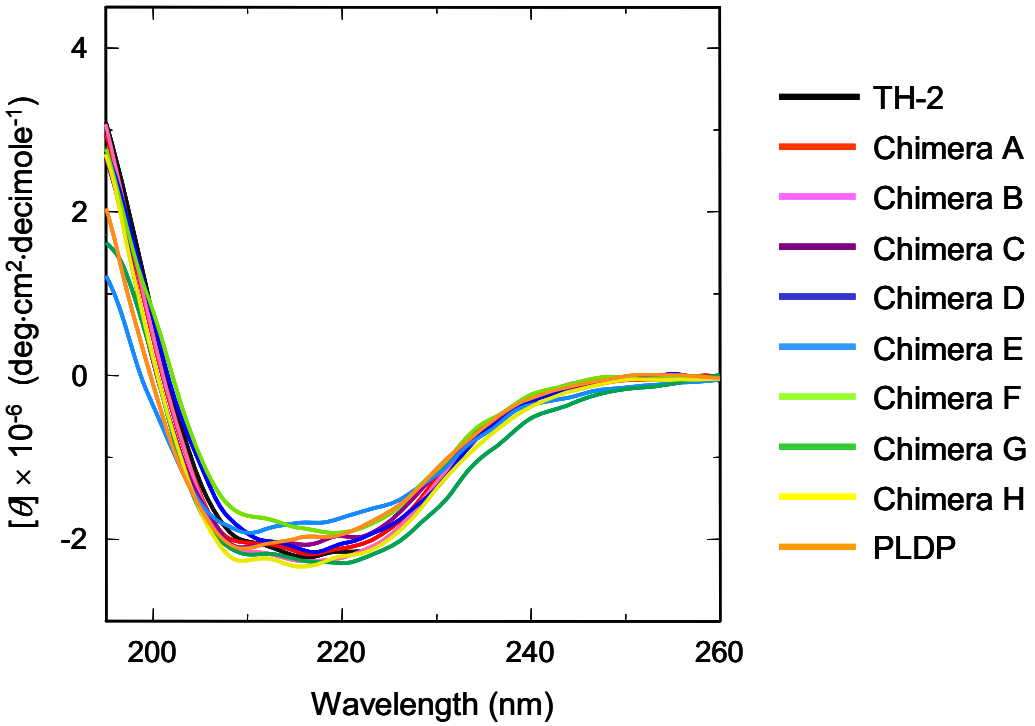

Figure 5. Circular dichroism spectra of TH-2, PLDP and chimeric PLDs (A-H). The spectrum of protein (0.1 mg/ml) in 10 mM potassium phosphate buffer (pH 7.0) was measured at 25°C.

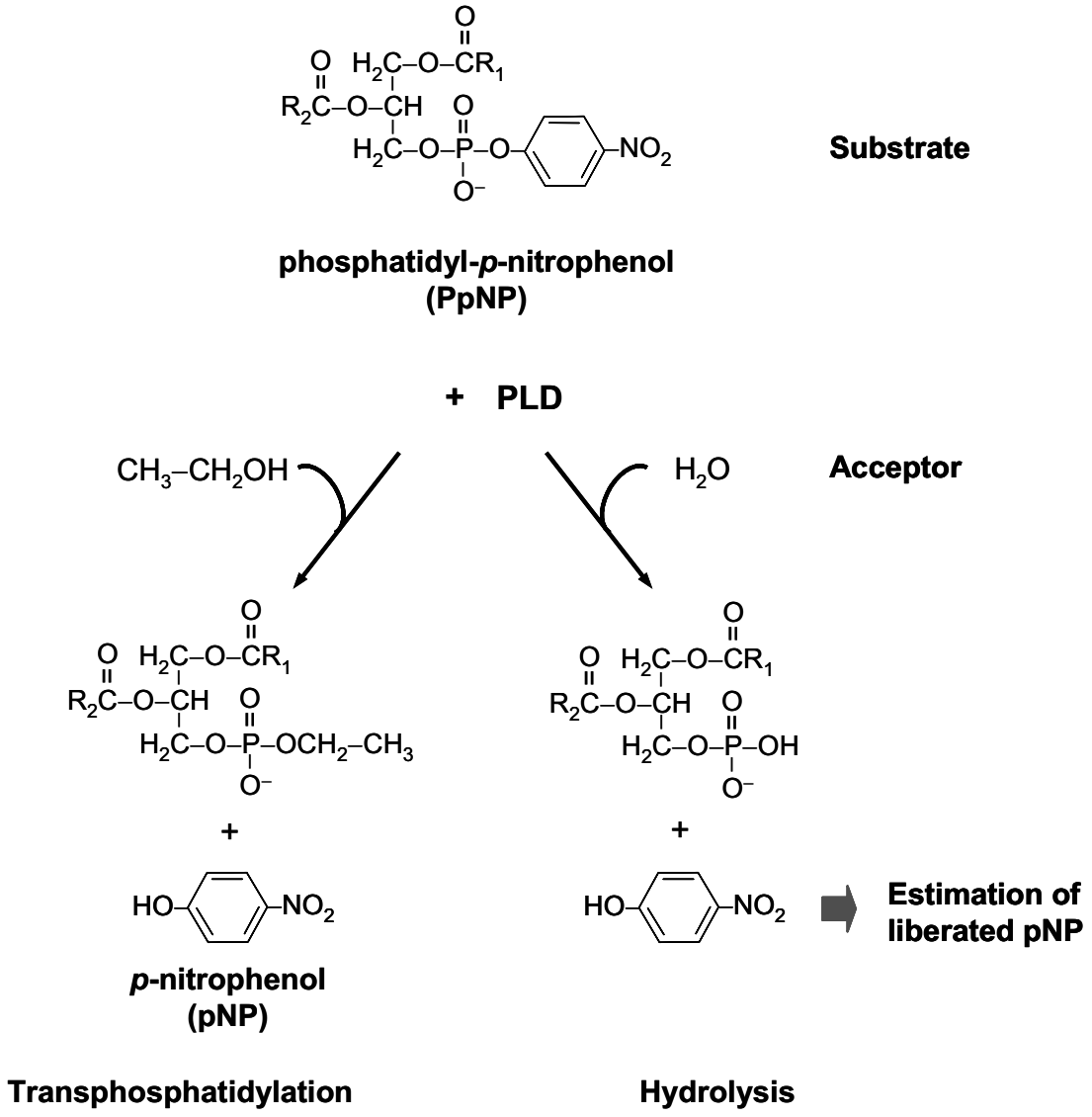

Figure 6. PLD-catalyzed transphosphatidylation and hydrolysis assay by measuring the production of *p*-nitrophenol from phosphatidyl-*p*-nitrophenol.

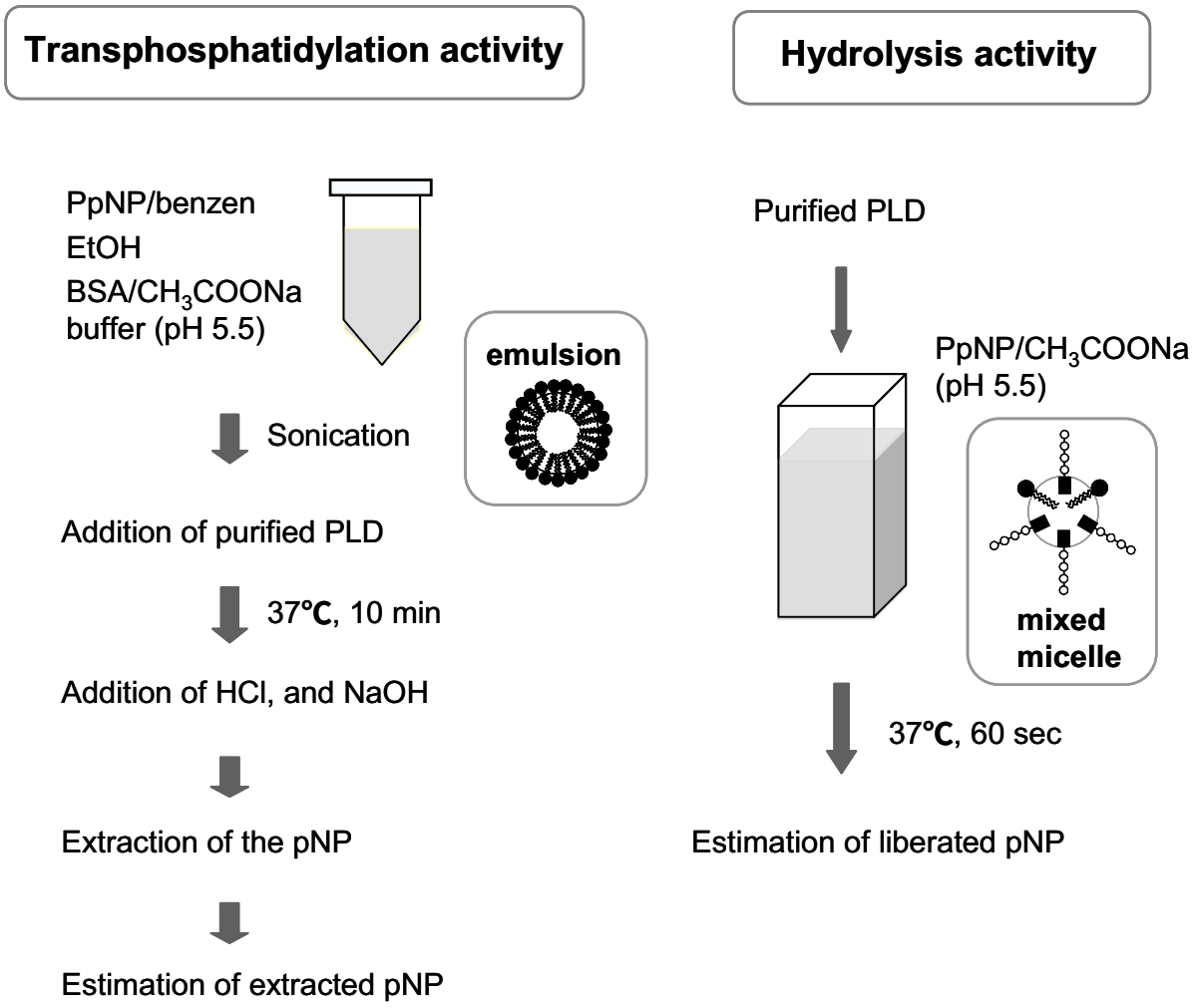

Figure 7. Assay for PLD activities using phosphatidyl-*p*-nitrophenol (PpNP).

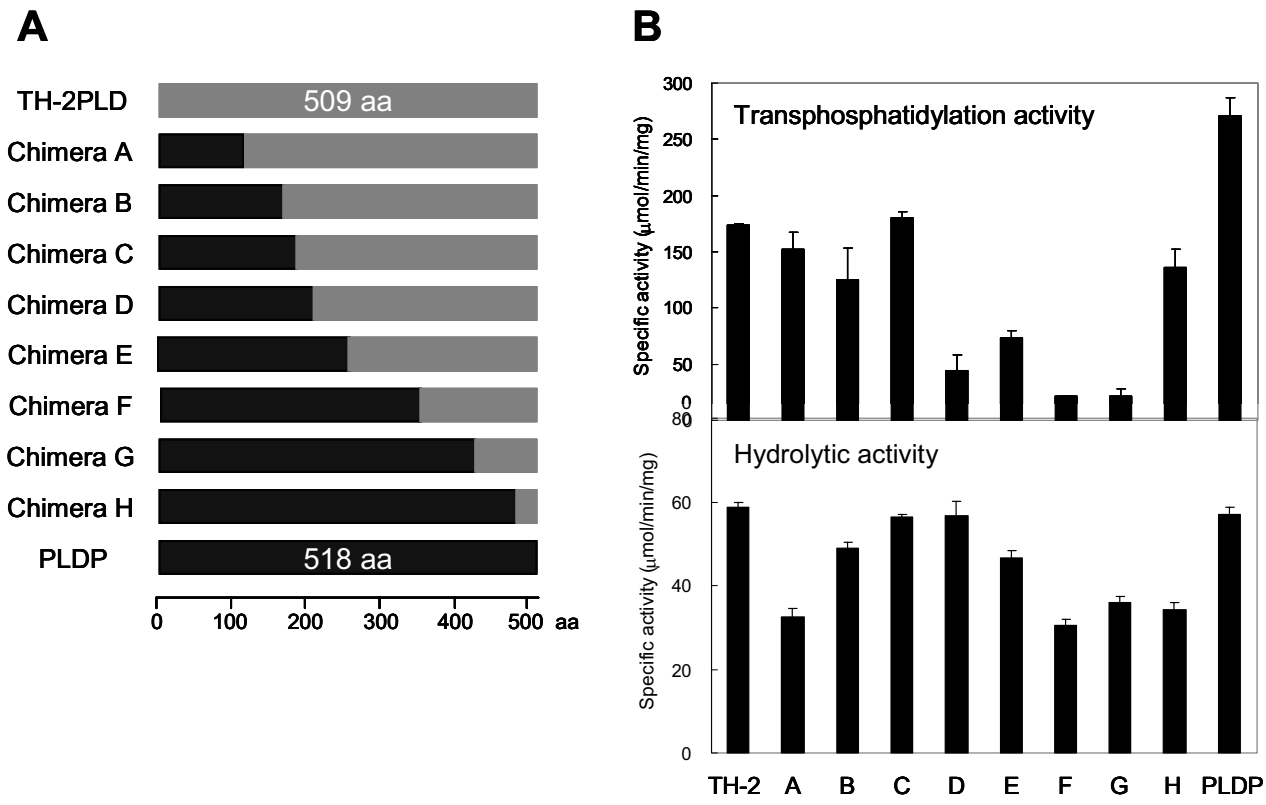

Figure 8. Comparison of activities for chimeras A-H, and parental PLD, TH-2PLD and PLDP. Primary structures of TH-2PLD, chimeras A to H, and PLDP are illustrated schematically (A). The map is drawn to scale (aa, amino acids). (B) Specific activities of PLDs in the transphosphatidylation reaction (upper) and hydrolytic reaction (lower). Transphosphatidylation activities were measured at pH 5.5 with 13 mM PpNP. Hydrolytic activities were determined at pH 5.5 with 2 mM PpNP. Data are expressed as means ± SD of three independent experiments.

4. Discussion

To investigate the contribution of amino acid residues to the enzyme reaction of *Streptomyces* PLD, a chimeric gene library between two highly homologous *plds*, which indicated different activity in transphosphatidylation, were constructed using RIBS *in vivo* DNA shuffling. The success of chimeragenesis for *Streptomyces* PLDs verified the advantage of the application of this system to cytotoxic targets such as PLD. Moreover, chimeric *pld* genes obtained from this system could be expressed easily, and applied to functional studies directly (Figs. 4, 8). Because the two parental *pld* genes used in this thesis, *th-2pld* and *pldp*, are 76% homologous in DNA sequences (Fig. 1), the *pld* genes are suitable for chimeragenesis. By this system, 21 chimeric *pld* genes were obtained with large variety (Fig. 3). As shown in Fig. 9, the recombination sites highly occurred in β sheets and turns, and rarely occurred in α helices. By comparing the activities of chimeras, it suggested that the two regions, residues 188-203 and 425-442 of TH-2PLD, are related to transphosphatidylation activity (Fig. 8).

Recently, several homology-independent protein recombination methods, such as incremental truncation for the creation of hybrid enzyme (ITCHY) (Lutz *et al*., 2001; Ostermeier *et al*., 1999) and sequence homology-independent protein recombination (SHIPREC) (Sieber *et al*., 2001), have been reported. These homology-independent methods are required a system for selecting functional chimeras because many nonfunctional chimeric genes could be formed. On the other hand, most of chimeric PLD plasmids generated correct chimeric genes in RIBS *in vivo* DNA shuffling (Fig. 3).

Leiros *et al.* solved the tertiary structure of PMFPLD as the first crystal structure of PLD (Leiros *et al.*, 2000). They revealed that the PLD consists of 18 α helices and 17 β sheets, with the overall structure being an α-β-α-β-α-sandwich structure. The two HKD motifs were opposed, forming an active well. Based on the crystal structure of PMFPLD, two regions related to the transphosphatidyl activity, residues 188-203 and 425-442 of TH-2PLD, are

present in the two flexible loop regions between β7 and α7 (residues 188-203), respectively, and between β13 and β14 (residues 425-442) and are face-to-face in the domain-domain interface, and the regions locate at the entrance of the active well formed by the two HKD motifs (Fig. 10). I considered that the two regions may be the entrance gate for phospholipid substrates.

5. Conclusions

Using RIBS *in vivo* DNA shuffling, 21 chimeric PLDs were obtained. Their recombinations were occurred between short homologous sequences at corresponding position and with large variety. By comparing the activities of chimeras, it suggested that the two regions, residues 188-203 and 425-442 of TH-2PLD, are related to transphosphatidylation activity.

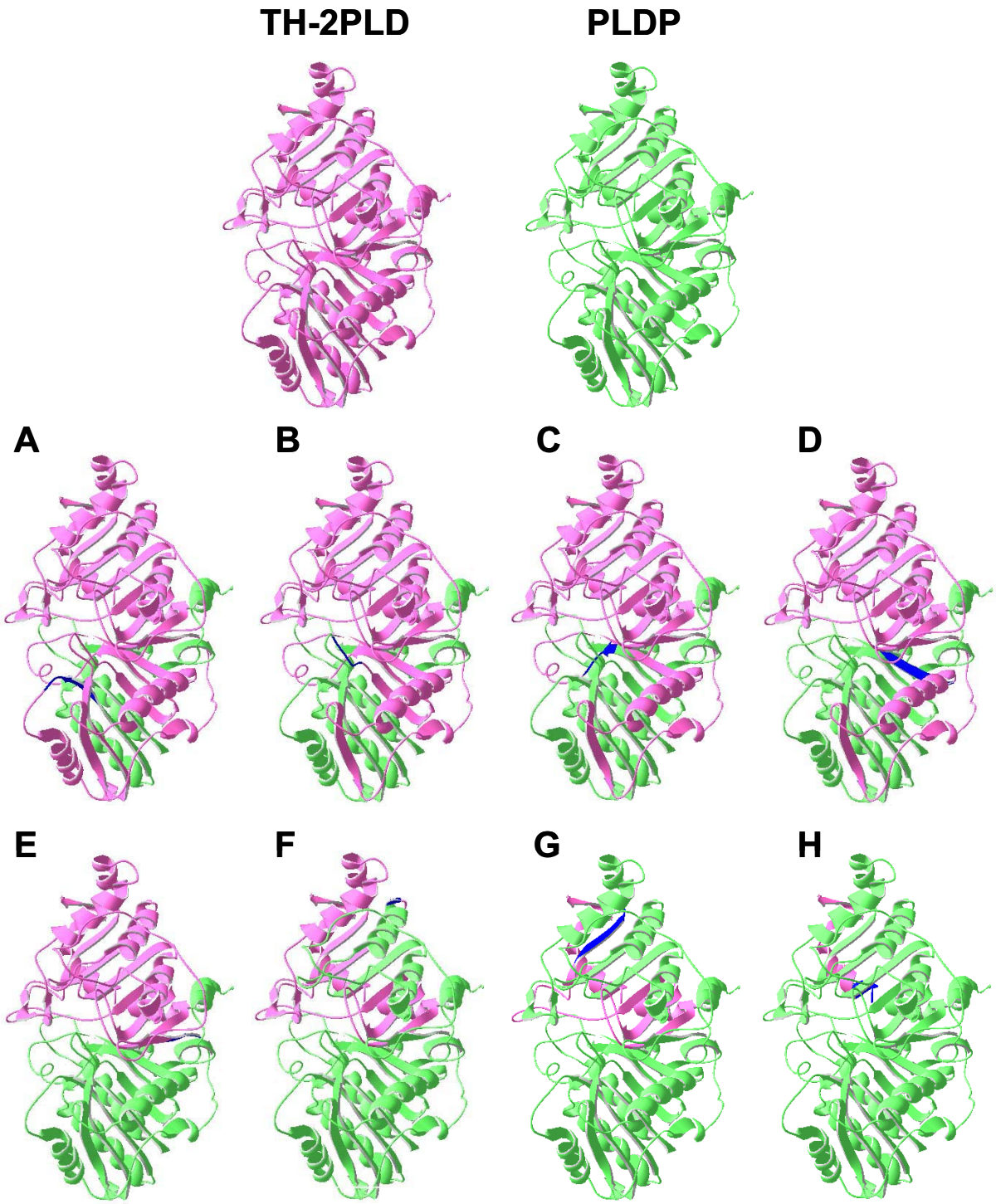

Figure 9. The tertiaty structure of TH-2PLD, PLDP and chimeras A to H. Recombination sites are indicated in blue, respectively.

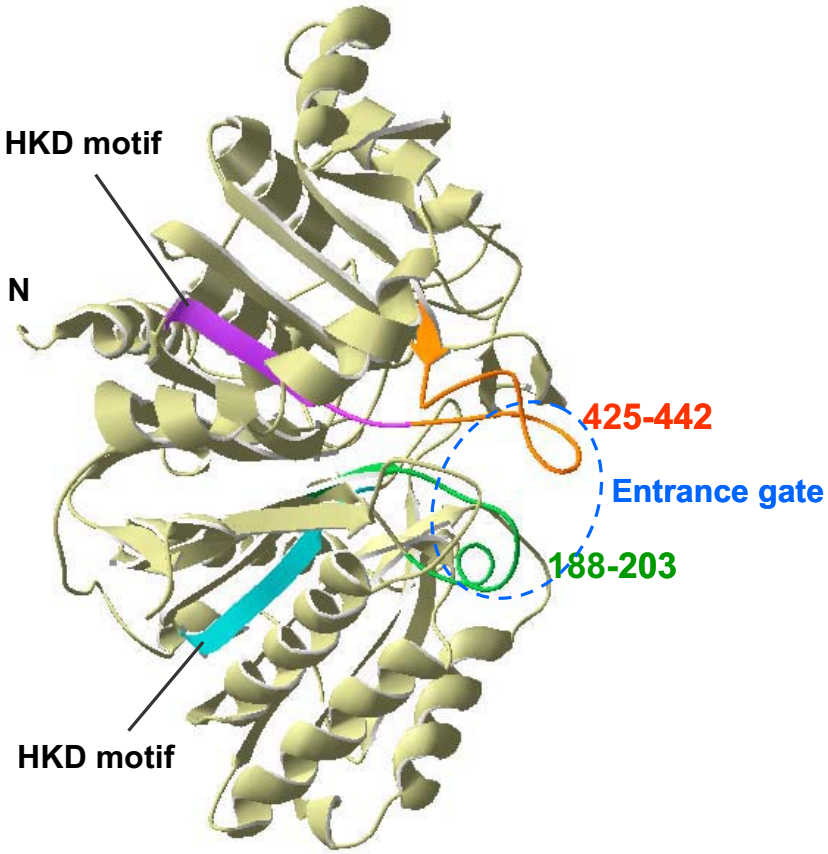

Figure 10. The three-dimensional structure around the regions related to activities. Overall structure of TH-2PLD is shown using the Swiss-pdb viewer on the basis of the crystal structure of PMFPLD. The two regions related to activities are indicated in green (residues 188-203 of TH-2PLD) and orange (residues 425-442 of TH-2PLD). The N-terminal and C-terminal HKD motifs are shown in light blue and purple, respectively.

CHAPTER 3

IDENTIFICATION OF THE KEY AMINO ACID RESIDUES RELATED TO ACTIVITIES OF PHOSPHOLIPASE D

1. Introduction

PLD-catalyzed reactions are beset by several unique problems. The reactions depend on the chemical and physical characteristics of the phospholipids in the reaction systems.

In the hydrolysis reaction, phospholipids exist in many different aggregated forms because of its insolubility in water (Reynolds *et al*., 1991). Synthetic short-chain phospholipids and lysophospholipids either exist as monomers or micelles. At lower concentrations below the critical micelle concentration (CMC), they exist as monomeric state, while they form micelles above the CMC. As the length of a fatty acid chain longer, the CMC of a particular phospholipids to be decreased. For example, dihexanoyl-PC has a CMC of about 14 mM whereas diheptanoyl-PC has a CMC of about 1.5 mM (Bian & Roberts, 1992). Phospholipids with long fatty acid chains do not readily form micelles, but they are soluble into mixed micelles with detergents (Lichtenberg *et al*., 1983). The uncharged detergent, Triton X-100, has been widely used for this purpose (Dennis, 1973). Long-chain phospholipids also form vesicles. The vesicles consist of small unilamellar, large unilamellar, or multilamellar forms. These structures have the bilayer organization and can serve as the models of biological membrane. The packing and conformation of phospholipids in the bilayer membranes are highly dependent on the chemical and physical characteristics of the phospholipids used and on its thermotropic phase transition.

In the transphosphatidylation assay of PLDs, it is usually performed in two-phase systems consisting of water and an organic solvent. In this system, phospholipids are only presented in an organic phase. On the other hand, enzymes and nucleophile substrates are only at an

aqueous phase. The reaction is assumed to take place at the inter-phase of the organic and aqueous phases. In the previous kinetic studies about PLDs, most reactions were carried out in the emulsion systems (Hirche *et al*. 1997, Hagishita *et al*. 1999). Thus, the physical state of the substrates in the transphosphatidylation reaction is different from that of in the hydrolysis reaction.

The transphosphatidylation activity of PLDs is expected to be a powerful tool for the synthesis of various phospholipids employed in many biological and industrial processes. The selectivity of transphosphatidylation depends on the production of phosphatidic acid (PA), which is a side-reaction product during the hydrolysis of phospholipids. The reaction selectivity is an important factor especially in the industrial applications. Recently, the PA contents by the side-reaction of *Streptomyces* PLDs have been shown differ significantly during the transphosphatidylation from PC to PG (Sato *et al*., 2004). This phenomenon was considered that the synthesized PG was hydrolyzed to PA during the transphosphatidylation reaction, and suggested the reaction selectivity is different in each *Streptomyces* PLDs.

In Chapter 2, it was found that the two regions, residues 188-203 and 425-442 of TH-2PLD, are related to transphosphatidylation activity. In this chapter, the key amino acid residues relating to transphosphatidylation and hydrolysis activities were identified. The effect of the identified residues on the recognition of phospholipids and different physical state of phospholipids were also estimated using SPR analysis. Furthermore, the reaction selectivity was evaluated by measuring the amounts of the hydrolysis product PA during transphosphatidylation reaction.

2. Experimental procedures

2.1. Materials

pETKmS2 (Mishima *et al*., 1997) was kindly provided by Dr. Tsuneo Yamane, Nagoya University, Japan. Phosphatidyl-*p*-nitrophenol (PpNP) was prepared from soybean phosphatidic acid and *p*-nitrophenol according to the procedure of D'Arrigo *et al*. (D'Arrigo *et al*., 1995). 1-Palmitoyl-2-oleoyl-*sn*-glycero-3-phosphocholine (POPC) was purchased from Avanti. 1, 2-diheptanoyl-*sn*-glycero-3-phosphocholine (diC_7PC) was purchased from Sigma. All the other chemicals were of the highest purity available.

2.2. Construction of expression vectors of chimeras C and D mutants

In order to identify the amino acid residues related to activities, I constructed chimera C and D mutants by PCR amplification. To prepare the mutants (C-1, C-2, and D-GD), the following three mutagenic sense primers, where the *Hin*fI site (underlined) was substituted with a silent mutation, were synthesized, 5'-GGTG<u>G(C→A)ATC</u>AACG(G→A, Gly→Asp)CTGGAAG-3' (corresponding to the chimera C gene, nucleotide (nt) 574-594), 5'-GTG<u>G(C→A)ATC</u>AACG(G→A, Gly→Asp)CTGGAAGG(A→C, Asp→Ala)CGAC-3' (corresponding to the chimera C gene, nt 575-600), and 5'- GGTG<u>G(C→A)ATC</u>AACG(A→G, Asp→Gly)CTGGAAGG(C→A, Ala→Asp)CGAC-3' (corresponding to the chimera D gene, nt 575-600), respectively. The target mutation was introduced with the primer sets of 5'-TTGTGGTGCTGCGCGTACGGC-3' (a reverse primer, corresponding to the chimera C gene, nt 1314-1334) and each of the mutagenic primers using the GC-RICH PCR system. The partial *pldp* gene was amplified by PCR with a combination of a forward primer 5'-GCACCGAGGGCAACGCGCTGGA-3' (a forward primer, corresponding to the chimera C gene, nt 119-140) and a reverse primer (5'-CGTT<u>GAT(G→T)C</u>CACCGGTGATCACGC-3' for silent mutation of the *Hin*fI site (underlined),

corresponding to the nucleotide sequence from the chimera C gene, 563-586). The amplified DNA fragments were cloned into the T-vector pGEM-TEasy (Promega), and the resultant plasmids were confirmed by DNA sequencing. The plasmids representing C-1, C-2, and D-GD were digested with *Hin*fI and *Bam*HI. The plasmid containing *Hin*fI site was digested with *Pst*I and *Hin*fI. The fragments were ligated into the *Pst*I-*Bam*HI gap of vector pACTIS4b chimera D to construct the expression vector.

To prepare the mutants (C-3, C-4, and C-5), the following three mutagenic anti-sense primers, where the *Apa*I site (underlined) was substituted with a silent mutation, were synthesized, 5'-GGC(C → G)GGCCCGGTCAGCGCGAGGTC(GG → GA, Ala → Val)C GTC(GGT → CGA, Thr → Ser)CACCGGGTGGGAGGT(C → G, Gln → Asp)TC-3' (corresponding to the chimera D gene, nt 588-633), 5'-GGC(C → G)GGCCCGGTCAGCGCGAGGTC(GG→GA, Ala→Val)CGTC(GGT→CGA, Thr→Ser)-3' (corresponding to the chimera D gene, nt 603-633), and 5'-GGC(C → G)GGCCCGGTCAGCGCGAGGTC(GG→GA, Ala→Val)CGTC-3' (corresponding to the chimera D gene, nt 604-633) , respectively. The target mutation was introduced with the primer sets of 5'-GCACCGAGGGCAACGCGCTGGA-3' (a forward primer, corresponding to the chimera D gene, nt 119-140) and each of the mutagenic primers described above using the GC-RICH PCR system. The partial *th-2pld* gene was amplified by PCR with a combination of a forward primer (5'-ACCGG(D→G)CCCGCCGCCGGCTCCGCGGGC-3' for silent mutation of the *Apa*I site (underlined), corresponding to the nucleotide sequence from the chimera D gene, 624-648) and a reverse primer (5'-TTGTGGTGCTGCGCGTACGGC-3', corresponding to the complement of the chimera D gene, nt 1314-1334). The amplified DNA fragments were cloned into the T-vector pGEM-TEasy (Promega), and the resultant plasmids were confirmed by DNA sequencing.

The plasmids representing C-3, C-4, and C-5 were digested with *Pst*I and *Apa*I. The plasmid containing *Apa*I site was digested with *Apa*I and *Aat*II. The fragments were ligated into the *Pst*I-*Aat*II gap of vector pACTIS4b chimera D to construct the expression vector.

2.3. Construction of inactive mutants (C(H170A), C(H443A), C-2(H170A) and C-2(H443A)

To investigate the effect of the identified residues on the recognition of phospholipids, independent of the two HKD motifs that are essential for catalysis, I constructed mutants in which the His170 or His443 of the N- or C-terminal HKD motifs of TH-2PLD was substituted with Ala. To prepare the mutants (C(H170A) and C-2(H170A)), the mutagenic gene was amplified by PCR with a combination of a forward primer (5'-CGACCGCTGCTGCTGGTCTGC-3', corresponding to part of the *pelB* signal sequence) and a reverse primer (5'-CCGTCGACCACCAGCAGCTTGGCG(TG → GC, His → Ala)GTTC-3' (corresponding to the *pldp* gene, nt 528-557). Then, the amplified DNA fragment was cloned, sequenced and digested with *Bst*XI and *Bam*HI. The plasmid (pUC19(*C*) or pUC19(*C-2*)) was digested with *Pst*I and *Bst*XI. The fragments were ligated into the *Pst*I-*Bam*HI gap of vector pETKmS2PLDP to construct the expression vector.

To prepare the mutants (C(H443A) and C-2(H443A)), the mutagenic gene was amplified by PCR with a combination of a forward primer (5'-CCCTGCGCGCGCTCGTCGGCA-3', corresponding to the *th-2pld* gene, 962-982) and a reverse primer (5'-ACCAGCTTGTGG(TG →GC, His→Ala)CTGCGCGTACG -3' (corresponding to the *th-2pld* gene, nt 1316-1340). Then, the amplified DNA fragment was cloned, sequenced and digested with *Bgl*II and *Van*91I. The plasmid (pUC19(*C*) or pUC19(*C-2*)) was digested with *Bgl*II and *Van*91I. The fragment was exchanged for the homologous region of the subcloned *chimera C or C-2* gene. The resultant mutant genes were digested with *Nco*I and *Bam*HI. The fragment was ligated into the *Nco*I-*Bam*HI gap of vector pETKmS2.

2.4. Construction of expression vectors of chimeras G and I mutants

In order to identify the amino acid residues related to activities, I constructed chimera G and I mutants by PCR amplification. To prepare the mutants (G-1, G-2, G-3 and G-F), the following four mutagenic sense primers, where the *Nhe*I site (underlined) was substituted with a silent mutation, were synthesized, 5'-CCTCCAGCT(C→A)GCC(A→G, Thr→Ala)CC(GC→TT, Ala→ Phe)CCG-3' (corresponding to the chimera G gene, nucleotide (nt) 1299-1319), 5'-CAGCT(C→A)GCC(A→G, Thr→Ala)CC(GC→TT, Ala→ Phe)CCG(T→C)(AGC→GCG, Ser→Ala)(T→G, Ser→Ala)CCG-3' (corresponding to the chimera G gene, nt 1303-1327), 5'-CAGCT(C→A)GCC(A→G, Thr→Ala)CC(GC→TT, Ala→ Phe)CCG(T→C)(AGC→GCG, Ser→Ala)(T→G, Ser→Ala)CC(GA→CC, Asp→Pro)CAGCGCC-3' (corresponding to the chimera G gene, nt 1303-1335), and 5'-CCTCCAGCT(C→A)GCCACC(GC→TT, Ala→phe)CCG-3' (corresponding to the chimera G gene, nt 1299-1319), respectively. The target mutation was introduced with the primer sets of 5'-TGGTGGTGGTGCTCGAGTGCGGC-3' (an anti-sense primer, corresponding to part of the *His6 tag* sequence) and each of the mutagenic primers using the GC-RICH PCR system. The partial *pldp* gene was amplified by PCR with a combination of a sense primer 5'-ATGACCACCGCCAAGACCTCC-3' (corresponding to the chimera G gene, nt 499-519) and an anti-sense primer (5'-GAAGGCGGCTAGCTGGAGGTTC-3' for silent mutation of the *Nhe*I site (underlined), corresponding to the nucleotide sequence from the chimera G gene, 1295-1317). The amplified DNA fragments were cloned into the T-vector pGEM-TEasy (Promega), and the resultant plasmids were confirmed by DNA sequencing. The plasmids representing G-1, G-2, G-3 and G-F were digested with *Nhe*I and *Bam*HI. The plasmid containing *Nhe*I site was digested with *Age*I and *Nhe*I. The fragments were ligated into the *Age*I-*Bam*HI gap of vector pETKmS2(*pldp*) to construct the expression vector.

To construct the mutant G-FH, the mutagenic gene was amplified by PCR with a combination of a sense primer 5'-CCTCCAGCT(C → A)GCCACC(GC → TT, Ala → phe)CCG-3' (corresponding to the chimera G gene, nt 1299-1319) and an anti-sense primer 5'-TGCGCGTACGG(CTT→GTG, Lys→His)GCCGTCG-3' (corresponding to the chimera G gene, nt 1344-1364). The amplified DNA fragment was cloned into the T-vector pGEM-TEasy (Promega), and the resultant plasmids were confirmed by DNA sequencing. The plasmid representing G-FH were digested with *Nhe*I and *Bsi*WI. The plasmid containing *Nhe*I site mentioned above was digested with *Age*I and *Nhe*I. The fragments were ligated into the *Age*I- *Bsi*WI gap of vector pETKmS2(*G-F*) to construct the expression vector.

To prepare the mutants (G-4, G-5, G-6 and G-H), the following four mutagenic anti-sense primers were synthesized, 5'-CGCGTACGG(GTG → CTT, His → Lys)GCCGTCGGCCCA(GG→CT, Thr→Lys)TG(TC→GC, Asp→Ala)G-3' (corresponding to the chimera I gene, nt 1332-1362), 5'-CGCGTACGG(GTG → CTT, His → Lys)GCCGTCGGCCCA(GG→CT, Thr→Lys)TGTCGCC-3' (corresponding to the chimera I gene, nt 1330-1362), 5'-TGCGCGTACGG(GTG → CTT, His → Lys)GCCGTCG-3' (corresponding to the chimera I gene, nt 1344-1364) , and 5'-TGCGCGTACGG(CTT→GTG, Lys→His)GCCGTCG-3' (corresponding to the chimera G gene, nt 1344-1364), respectively. The target mutation was introduced with the primer sets of a sense primer 5'-ATGACCACCGCCAAGACCTCC-3' (corresponding to the chimera G gene, nt 499-519) and each of the mutagenic primers described above using the GC-RICH PCR system. The amplified DNA fragments were cloned into the T-vector pGEM-TEasy (Promega), and the resultant plasmids were confirmed by DNA sequencing. The plasmids representing G-4, G-5, G-6 and G-H were digested with *Age*I and *Bsi*WI. The plasmid pUC19(*th-2pld*) was digested with *Bsi*WI and *Bam*HI. The fragments were ligated into the *Age*I-*Bam*HI gap of vector

pETKmS2(*pldp*) to construct the expression vector.

To prepare the other mutants (G-D, G-FD, G-DH and G-FDH), the following two mutagenic anti-sense primers were synthesized, 5'-CGCGTACGGCTTGCCGTCGGCCCACTTG(G→T, Ala→Asp)CGC-3' (corresponding to the chimera G gene, nt 1331-1362) for G-D and G-FD, and 5'-CGCGTACGG(CTT→GTG, Lys →His)GCCGTCGGCCCACTTG(G→T, Ala→Asp)CGC-3' (corresponding to the chimera G gene, nt 1331-1362) for G-DH and G-FDH. Using the GC-RICH PCR system, the target mutation was introduced with the primer sets of a sense primer 5'-CGTCGGCATCCAGAGCGTCGA-3' (corresponding to the chimera G gene, nt 846-866) and each of the mutagenic primers described above with pATIS4b(*G*), pETKmS2(*G-F*), pETKmS2(*G-H*) and pETKmS2(*G-FH*) as template for G-D, G-FD, G-DH and G-FDH, respectively. The amplified DNA fragments were cloned into the T-vector pGEM-TEasy (Promega), and the resultant plasmids were confirmed by DNA sequencing. The plasmids representing G-D, G-FD, G-DH and G-FDH were digested with *Eco*O109I and *Bsi*WI. The plasmid pUC19(*pldp*) was digested with *Pst*I and *Eco*O109I. The fragments were ligated into the *Pst*I-*Bsi*WI gap of vector pETKmS2(*G-F*) to construct the expression vector.

2.5. Expression and purification of PLDs

E. coli BL21-Gold(DE3) (Invitrogen) was transformed with PLD expression plasmids. Expression was carried out according to a method described previously (Hatanaka *et al*., 2002) in the presence of appropriate antibiotics (chloramphenicol (50 μg/ml) and kanamycin (50 μg/ml) for strains harboring plasmids obtained from the random chimeragenesis and plasmids derived from pETKmS2, respectively) except for the addition of premixed protease inhibitor tablet Complete^{TM}, Mini, EDTA-free (Roche) at the induction period (one tablet per culture). Cultures were centrifuged for 60 min at 3,500 × g. The culture broth was

concentrated with an ultrafiltration device using Amicon Ultra (Millipore, 30 kd cut), and dialyzed against 20 mM Tris-HCl (pH 8.0). His-tagged PLDs were purified using Magextractor-His Tag (TOYOBO). The purified PLDs were dialyzed against 10 mM acetate buffer (pH 5.5).

2.6. Gel electrophoresis of proteins

SDS-PAGE was performed by the method of Laemmli (Laemmli *et al*., 1970) using a 15% acrylamide gel. Proteins on the gels were stained with Coomassie brilliant blue R-250 (Bio-RAD) and destained with water.

2.7. Circular dichroism (*CD) spectroscopy*

The secondary structures of PLDs were determined by CD spectroscopy using a J-720WI spectrometer (Jasco). Proteins were dissolved to a final concentration of 0.1 mg/ml in 10 mM potassium phosphate buffer (pH 7.0). Spectra were acquired at 25°C using a 2-mm cuvette. Molar ellipticities (per residue) were calculated using the equation $[\theta] = 100(\theta) / (lcN)$, where $[\theta]$ is the molar ellipticity per residue, (θ) is the observed ellipticity in degrees, l is the optical path length in centimeters, c is the molar concentration of the protein, and N is the number of residues in the protein.

2.8. Assay for PLD activities using PpNP

Hydrolytic activity was determined based on the hydrolytic activity of PpNP. The procedure was similar to the method described previously (Hatanaka *et al*., 2002a). PLD-catalyzed transphosphatidylation activity was determined by measuring the production of *p*-nitro-phenol from PpNP and ethanol according to the method that used a biphasic system consisting of benzene and water as described previously (Hatanaka *et al*., 2002a). One unit of

PLD was defined as the amount of the enzyme that released 1 μmol of *p*-nitro-phenol per minute under the assay conditions. PLDs used in this study showed both hydrolysis and transphosphatidylation activities in the absence of Ca^{2+}. The kinetic assays for both activities were carried out as described previously (Hatanaka *et al*., 2002a). In the assay of hydrolytic activity, the reactions were carried out in 1.5-ml cuvettes; the 1-ml reaction mixture consisted of PpNP at final concentrations ranging from 0.11 to 2 mM in 0.1 M acetate buffer (pH 5.5) and the purified PLDs. In the assay for transphosphatidylation activity, the reactions were performed for 10 min in 1.5-ml sample tubes; the 400-μl reaction mixture consisted of PpNP at a final concentrations ranging from 1.8 mM to 20 mM, and ethanol at final concentration of 800 mM, in an emulsion containing benzene and acetate buffer (pH 5.5). The purified PLDs (200 ng) were used in the assay.

2.9. Thin-layer chromatography (TLC)

Another enzyme assay for PLD-catalyzed transphosphatidylation was performed by TLC using 10 mM PpNP, POPC or diC_7PC as the substrate. The reaction conditions were similar to those mentioned above except for the use of acetate buffer (pH 5.5) containing 4 mM $CaCl_2$. After centrifugation, the organic layer of the reaction mixture was applied to a TLC plate (Silica gel 60 F_{254}, Merck) and developed with chloroform : methanol : water (30 : 10 : 1, v/v). Lipids on the TLC plate were detected by spraying with 5% sodium phosphomolybdate/ethanol solution or the Dittmer-Lester reagent (Dittmer & Lester, 1964) for POPC or diC_7PC, respectively. Then, the plate was dried and scanned. The intensity of the spot corresponding to phosphatidylethanol (PEtOH) was analyzed using *Scion Image* software.

2.10. Preparation of vesicles

An appropriate aliquot of POPC dissolved in chloroform was evaporated and further dried under a vacuum for at least 3 h. The lipid was hydrated at a concentration of 10 mM in phosphate-buffered saline. Then, the lipid suspensions were vortexed vigorously and frozen and thawed 10 times in liquid nitrogen. The multilamellar vesicles (MLVs) were passed 30 times through polycarbonate membranes (50 nm pore diameter) using a Lipofast extruder (MacDonald *et al*., 1991) (Avestin), to obtain small unilamellar vesicles (SUVs).

2.11. Surface plasmon resonance (Biacore)

Real time interaction between PLD molecules and phospholipids were measured using a Biacore instrument (BIAcore 2000, Biacore AB, Uppsala, Sweden). Liposomes were captured onto the surface of a Sensor Chip L1 (Biacore AB, Uppsala, Sweden). The surface of the L1 sensor chip was first cleaned with 20 mM CHAPS at a flow rate of 5 μl/min followed by the injection of SUVs (60 μl, 0.5 mM lipid concentration) at a flow rate of 2 μl/min in buffer A (10 mM sodium acetate, pH 5.5, 4 mM $CaCl_2$) which resulted in the deposition of approximately 7000-8000 resonance units. To measure the association of PLDs with lipids, purified chimera C or C-2 (79-266 nM diluted in buffer A) was applied to the captured SUVs at a flow rate of 20 μl/min. After binding of PLDs to phospholipids, the dissociation process was observed at the same flow rate for 10 min. The evaluation of the kinetic parameters for PLD binding to lipids was performed by nonlinear fitting of binding data using the BIA evaluation 4.1 analysis software. The apparent association (k_a) and dissociation (k_d) rate constants were evaluated from the differential binding curves (sample-control) as shown in Fig. 6 assuming an A + B = AB association type for the protein-lipid interaction. The affinity constant K_D was calculated from the equation $K_D = k_d / k_a$.

2.12. Transphosphatidylation from PC to PG by PLDs

The progress of the PLD-catalyzed transphosphatidylation from PC to PG was monitored on a TLC. The reaction conditions were similar to those mentioned above using 10 mM POPC except for the use of acetate buffer (pH 5.5) containing 0.5 M glycerol and 4 mM $CaCl_2$. After centrifugation, the organic layer of the reaction mixture was applied to a TLC plate (Silica gel 60 F_{254}, Merck) and developed with chloroform : methanol : acetic acid (70 : 30 : 8, v/v). Lipids on the TLC plate were detected by spraying with 5% sodium phosphomolybdate/ethanol solution. Then, the plate was dried and scanned. The intensity of the spot corresponding to PA, PG and PC were analyzed using *Scion Image* software.

2.13. Statistical analysis

All statistical evaluations were performed by an unpaired Student's *t* test or analysis of variance (ANOVA). All data are presented as means ± standard deviations of at least three determinations.

3. Results

3.1. N-terminal region (residues 188-203 of TH-2PLD)

3.1.1. Preparation of chimeric PLDs and mutant

In Chapter 2, by comparing the activities of chimeras, the transphosphatidylation activity of chimera C was significantly different from that of chimera D, despite these two chimeras exhibiting equivalent hydrolytic activity. In the primary structure, chimera C differed from chimera D in six residues (Fig. 1A). This suggests that some of these residues are related to the difference in activities. Therefore, I constructed five chimera C mutants (from C-1 to C-5, the primary sequence of which is presented in Fig. 1A, and expressed the genes and purified the protein products. Fig. 1B showed the SDS-PAGE profiles of purified chimeric PLDs and mutant. PLDs indicated mostly a single band at the same molecular weight (approximately 57 kDa) position. CD spectra of chimeras C and D mutants were measured and used to check for overall structure of them. A large change might not be expected in secondary structure (Fig. 2).

3.1.2. Identification of amino acid residues related to activities

I estimated activities of purified PLDs using PpNP, and compared their specific activities. The transphosphatidylation activity of each chimera C mutant was considerably decreased in comparison to their hydrolytic activity (Fig. 3). This result suggests that Gly188 contributes to the increase in transphosphatidylation activity. It should be noted that mutant C-2 had the lowest transphosphatidylation activity, while it had the highest hydrolytic activity among these mutants. Chimeras C and C-2 differed in two amino acid residues, residues 188 and 191. From these results, I assumed that Gly188 and Asp191 of TH-2PLD were related to the transphosphatidylation activity. Furthermore, I constructed chimera D mutant, in which these two residues were substituted (D-GD) (Fig. 1A). The transphosphatidylation activity of D-GD

was 3-fold higher than that of chimera D (Fig. 3). This result supported the assumption that Gly188 and Asp191 of TH-2PLD were key amino acid residues related to the transphosphatidylation activity.

3.1.3. The kinetic analysis of PLD activities

The effect of the PpNP concentration on the transphosphatidylation and hydrolytic activities of PLDs is shown in Fig. 4. In the transphosphatidylation activity assay, the reaction velocities of chimera C and TH-2 rose with the increase in PpNP concentration (Fig. 4A). These two enzymes exhibited similar K_m and k_{cat} values (Table 1). On the other hand, the reaction velocity of chimera C-2 slightly increased at low PpNP concentration, but decreased at high concentration. The K_m and k_{cat} values of chimera C-2 were a tenth and a sixth of those of chimera C, respectively. Inversely, the reaction velocity of chimera C-2 was higher than that of C for all concentrations of PpNP in the hydrolysis reaction (Fig. 4B). The K_m value of C-2 was lower than that of C, and the k_{cat} value was the highest.

3.1.4. Transphosphatidylation activity of PLDs toward natural substrate

Natural substrates such as POPC have polar heads with properties different from those of PpNP, although POPC and PpNP similarly have a long chain of fatty acids. To evaluate the transphosphatidylation activity of chimeras C and C-2 toward natural substrates, I carried out TLC using POPC (Fig. 5). In comparison with synthesized PEtOH, chimera C converted PC to PEtOH approximately 6-fold higher than chimera C-2 (*t* test; $P < 0.001$). On the other hand, chimera C converted PC to PEtOH approximately 10-fold higher than chimera C-2 (*t* test; $P < 0.0001$) in the presence of PpNP and this result corresponded to that shown in Fig. 3. These results suggest that chimeras catalyze the conversion of natural substrates that is comparable to that of synthetic substrate.

3.1.5. The surface plasmon resonance (SPR) analysis of PLDs

To estimate the effect of the identified residues on the association with natural substrates, I analyzed the binding profiles of C and C-2 on POPC vesicles using surface plasmon spectroscopy (Biacore). Overlaid sensorgrams (Fig. 6A) of chimeras C and C-2 at 178 nM binding to different particle sizes of POPC (SUVs and MLVs) were obtained when chimeras were passed over the immobilized POPC vesicles at a flow rate of 20 μl/min. The maximal responses measured for PLD associations with POPC are shown in Fig. 6B. Chimera C exhibited significant interaction with the SUVs of POPC when compared with chimera C-2 (*t* test; $P < 0.05$), while there was no significant difference between C and C-2 with MLVs of POPC (*t* test; $P > 0.05$). Therefore, I carried out SPR analysis with SUVs of POPC.

3.1.6. Interaction of PLDs and POPC vesicles

Figs. 7A and B show overlaid sensorgrams demonstrating the interactions between captured POPC vesicles and different concentrations of chimeras C and C-2 (from 266 nM to 79 nM). The associations of chimeras C and C-2 with POPC vesicles are summarized in Fig. 7C. For both chimeras C and C-2, the association increased in a dose-dependent manner. Chimera C showed a significantly higher interaction rate than that of C-2 at all concentrations (ANOVA; $P < 0.0001 – 0.01$). The values of k_a, k_d, and affinity constant K_D were calculated from each sensorgram, and the averages of each parameter representing the kinetic parameters of chimeras C and C-2 are shown in Table 2. The association rate constants (k_a) were 2.97×10^5 M^{-1} s^{-1} and 2.82×10^4 M^{-1} s^{-1} for chimeras C and C-2, respectively. The dissociation rate constants (k_d) were 5.56×10^{-5} s^{-1} and 1.80×10^{-4} s^{-1} for chimeras C and C-2, leading to affinity constants (K_D values) of 2.04×10^{-10} and 1.47×10^{-8} M, respectively. The affinity constant of chimera C was lower than that of C-2 by 2 orders of magnitude. Hence, chimera C bound to POPC with high affinity compared to C-2.

3.1.7. Preparation of chimeras C and C-2 mutants

To investigate the effect of the identified residues on the recognition of phospholipids, independent of the two HKD motifs that are essential for catalysis, I constructed mutants in which the His170 or His443 of the N- or C-terminal HKD motifs of TH-2PLD was substituted with Ala. Preparation of these inactive mutants were carried out similarly as mentioned above. The purified mutants showed a single band at the same molecular weight position as chimeras C and C-2 on SDS-PAGE (Fig. 8A). Furthermore, upon Western blot analysis using anti-wild-type TH-2PLD antibody, these mutants and chimeras C and C-2 demonstrated similar results. To confirm the folding of chimeras C, C-2 and their inactive mutants (C(H170A), C(H443A), C-2(H170 A), and C-2(H443A)), their CD spectra were measured. As shown in Fig. 8B and C, a large change might not be expected in secondary structure. Chimeras C and C-2 had high activities (Fig. 3), while each of the inactive mutants had no detectable activity. These results suggested that inactive mutant enzymes were successfully prepared, and therefore SPR analysis were carried out using these PLDs.

3.1.8. Comparison of affinities of inactive mutants toward POPC vesicles

To compare the association of the inactive mutants toward POPC vesicles, the binding profiles were analyzed by surface plasmon spectroscopy. Overlaid sensorgrams of the mutants (C(H443A), C-2(H443A), C(H170A), and C-2(H170A)) are superimposed in Fig. 9A, and the association values are summarized in Fig. 9B. The injection of 0.79 μM C(H443A) resulted in a binding signal of 208 RU, whereas the association of C-2(H443A) was significantly ($P < 0.05$) lower (126 RU). There was no significant difference between C(H170A) and C-2(H170A). This result suggested that Gly188 and Asp191 of TH-2PLD play a role independently of the N-terminal HKD motif in reactions. Interestingly, C(H443A) bound to POPC with 2.4-fold higher affinity compared to C(H170A). In Chapter 1, a similar significant

difference in affinity was observed using inactive mutants in which the His170 or His443 of the N- or C-terminal HKD motifs of TH-2PLD was substituted with Ala. This result supported that the N-terminal HKD motif of PLD acts as the nucleophile which attacks the phosphorus atom of the substrate phospholipids.

A

PLDs		Amino acid sequence															
C	188	G	W	K	D	D	Y	V	D	T	S	H	P	V	S	D	V	203
C-1		D	W	K	D	D	Y	V	D	T	S	H	P	V	S	D	V	
C-2		D	W	K	A	D	Y	V	D	T	S	H	P	V	S	D	V	
C-3		D	W	K	A	D	Y	L	D	T	S	H	P	V	S	D	V	
C-4		D	W	K	A	D	Y	L	E	T	S	H	P	V	S	D	V	
C-5		D	W	K	A	D	Y	L	E	T	S	H	P	V	T	D	V	
D		D	W	K	A	D	Y	L	E	T	S	H	P	V	T	D	A	
D-GD		G	W	K	D	D	Y	L	E	T	S	H	P	V	T	D	A	

B

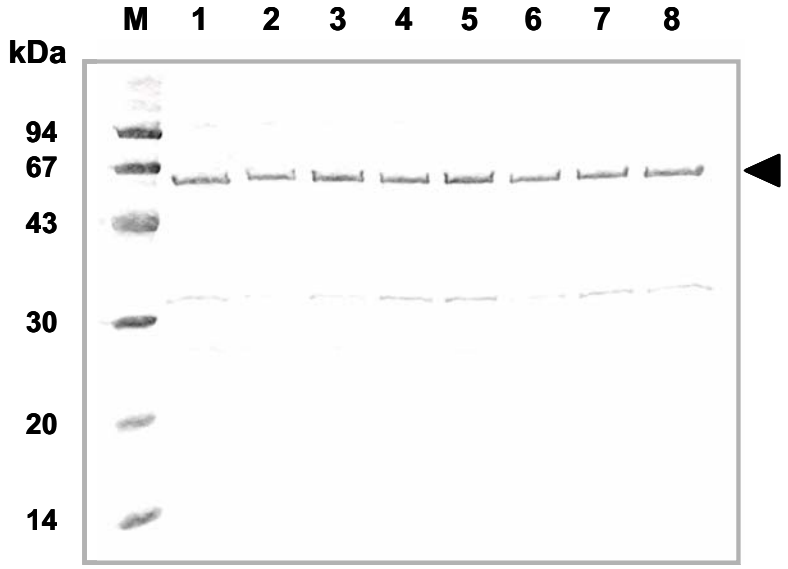

Figure 1. Preparation of chimeras C and D mutants. (A) Primary structures of chimeras C to D and mutant. (B) SDS-PAGE of purified PLDs. Lane 1 and 7 contained 1.5 μg of chimeras C and D, respectively. Lanes 2-6 contained 1.5 μg of chimeras C-1 to C-5, respectively. Lane 8 contained 1.5 μg of chimera D mutant D-GD. Lane M indicates low-molecular-weight marker proteins (molecular weights, 94,000, 67,000, 43,000, 30,000, 20,100 and 14,400). Samples were loaded on a 15% acrylamide gel. Arrow indicates the position of purified PLDs.

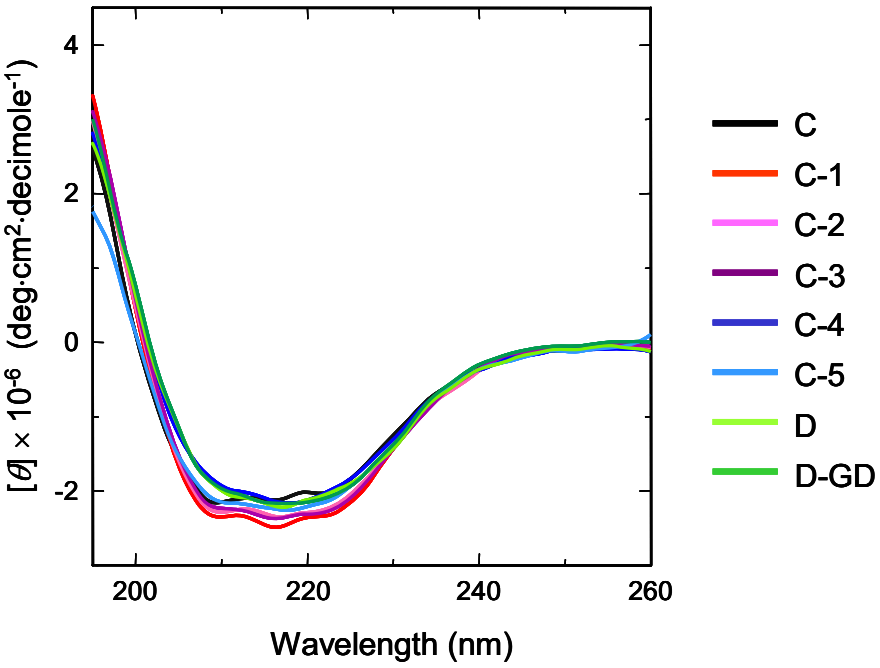

Figure 2. Circular dichroism spectra of chimeras C and D mutants. The spectrum of protein (0.1 mg/ml) in 10 mM potassium phosphate buffer (pH 7.0) was measured at 25°C.

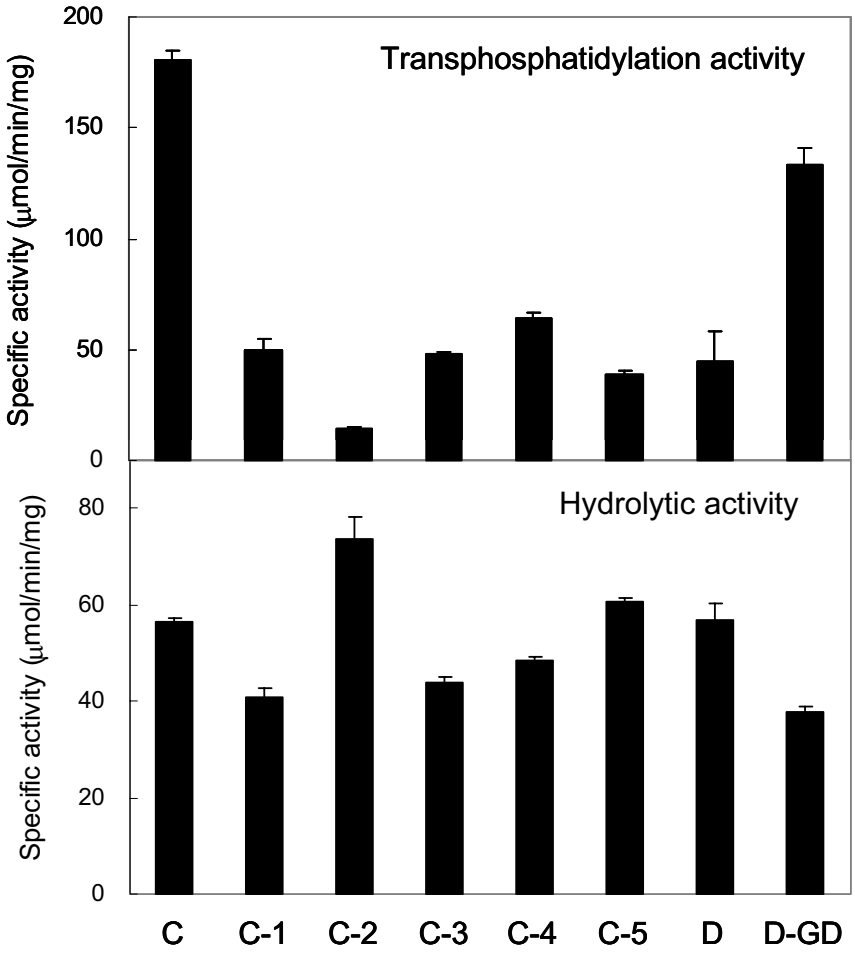

Figure 3. Identification of amino acid residues related to activities. Specific activities of chimeras C and D mutants in the transphosphatidylation reaction (upper) and hydrolytic reaction (lower). Transphosphatidylation activities were measured at pH 5.5 with 13 mM PpNP. Hydrolytic activities were determined at pH 5.5 with 2 mM PpNP. Data are expressed as means ± SD of three independent experiments.

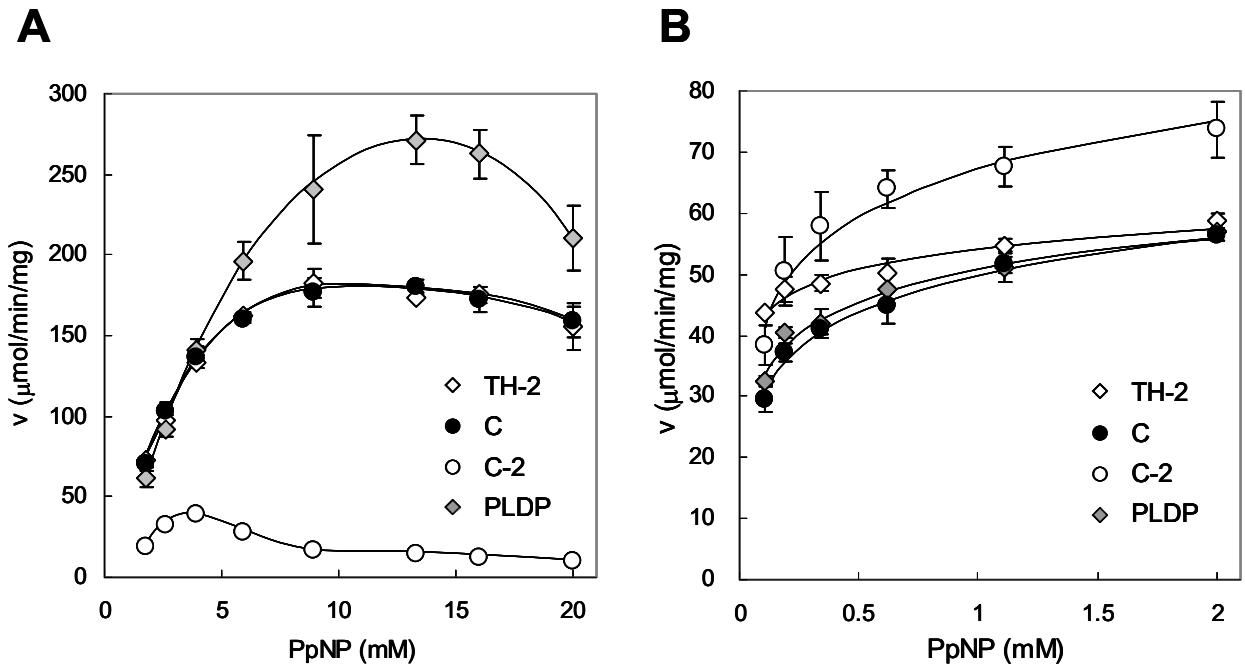

Figure 4. Effects of substrate concentration on transphosphatidylation (A) and hydrolytic (B) activities of PLDs. Enzyme activities were assayed by standard conditions described under Experimental Procedures, except that PpNP was used at the indicated concentrations. The reaction velocity (v) was expressed as mmol *p*-nitrophenol released min^{-1} mg $enzyme^{-1}$.

Table 1 Kinetic parameters of the transphosphatidylation and hydrolysis activities of PLDs toward PpNP

	K_m (mM)	k_{cat} (s^{-1})
Transphosphatidylation [a]		
TH-2	1.16 ± 0.52	174.8 ± 12.3
C	1.54 ± 0.19	179.3 ± 6.2
C-2	0.13 ± 0.08	33.3 ± 4.5
PLDP	4.92 ± 0.55	326.0 ± 7.0
Hydrolysis [b]		
TH-2	0.075 ± 0.020	68.8 ± 1.3
C	0.147 ± 0.018	68.3 ± 0.7
C-2	0.119 ± 0.016	88.5 ± 4.9
PLDP	0.126 ± 0.004	68.2 ± 2.2

[a] The transphosphatidylation assay of TH-2, C and PLDP was performed with 1.8 - 20 mM PpNP at pH 5.5. For C-2, transphosphatidylation assay was performed with 2.2 - 3.5 mM PpNP.
[b] The hydrolysis assay of PLDs was carried out with 0.06 - 2 mM PpNP at pH 5.5. Data are expressed as means ± SD.

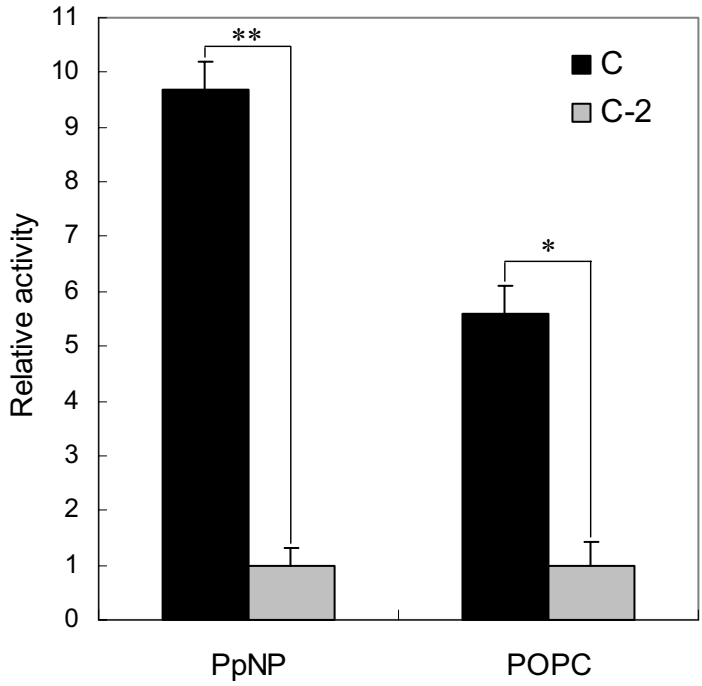

Figure 5. TLC of PLD-catalyzed transphosphatidylation. The reaction was performed for 10 min using 10 mM PpNP or POPC with 4 mM $CaCl_2$ present in acetate buffer (pH 5.5). The relative activity of PLD was then determined by measuring the intensity of the spot corresponding to phosphatidylethanol using *Scion Image* software, and indicated as chimera C-2 activity toward POPC or PpNP. The relative activity of chimera C was significantly different from that of chimera C-2 toward POPC and PpNP (∗: $P < 0.001$, ∗∗: $P < 0.0001$, calculated by *t* test).

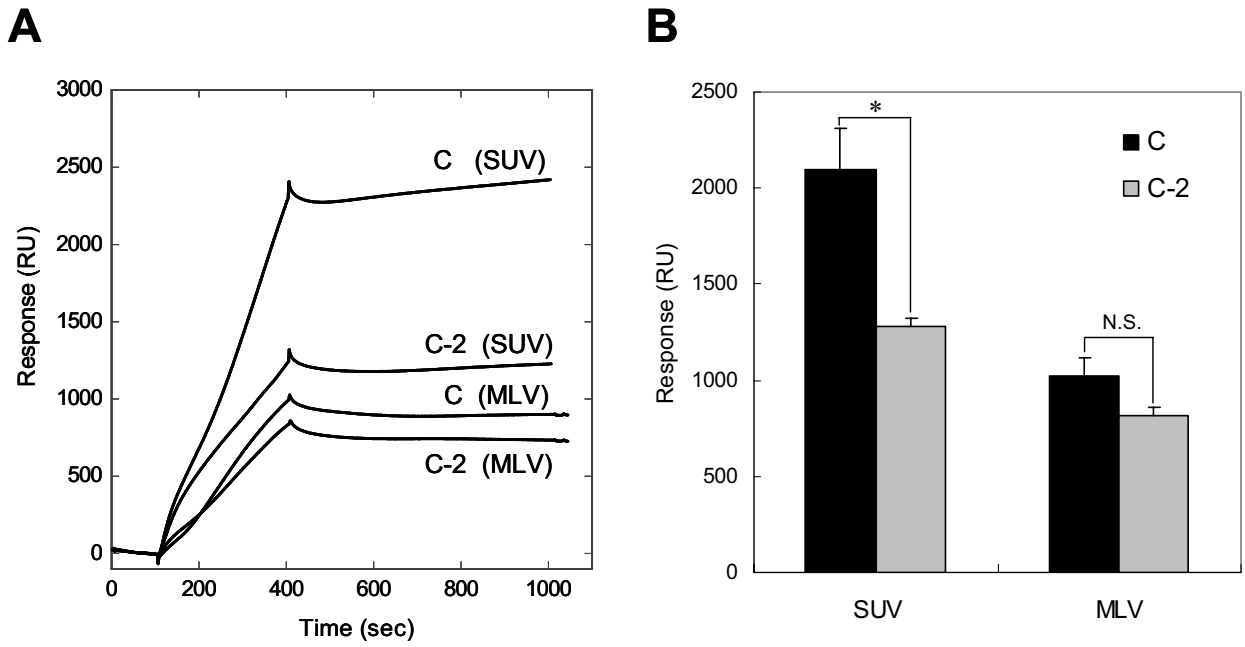

Figure 6. Quantitative biosensor analysis of PLD interactions with different sized POPC vesicles. (A) Overlay plots of chimeras C and C-2 at 178 nM binding to POPC vesicles (SUV and MLV) obtained when C or C-2 were passed over the POPC vesicles immobilized on a sensor chip L1 at a flow rate of 20 μl/min. (B) The *bar graph* represents the maximal responses measured for specific PLD associations with POPC (SUVs and MLVs). Each value represents the mean ± SD from three independent experiments. Chimera C induced significant interaction with POPC vesicles (SUVs) when compared with chimera C-2 (∗: $P < 0.05$, calculated by *t* test). There was no significant difference between chimera C and C-2 with MLVs of POPC (N.S.: $P > 0.05$, calculated by *t* test).

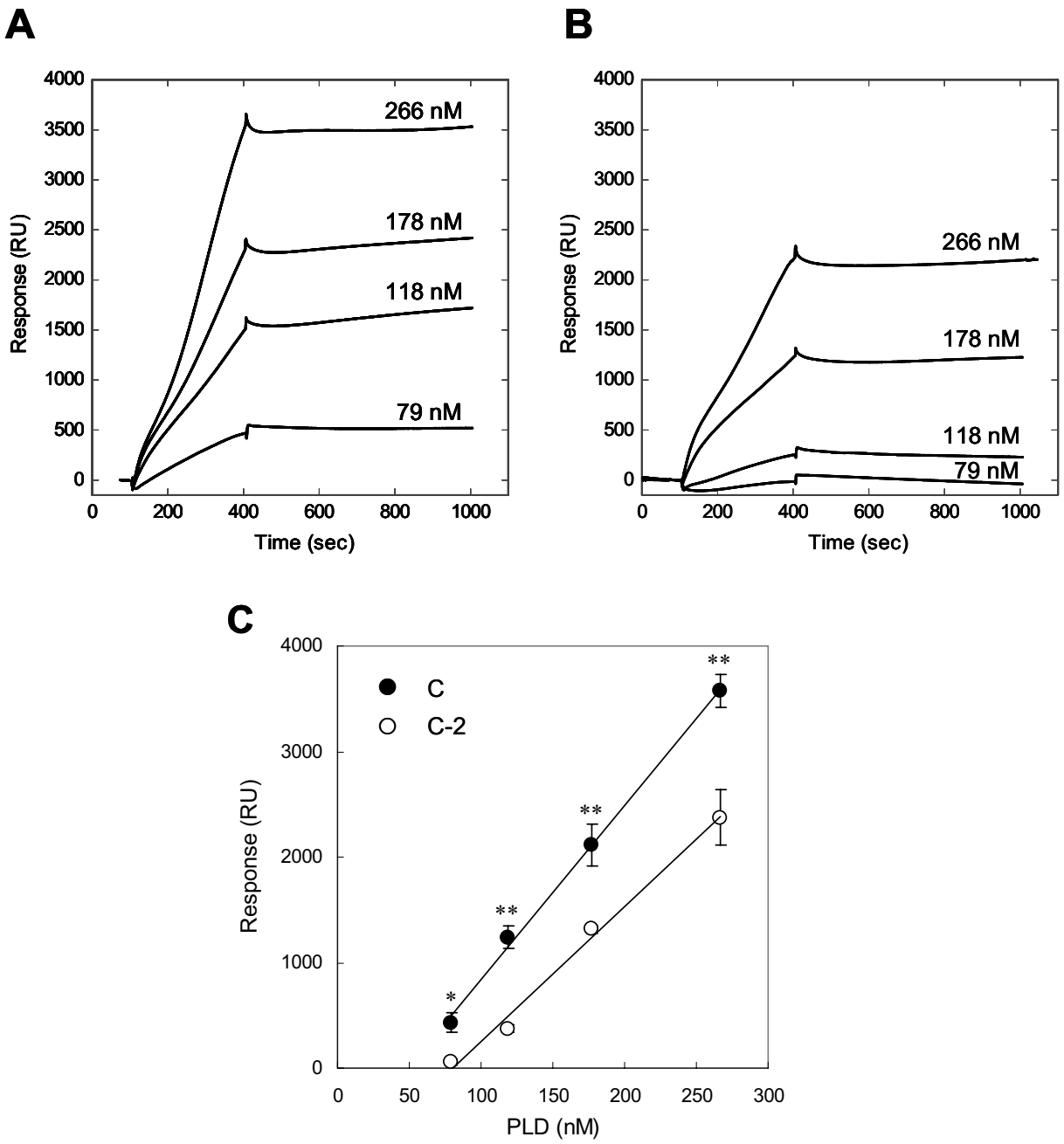

Figure 7. Interaction of PLDs and POPC vesicles. Sensorgrams with different concentrations (266 nM, 178 nM, 118 nM and 79 nM, from top to bottom) of chimera C (A) and chimera C-2 (B) are shown. (C) The values of maximal responses measured for PLD interactions with POPC vesicles were obtained from sensorgrams of chimeras C (A) and C-2 (B). Each value represents the mean ± SD from three independent experiments. Chimera C induced significant interaction with POPC vesicles when compared with chimera C-2 (*: $P < 0.01$, **: $P < 0.0001$, calculated by ANOVA).

Table 2 Kinetic parameters for interactions of chimeras C and C-2 toward POPC vesicles

	k_a (1/Ms)	k_d (1/s)	K_D (M) [a]
C	2.97×10^{5}	5.56×10^{-5}	2.04×10^{-10}
C-2	2.82×10^{4}	1.80×10^{-4}	1.47×10^{-8}

[a] Apparent affinity constants K_D were calculated from k_d/k_a.

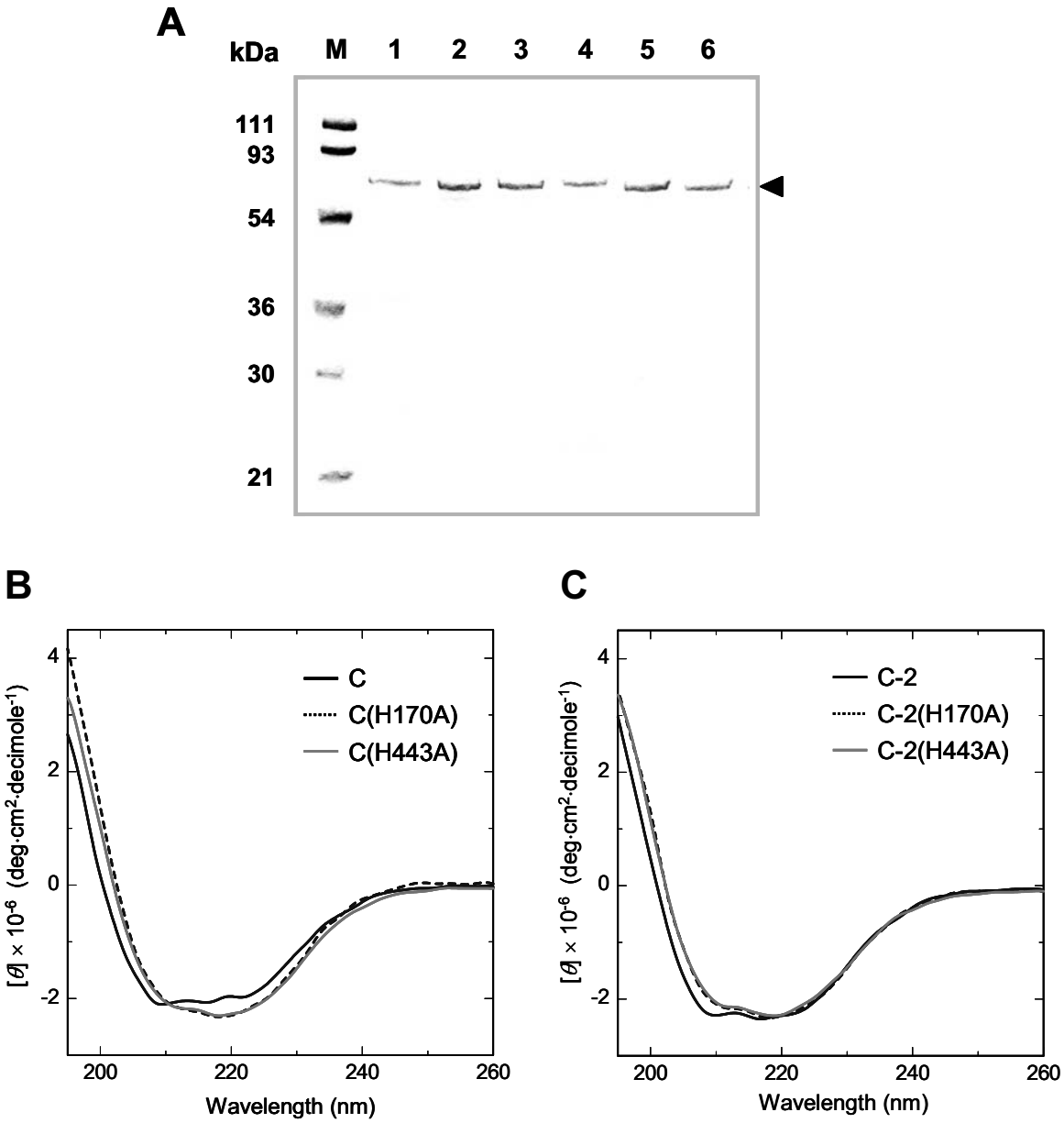

Figure 8. Preparation of chimeras C and C-2 mutants. (A) SDS-PAGE of purified chimeras C, C-2 and their mutants. Lane 1 contained 1.5 μg of chimera C. Lanes 2 and 3 contained 1.5 μg of C(H170A) and C(H443A), respectively. Lane 4 contained 1.5 μg of chimera C-2. Lanes 5 and 6 contained 1.5 μg of C-2(H170A) and C-2(H443A), respectively. Lane M indicates SDS-PAGE standard proteins (molecular weights, 111,000, 93,000, 53,500, 36,100, 29,500 and 21,300). Samples were loaded on a 15% acrylamide gel. Arrow indicates the position of purified PLDs. CD spectra of chimera C and its mutants (B), and chimera C-2 and its mutants (C) were shown. The spectrum of protein (0.1 mg/ml) in 10 mM potassium phosphate buffer (pH 7.0) was measured at 25°C.

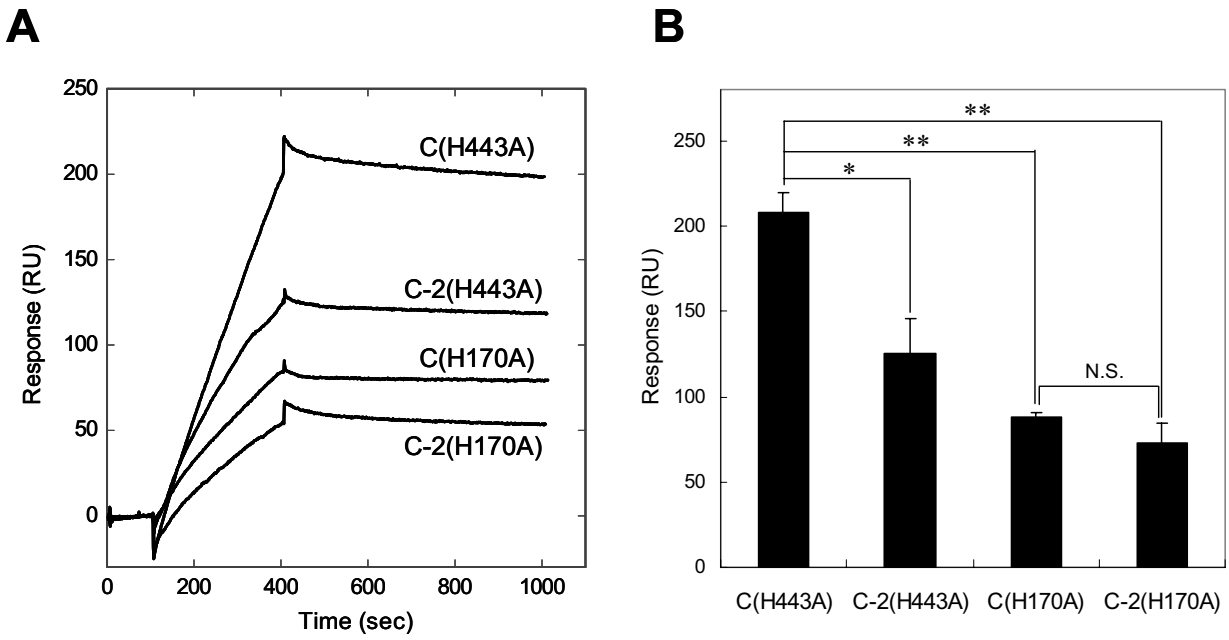

Figure 9. Difference in affinity among chimeras C and C-2 inactive mutants. (A) Sensorgrams of the mutants (C(H443A), C-2(H443A), C(H170A), and C-2(H170A)) were superimposed to facilitate comparison. Each mutant (0.79 μM) was injected at a flow rate of 20 μl/min. (B) The *bar graph* represents the maximal responses measured for specific PLD associations with POPC. Each value represents the mean ± SD from three independent experiments. C(H443A) induced significant interaction with POPC vesicles when compared with the other mutants (∗: $P < 0.05$, ∗∗: $P < 0.01$, calculated by *t* test). There was no significant difference between C(H170A) and C-2(H170A) (N.S.: $P > 0.05$, calculated by *t* test).

3.2. C-terminal region (residues 425-442 of TH-2PLD)

3.2.1. Preparation of chimeric PLDs

As shown in Fig. 10A, chimera G differed from chimera I in ten residues in the primary structure. This suggests that some of these residues are related to the difference in activities. Therefore, I constructed six chimera G mutants (from G-1 to G-6, the primary sequence of which is presented in Fig. 10A), and expressed the genes and purified the protein products. The purified chimeric PLDs showed mostly a single band at the same molecular weight position (Fig. 10B). CD spectra of chimeras G to I were measured and used to check for overall structure. A large change might not be expected in secondary structure (Fig. 11).

3.2.2. Comparison of activities for chimeras G to I

The purified chimeric PLDs were compared in the transphosphatidylation and hydrolysis activities (Fig. 12). By comparing specific activities of chimeric PLDs, large differences in the transphosphatidylation activities were observed than those in the hydrolysis activities. Interestingly, the transphosphatidylation activities of chimeras G-3 and G-4 were similar to that of chimera G, although those of chimeras G-1, G-2, G-5 and G-6 were higher than that of chimera G. Thus, I focused on the different amino acid residues between chimeras G and G-1, chimeras G-4 and G-5, and chimeras G-6 and I, respectively (Fig. 10A). Comparing each set of mutants, it was suggested that three amino acid residues, Ala426, Ala432 and Lys438 of TH-2PLD, are related to the transphosphatidylation activity.

3.2.3. Identification of amino acid residues relating to activities

To determine the contribution of Ala426, Ala432 and Lys438 in transphosphatidylation and hydrolysis activities, I constructed seven chimera G mutants that had a substitution of one, two or three of the candidate residues from the chimera G type to the chimera I type. Their

primary sequences are presented in Fig. 13A. These mutants were expressed and purified similarly as mentioned above. The purified mutant PLDs showed mostly a single band at the same molecular weight position as chimeras G and I (Fig. 13B).

To confirm the folding of chimera G mutants, their CD spectra were measured. As shown in Fig. 14, a large change might not be expected in secondary structure.

The purified chimera G mutants were evaluated in the transphosphatidylation and hydrolysis activities (Fig. 15). By comparison of specific activities among single-substitutions, mutant G-F exhibited the highest activity in the transphosphatidylation reaction. Among double-substitutions examined, each mutant showed significantly higher activity than chimera G (*t* test; $P < 0.0001$). In particular, mutant G-FH had 2.5-fold and 2-fold higher activity than chimera G in transphosphatidylation and hydrolysis reactions, respectively. The transphosphatidylation and hydrolysis activities of triple-substitution G-FDH were similar to those of mutant G-FH. Chimera G and mutant G-FH differed in two amino acid residues, residues 426 and 438. From these results, I assumed that Ala426 and Lys438 of TH-2PLD were key amino acid residues relating to the activities.

3.2.4. The kinetic analysis of PLD activities

Fig. 16 shows the effect of the substrate concentration on the transphosphatidylation and hydrolytic activities of PLDs. In the transphosphatidylation activity assay toward PpNP, the reaction velocities of chimera G and mutant G-FH rose with the increase in PpNP concentration, and that of chimera G reached the plateau above 5 mM (Fig. 16A). The K_m value of chimera G was lower than that of mutant G-FH by 1 order of magnitude (Table 3). The k_{cat} value of mutant G-FH was 3-fold higher than that of chimera G. As shown in Fig. 16B, both of the reaction velocities of chimera G and mutant G-FH rose with the increase in EtOH concentration, but decreased above 0.8 M. These enzymes exhibited similar K_m value toward

EtOH (Table 3). On the other hand, in the hydrolysis activity assay toward PpNP, the reaction velocities of chimera G and mutant G-FH rose with the increase in PpNP concentration (Fig. 16C). As shown in Table 3, these enzymes exhibited similar K_m value. The k_{cat} value of mutant G-FH was 2-fold higher than that of chimera G.

3.2.5. Transphosphatidylation activity of PLDs toward phosphatidylcholine

To evaluate the transphosphatidylation activity of chimeras G and mutant G-FH toward phosphatidylcholine, I carried out TLC using POPC (Fig. 17). In comparison with synthesized PEtOH, mutant G-FH converted PC to PEtOH approximately 2-fold higher than chimera G (*t* test; $P < 0.001$). Furthermore, I examined activity of PLDs toward short-chain phospholipid. For diC_7PC, mutant G-FH also converted PC to PEtOH 1.7-fold higher than chimera G (*t* test; $P < 0.01$). These results suggest that difference of the activities of chimera G and mutant G-FH was independent of the length of fatty acid chains.

3.2.6. Estimation of PA-production in transphosphatidylation reaction

I analyzed the amount of the hydrolysis product, PA, during transphosphatidylation reaction catalyzed by chimera G and mutant G-FH by TLC. The relative contents of the reaction products determined with chimera G and mutant G-FH was shown in Fig. 18. After 10 min of reaction, mutant G-FH converted PC to PG 1.7-fold higher than chimera G. With mutant G-FH, the relative contents of PG was 33.4% after 10 min, and increased as the reaction time elapsed, most of the PC was transformed into PG after 3 h of reaction (Fig. 18B). On the other hand, PG contents of chimera G were lower than that of mutant G-FH over a reaction time from 10 min to 6 h (Fig. 18A). Inversely, PA content of chimera G was 3.7-fold higher than that of mutant G-FH after 6 h of reaction. The PA content of chimera G was 16.6%, and similar to that of TH-2PLD (20.5%). These results suggested mutant G-FH has not only

higher activities but also higher selectivity on the transphosphatidylation activity than those of original chimera G.

A

PLDs		Amino acid sequence																	
G	425	T	A	R	S	S	D	S	A	K	W	A	D	G	K	P	Y	A	Q	442
G-1		A	F	R	S	S	D	S	A	K	W	A	D	G	K	P	Y	A	Q	
G-2		A	F	R	A	A	D	S	A	K	W	A	D	G	K	P	Y	A	Q	
G-3		A	F	R	A	A	P	S	A	K	W	A	D	G	K	P	Y	A	Q	
G-4		A	F	R	A	A	P	G	A	K	W	A	D	G	K	P	Y	A	Q	
G-5		A	F	R	A	A	P	G	D	K	W	A	D	G	K	P	Y	A	Q	
G-6		A	F	R	A	A	P	G	D	T	W	A	D	G	K	P	Y	A	Q	
I		A	F	R	A	A	P	G	D	T	W	A	D	G	H	P	Y	A	L	

B

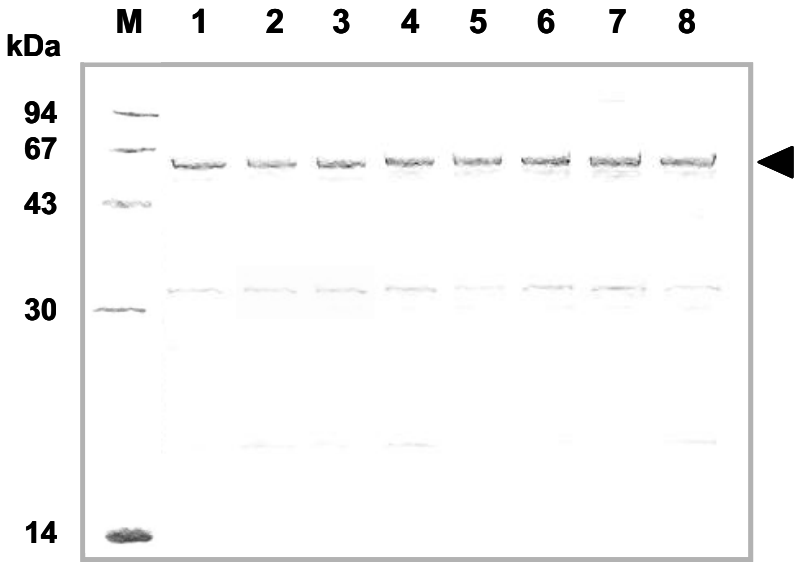

Figure 10. Preparation of chimeras G to I. (A) Primary structures of chimeras G to I. (B) SDS-PAGE of purified chimeric PLDs. Lane 1 contained 1.5 μg of chimera G. Lanes 2-7 contained 1.5 μg of chimeras G-1 to G-6, respectively. Lane 8 contained 1.5 μg of chimera I. Lane M indicates low-molecular-weight marker proteins (molecular weights, 94,000, 67,000, 43,000, 30,000, 20,100 and 14,400). Samples were loaded on a 15% acrylamide gel. Arrow indicates the position of purified PLDs.

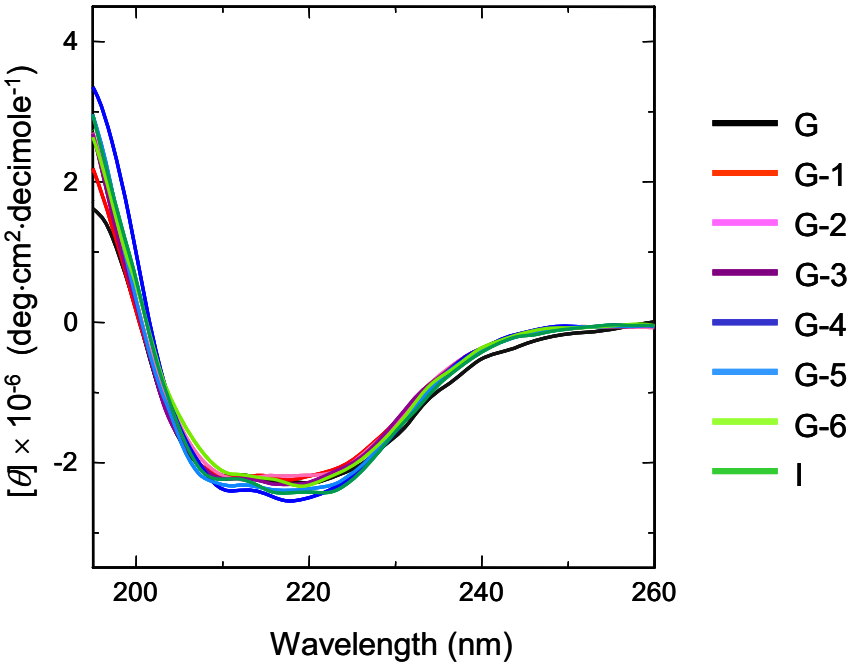

Figure 11. Circular dichroism spectra of chimeras G to I. The spectrum of protein (0.1 mg/ml) in 10 mM potassium phosphate buffer (pH 7.0) was measured at 25°C.

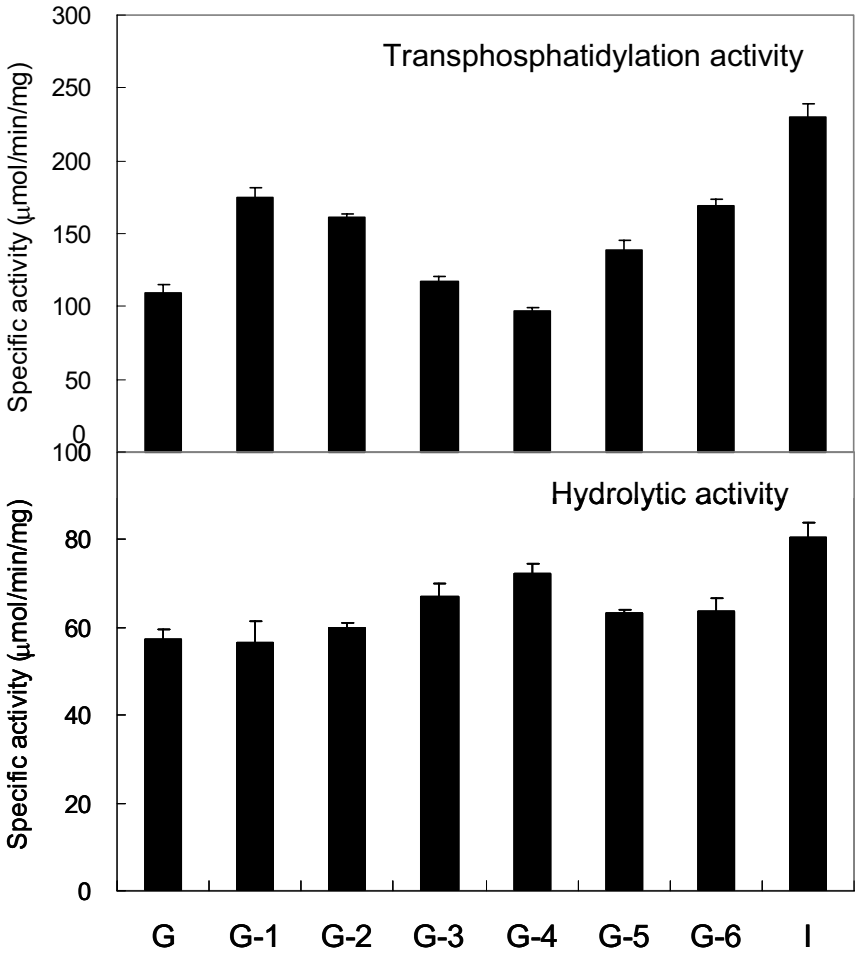

Figure 12. Comparison of activities for chimeras G to I. Specific activities of PLDs in the transphosphatidylation reaction (upper) and hydrolytic reaction (lower). Transphosphatidylation activities were measured at pH 5.5 with 13 mM PpNP. Hydrolytic activities were determined at pH 5.5 with 2 mM PpNP. Data are expressed as means ± SD of three independent experiments.

A

PLDs		Amino acid sequence																	
G	425	T	A	R	S	S	D	S	A	K	W	A	D	G	K	P	Y	A	Q	442
G-F		T	**F**	R	S	S	D	S	A	K	W	A	D	G	K	P	Y	A	Q	
G-D		T	A	R	S	S	D	S	**D**	K	W	A	D	G	K	P	Y	A	Q	
G-H		T	A	R	S	S	D	S	A	K	W	A	D	G	**H**	P	Y	A	Q	
G-FH		T	**F**	R	S	S	D	S	A	K	W	A	D	G	**H**	P	Y	A	Q	
G-FD		T	**F**	R	S	S	D	S	**D**	K	W	A	D	G	K	P	Y	A	Q	
G-DH		T	A	R	S	S	D	S	**D**	K	W	A	D	G	**H**	P	Y	A	Q	
G-FDH		T	**F**	R	S	S	D	S	**D**	K	W	A	D	G	**H**	P	Y	A	Q	
I		**A**	**F**	R	**A**	**A**	**P**	**G**	**D**	**T**	W	A	D	G	**H**	P	Y	A	**L**	

B

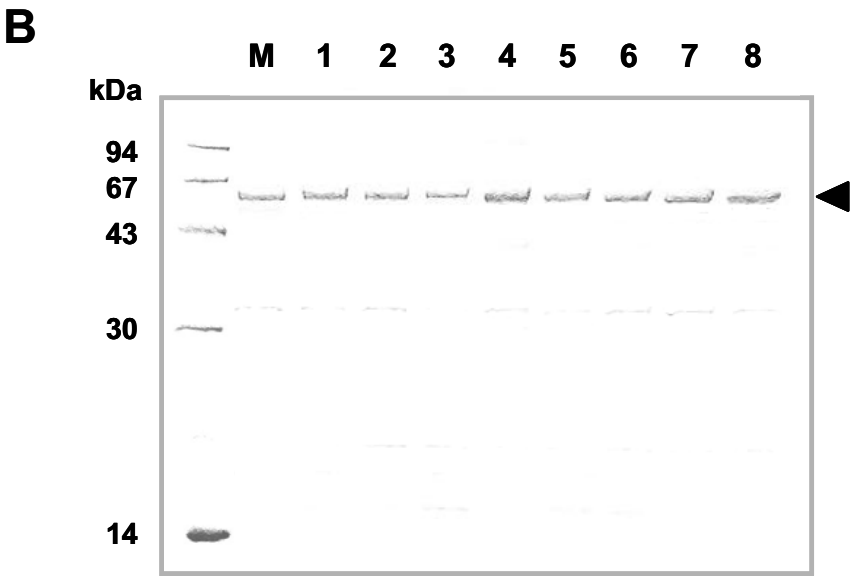

Figure 13. Preparation of chimera G mutants. (A) Primary structures of chimeras G, I and their mutants. (B) SDS-PAGE of purified PLDs. Lane 1 contained 1.5 μg of chimara G. Lanes 2-8 contained 1.5 μg of chimera G mutants G-F, G-D, G-H, G-FH, G-FD, G-DH, and G-FDH, respectively. Lane 9 contained 1.5 μg of chimera I. Lane M indicates low-molecular-weight marker proteins (molecular weights, 94,000, 67,000, 43,000, 30,000, 20,100 and 14,400). Samples were loaded on a 15% acrylamide gel. Arrow indicates the position of purified PLDs.

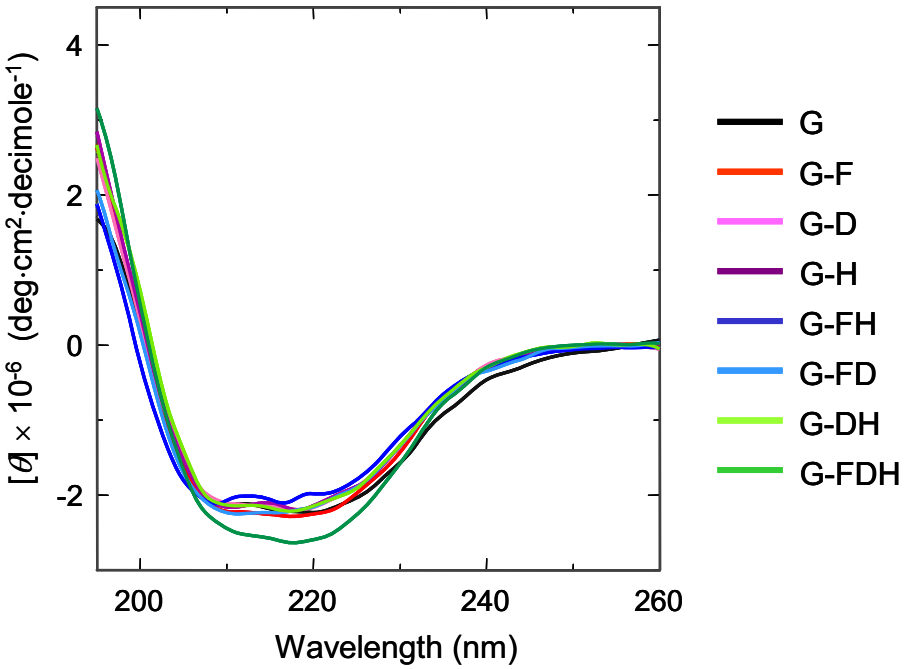

Figure 14. Circular dichroism spectra of chimera G mutants. The spectrum of protein (0.1 mg/ml) in 10 mM potassium phosphate buffer (pH 7.0) was measured at 25°C.

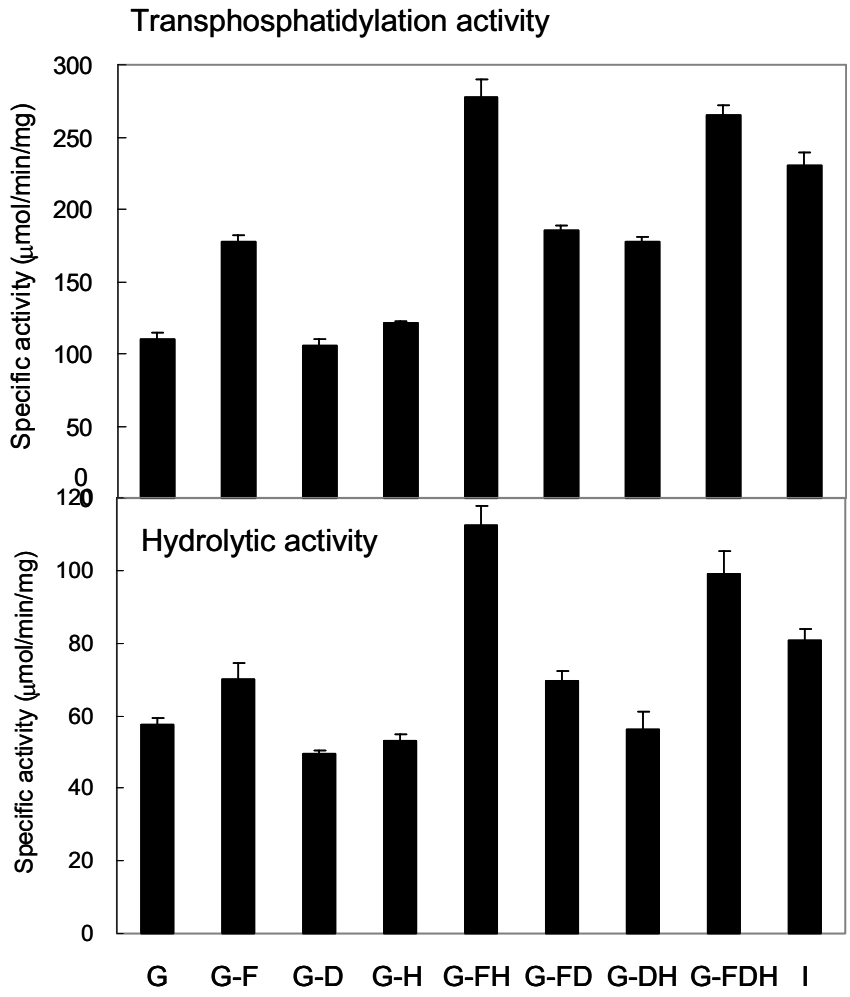

Figure 15. Identification of amino acid residues relating to activities. Specific activities of chimeras G, I and mutants in the transphosphatidylation reaction (upper) and hydrolytic reaction (lower). Transphosphatidylation activities were measured at pH 5.5 with 13 mM PpNP. Hydrolytic activities were determined at pH 5.5 with 2 mM PpNP. Data are expressed as means ± SD of three independent experiments.

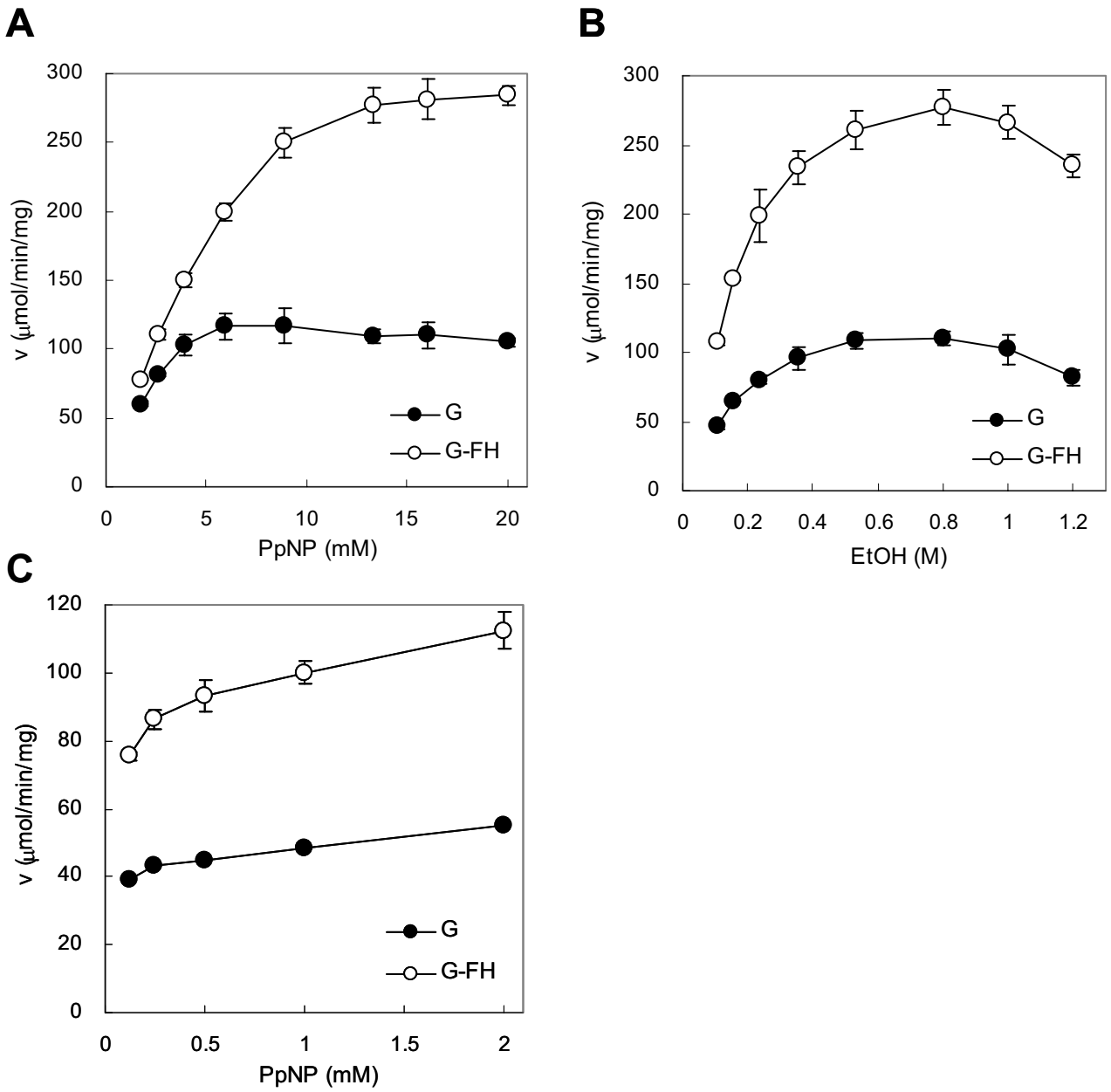

Figure 16. Effects of substrate (PpNP; A and EtOH; B) concentration on transphosphatidylation and hydrolytic (C) activities of PLDs. Enzyme activities were assayed by standard conditions described under Experimental Procedures, except that PpNP was used at the indicated concentrations. The reaction velocity (v) was expressed as mmol *p*-nitrophenol released min^{-1} mg $enzyme^{-1}$.

Table 3 Kinetic parameters of the transphosphatidylation and hydrolysis activities of PLDs toward PpNP and EtOH

	K_m (PpNP) (mM)	k_{cat} (PpNP) (s^{-1})	K_m (EtOH) (mM)	k_{cat} (EtOH) (s^{-1})
Transphosphatidylation [a]				
G	0.84 ± 0.06	113.7 ± 9.4	79 ± 14	105.0 ± 6.4
G-FH	5.69 ± 0.18	350.9 ± 10.7	97 ± 15	273.2 ± 11.8
Hydrolysis [b]				
G	0.104 ± 0.023	65.1 ± 2.3		
G-FH	0.106 ± 0.009	133.8 ± 6.4		

[a] The transphosphatidylation assay of chimera G and mutant G-FH toward PpNP was performed with 1.8 - 20 mM PpNP at pH 5.5, and toward EtOH was performed with 0.11 – 1.20 M EtOH at pH 5.5.
[b] The hydrolysis assay of PLDs was carried out with 0.13 - 2 mM PpNP at pH 5.5. Data are expressed as means ± SD.

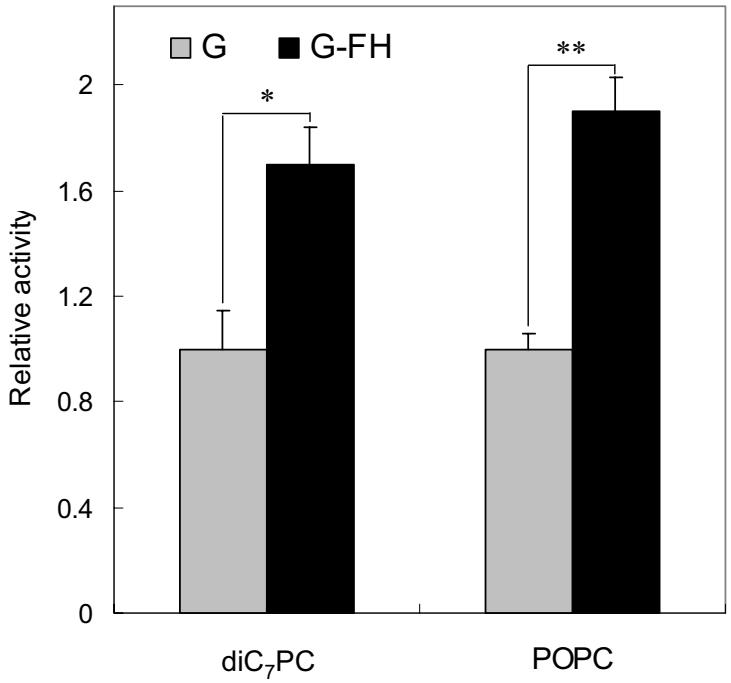

Figure 17. TLC of PLD-catalyzed transphosphatidylation. The reaction was performed for 10 min using 10 mM diC_7PC or POPC with 4 mM $CaCl_2$ present in acetate buffer (pH 5.5). The relative activity of PLD was then determined by measuring the intensity of the spot corresponding to phosphatidylethanol using *Scion Image* software, and indicated as chimera G activity toward diC_7PC or POPC. The relative activity of mutant G-FH was significantly different from that of chimera G toward diC_7PC and PpNP (*: $P < 0.01$, **: $P < 0.001$, calculated by *t* test).

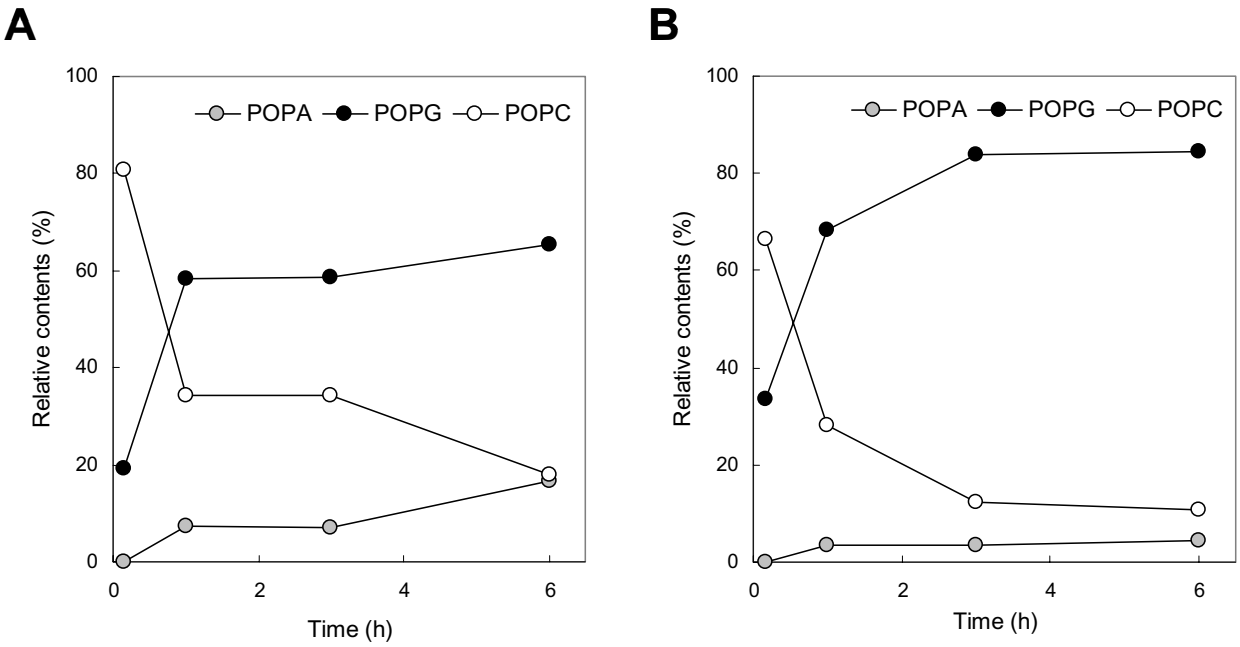

Figure 18. Transphosphatidylation from POPC to POPG by chimera G (A) and mutant G-FH (B). The reaction was performed using 10 mM POPC with 0.5 M glycerol and 4 mM $CaCl_2$ present in acetate buffer (pH 5.5) for 10 min, 1 h, 3 h and 6 h. The relative contents were determined by measuring the intensity of the spot corresponding to phosphatidic acids, phosphatidylglycerol and phosphatidylcholine using *Scion Image* software, respectively.

4. Discussion

In chapter 2, I found that the two regions, corresponding to the amino acid residues 188-203 and 425-442 of TH-2PLD, are related to transphosphatidylation activity. I first focused on N-terminal region of TH-2PLD (chimeras C and D). I investigated the difference in transphosphatidylation activity between chimeras C and D. Gly188 and Asp191 of TH-2PLD were determined to be the key residues related to the activity. Chimeras C and C-2 differed in these two residues (Fig. 1A). They exhibited considerably different transphosphatidylation activities, despite their similar hydrolytic activities. I also confirmed that chimeras C and C-2 were not denatured by organic solvents, such as benzene, which was used in our transphosphatidyalation assay, and they were folded with similar secondary structures (Fig. 2). I consider that this discrepancy was caused by substrate formed by two different reaction systems. In a previous study, the transphosphatidylation reaction catalyzed by *Streptomyces* PLD with two HKD motifs was influenced by the structure of substrate aggregates (Hirche *et al*., 1997). The substrate specificity and sensitivity to interfaces of PMFPLD were examined with a variety of phospholipids (Yang *et al*., 2003). PLD exhibited good activity toward monomeric short-chain lipids, while it exhibited lower activity toward PC packed in vesicles compared to PC dissolved in mixed micelles. Chimeras C and C-2 may also be sensitive to substrate form. That is to say, in the hydrolysis reaction, both chimeras C and C-2 reacted easily to monomeric and mixed micelles substrates, although in the transphosphatidylation reaction, C-2 reacted hard to emulsified substrates. In fact, there was no discrepancy in the results of SPR analysis; no obvious difference was observed in the interaction between chimera C and C-2 toward larger vesicles and more pronounced smaller vesicles, respectively (Fig. 6). Under the conditions of SPR analysis using SUVs, these differences in reactivity were manifested in the affinity for neutral substrate. A comparison of the binding kinetics of chimeras C and C-2, showed that the K_D value of C was smaller than

that of C-2 by 2 orders of magnitude (2.04×10^{-10} M, Table 2). From these results, Gly188 and Asp191 of TH-2PLD were indicated to play a crucial role in recognizing phospholipids.

The local environment around the key residues (Gly188 and Asp191 of TH-2) is shown in Fig. 19A. The residue Asp191 was located at the entrance of the predicted pocket for recognition of phospholipids, and exposed to a solvent. These residues were apart from the two histidine residues of the HKD motifs (approximately 11-20 Å in length). These results suggest that residues Gly188 and Asp191 contribute to the transphosphatidylation reaction, although they do not directly affect the histidine residues of the HKD motifs. Recently, Aikens *et al.* have characterized an interaction between PMFPLD and phospholipids by computer analysis using the automated docking program, 'AutoDock' (Aikens *et al*., 2004). They showed that a second residue of PA, phosphatidylethanolamine or PS was occasionally bound to a slightly negatively charged surface composed of Pro87, Asn90, Ser183, Trp184, Lys185, Asp186 and Asp187 of PMFPLD. Because PMFPLD and TH-2PLD shares 85% homology in their primary structures, the homology modeling of TH-2PLD indicated that Ser183 and Asp186 of PMFPLD correspond to Gly188 and Asp191 of TH-2PLD. Therefore, the two residues may recognize a secondary fatty acid of phospholipids.

Furthermore, I determined that the two residues play a role independent of the N-terminal HKD motif in reactions by SPR analysis using inactive mutants (Fig. 9). Chimera C mutant, in which the His443 of the C-terminal HKD motif was substituted with Ala (C(H443A)), showed higher affinity to substrate than the mutant in which the His170 of the N-terminal HKD motif was substituted with Ala (C(H170A)) (Fig. 9). These results agree with the result of Chapter 1 and indicating that histidine residue in the N-terminal HKD motif of TH-2PLD involves the catalytic nucleophile.

Next, I investigated amino acid residues related to the activities on C-terminal region of TH-2PLD (chimeras G and I in Fig. 10A). The results suggested that Ala426 and Lys438 of

TH-2PLD were key residues related to the both transphosphatidylation and hydrolytic activities. Although, chimeras G and G-FH only differed in these two residues (Fig. 13A), they exhibited considerably different activities (Figs. 15, 16 and Table 3). These differences in activities were also shown using different chain-length phospholipids (Fig. 17).

The local environment around the residues Ala426 and Lys438 of TH-2 is shown in Fig. 19B. The residue 426 of TH-2PLD was located inside the enzyme. When residue Ala426 was substituted with the hydrophobic amino acid residue Phe, both of transphosphatidylation and hydrolytic activities increased significantly. This residue was reported as one of the reliable thermostability-related residues (Mori *et al*., 2005). These results suggest that residue 426 participates in the conformational stability. On the other hand, residue 438 was present in the loop region, and exposed to a solvent. When residues Ala426 and Lys438 were substituted concurrently with the Phe and His respectively (mutant G-FH), the activities increase substantially than chimera G (Figs. 15, 16 and Table 3). Furthermore, the mutant G-FH showed higher selectivity of transphosphatidylation activity than chimera G (Fig. 18).

Considering the findings mentioned above, I speculate that residues 426 and 438 of TH-2PLD have different role from residues 188 and 191. Although residues 188 and 191 affect on the reaction differently toward mixed micelle, emulsion, SUV and MLV, the residues 426 and 438 affect on the reaction similarly with different physical states of substrate. Therefore, I consider that the residues 188 and 191 involve in sensitivity of the physical states of substrate, and residues 426 and 438 participate in the enhancement of activities and selectivity of transphosphatidylation activity catalyzed by TH-2PLD.

Because Asp191 of TH-2PLD was located at the entrance of the predicted pocket for recognition of phospholipids, anion charge of side chain of Asp191 make easily interact to head group of phosphatidylcholine. Asp191 is highly conserved residue among PLDs from *Streptomyces*, thus this residue may be an indispensable amino acid residue during evolutional

process. On the other hand, Gly188 of TH-2PLD was located inside the protein, which was near the alpha-7 helix. Gly has the smallest side-chain and a flexible dihedral angle. I speculate that the local environment around Gly188 affects on flexibility of the loop, therefore chimera C recognizes easily highly curved surface of SUV than chimera C-2. Moreover, the dissociation rate of phospholipids dislocated from bilayer membrane of SUV is higher than that of MLV. This fact also may explain the reason why chimera C could recognize substrates with ease.

5. Conclusion

Gly188, Asp191, Ala426 and Lys438 of TH-2PLD are key amino acid residues relating the PLD-catalyzed activities. Gly188 and Asp191 have an effect on sensitivity to substrate form. Moreover, it is suggested that Gly188 and Asp191 affect on recognition of phospholipids independently of HKD motifs in the reaction. On the contrary, the residues 426 and 438 of TH-2PLD participate in the enhancement of the transphosphatidylation and hydrolytic activities, and affect on the reaction independently of substrate form. By substituting these two residues of chimera G with Phe and His, respectively, the mutant G-FH express not only higher activities but also higher selectivity on the transphosphatidylation activity than those of original chimera G.

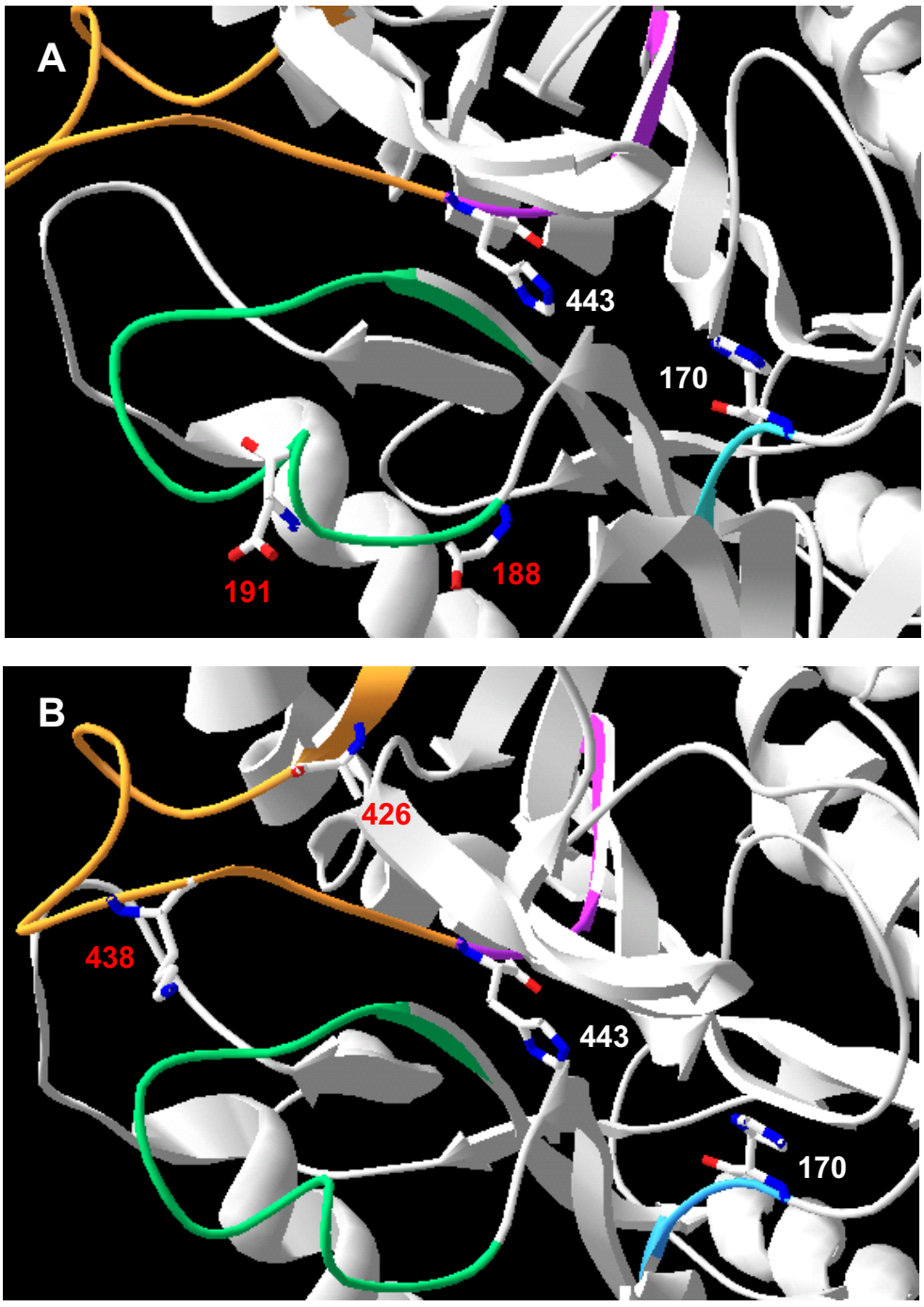

Figure 19. The local environment around the identified key residues (188, 191 (A), 426 and 438 (B) of TH-2PLD) is represented using the Swiss-pdb viewer. The identified key residues are indicated red characters.

GENERAL CONCLUSION

This thesis is concerned with the catalytic reaction mechanism of *Streptomyces* PLD. PLD is useful for the synthesis of rare natural phospholipids and novel artificial phospholipids because of its transphosphatidylation activity. Phospholipids have various biological functions in living organism, and are employed in many applications to the pharmaceuticals, foods, cosmetics, and other industries. The reaction mechanism of PLD has already been studied extensively, and the role of the HKD motifs in the enzyme reaction was described. However, it has still been discussed which HKD motif contains the initial catalytic nucleophile attacking the phosphatidyl group of the substrate phospholipids. Furthermore, amino acid residues other than those in the HKD motifs, which are related to PLD-catalyzed activities, have not yet been identified experimentally. Therefore, the general purpose of this thesis is an elucidation of catalytic mechanism of PLD. The results of each chapter are summarized as follows.

In Chapter 1, first of all, to determine which HKD motif contains the initial catalytic nucleophile in *Streptomyces* PLD, binding of inactive mutants, in which the His170 or His443 of the N- or C-terminal HKD motif in TH-2PLD was substituted with Ala, to several phospholipids was analyzed by surface plasmon spectroscopy. The results revealed that each histidine residue of the two HKD motifs indeed show distinct role in the catalytic reaction. It found that His170 of the N-terminal HKD motif in TH-2PLD acts as an initial catalytic nucleophile, which attacks the phosphorus atom of the phospholipids, and that His443 of the C-terminal HKD motif in TH-2PLD should act as a general acid. Furthermore, it suggested that His443 significantly affects the interaction with PG vesicles, and also suggested that the other amino acid residues than the HKD motifs relates the recognition of POPC.

In Chapter 2, to determine the other amino acid residues relating the catalytic reactions than the two HKD motifs, I constructed a chimeric gene library between two highly homologous *plds* from *Streptomyces*, which show different activities in the

transphosphatidylation, using RIBS *in vivo* DNA shuffling. According to this method, 21 chimeric PLDs were obtained. The recombination was occurred between short homologous sequences at corresponding position with large variety. By comparing the activities of the chimeras, it was suggested that the two regions, residues 188-203 and 425-442 of TH-2PLD, relate to transphosphatidylation activity. Based on the crystal structure of PMFPLD (Leiros *et al*., 2000), residues 188-203 and 425-442 of TH-2PLD may locate in the two flexible loop regions between β7 and α7 (residues 188-203), and between β13 and β14 (residues 425-442), respectively, and are face to face at the domain-domain interface.

In Chapter 3, I first focused on N-terminal region, residues 188-203 (corresponding to chimeras C and D) of TH-2PLD, and constructed several mutants to identify the key residues involved in the recognition of phospholipids. By kinetic analysis, it showed that Gly188 and Asp191 in PLD from *Streptomyces septatus* TH-2 are key amino acid residues related to the transphosphatidylation activity. To investigate the role of two residues in the recognition of phospholipids, the effects of these residues on binding of substrates were evaluated using surface plasmon resonance analysis. The result suggests that Gly188 and Asp191 are involved in the recognition of phospholipids. I further studied on the other residues related to the reaction among 425-442 residues (corresponding to chimeras G and I) of TH-2PLD. By comparative study of the chimeras, ten candidate residues related to the activities were found. To identify the key residues, I then constructed thirteen mutants, and evaluated their hydrolytic and transphosphatidylation activities. From these results, the relation of Ala426 and Lys438 in TH-2PLD to the activities is elucidated. By substitution of these two residues in chimera G with Phe and His, respectively, the k_{cat} in the transphosphatidylation activity increased 3-fold than that of the original chimera. Furthermore, the mutant decreased PA production that formed by the side-reaction during transphospatidylation from PC to PG.

In this study, I identified that Gly188, Asp191, Ala426 and Lys438 of TH-2PLD are key

amino acid residues relating the activities (Fig. 1). These residues are not present in the highly conserved catalytic HxKxxxxD (HKD) motifs. It was found that Gly188 and Asp191 effect on sensitivity to the physical state of substrate, while Ala426 and Lys438 play a role independently of substrate form. The residues 426 and 438 are important for enhancement of both transphosphatidylation and hydrolytic activities, and related to selectivity of transphosphatidylation. Among these four residues, residues 188 and 426 are also the thermostability-related residues (Mori *et al*., 2005; Negishi *et al*., 2005), suggesting that residues 188 and 426 participate in the conformational stability.

In mechanism of PLD-catalyzed reactions, previous enzymatic studies proposed a two-step mechanism (Stanacev & Stuhne-Sekalec, 1970; Gottlin *et al*., 1998; Waite, 1999; Xie *et al*., 2000; Raetz *et al*., 1987). A covalently linked phosphohistidine moiety is the most probable reaction intermediate for enzymes in the PLD superfamily (Gottlin *et al*., 1998; Rudolph *et al*., 1999). It has also been shown that mutations of either His or Lys residues in the active site of Nuc, Ymt or Tdp1 resulted in an enzyme without activity hydrolyzing a phosphodiester substrate (Gottlin *et al*., 1998; Rudolph *et al*., 1999; Interthal *et al*., 2001). Other mutational studies on human PLD1 demonstrated the catalytic importance of the corresponding residues, although a serine was suggested to form the covalent phosphatidyl intermediate (Sung *et al*., 1997). A report on chemical modifications of the *Streptomyces* sp. PMF PLD (PMFPLD) suggested that Lys and not His is essential for the activity (Secundo *et al*., 1996). Other report indicated that the histidine residue in the C-terminal HKD motif of PLD from *Streptomyces antibioticus* included the catalytic nucleophile that bound directly to the phosphatidyl group of the substrate (Iwasaki *et al.*, 1999). Furthermore, the crystal structure of PMFPLD indicated that a histidine residue in the N-terminal HKD motif acts as the nucleophile (Leiros *et al*., 2004). These results are consistent with the conclusion of this study that N-terminal HKD motif involves the catalytic nucleophile (Chapter 1). As shown in

Fig. 2, the conformation of the active site in unliganded PMFPLD is almost the same as that in PMFPLD in the presence of short-chain substrate. The two aspartate residues in the active site (Asp202 and Asp473) formed strong hydrogen bonds to the two histidine residues of the HKD motifs in unliganded PMFPLD, while the side-chain of Asp473 formed an ion-pair interaction to His170 in PMFPLD in the presence of substrate. In addition, the interaction between PMFPLD and phospholipids was also investigated by computational analysis using the automated docking program, 'AutoDock' (Aikens *et al*., 2004). This study coincide with the experimental results that the N-terminal HKD motif contains the catalytic nucleophile which attacks the phosphatidyl group of the substrate.

In conclusion, previous reports and the results in this study lead to the hypothesis for the PLD-catalyzed reaction mechanism as follows (Fig. 1): (i) residues188 and 191 of TH-2PLD, which locate at the entrance of the active well formed by the two HKD motifs, effect on sensitivity to the physical state of the substrate, (ii) the imidazole nitrogen of His170 in the N-terminal HKD motif attacks the phosphorus atom of the substrate as a nucleophile, and His443 in the C-terminal HKD motif deliver a hydrogen to the OR' leaving group. Then, (iii) PLD and phospholipids form a phosphatidylhistidine intermediate and an alcohol is released, (iv) an alcohol or water activated by the imidazole nitrogen of His443 attack the phosphatidyl intermediate, followed by (v) dissociation of PLD from the intermediate and production of a new phospholipid or phosphatidic acid. The residues 426 and 438 of TH-2PLD act on enhancement of activities during reaction.

The catalytic mechanism of *Streptomyces* PLD proposed from this thesis is applicable to elucidation of those of PLDs from other sources, because *Streptomyces* PLD has most compact structure including conserved catalytic regions among many sources.

The most important future prospect is creation of a high-performance PLD having high selectivity ratio of transphosphatidylation/hydrolytic activity is aimed. Based on the obtained

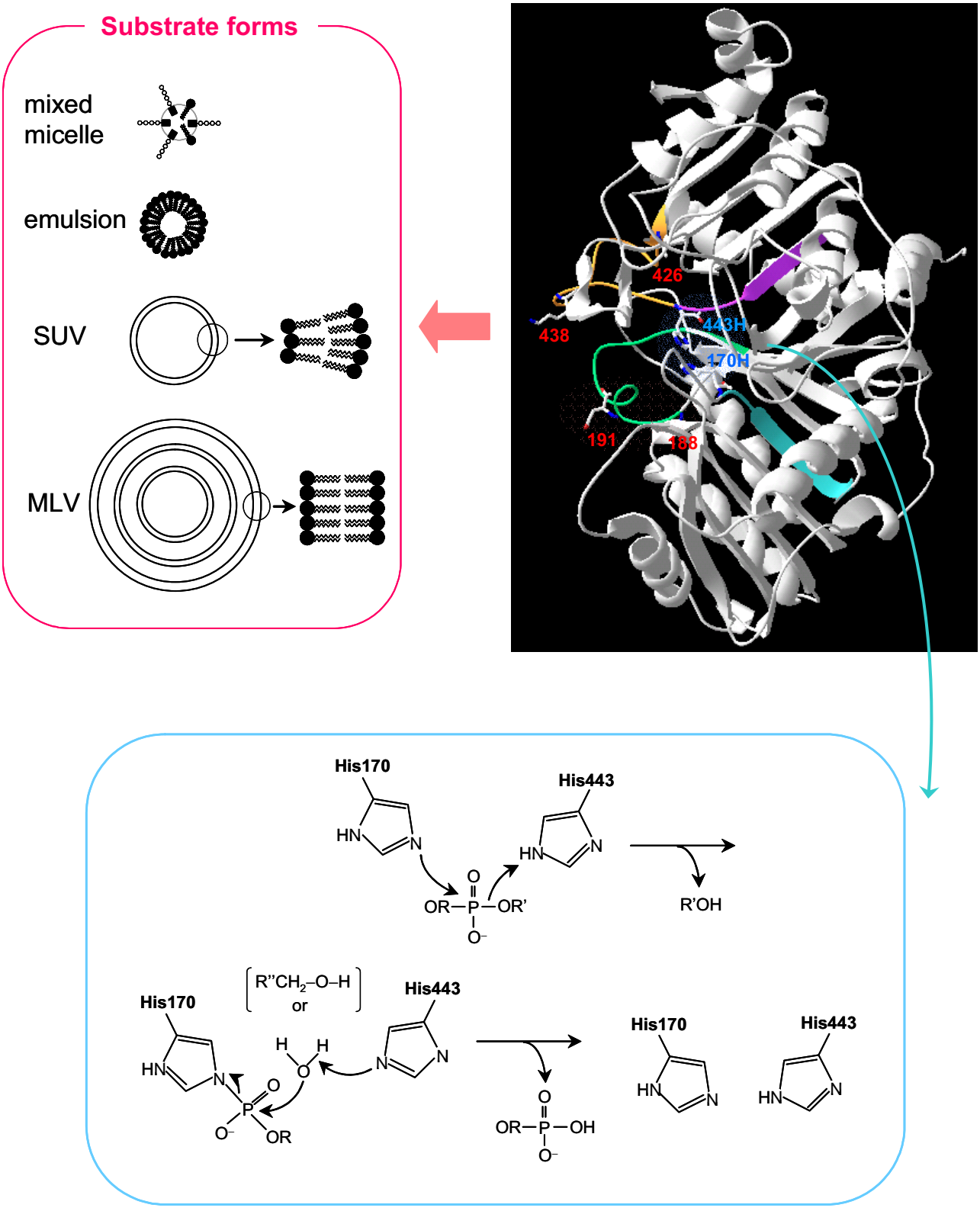

Figure 1. The identified key amino acid residues and proposed reaction mechanism of *Streptomyces* PLD.

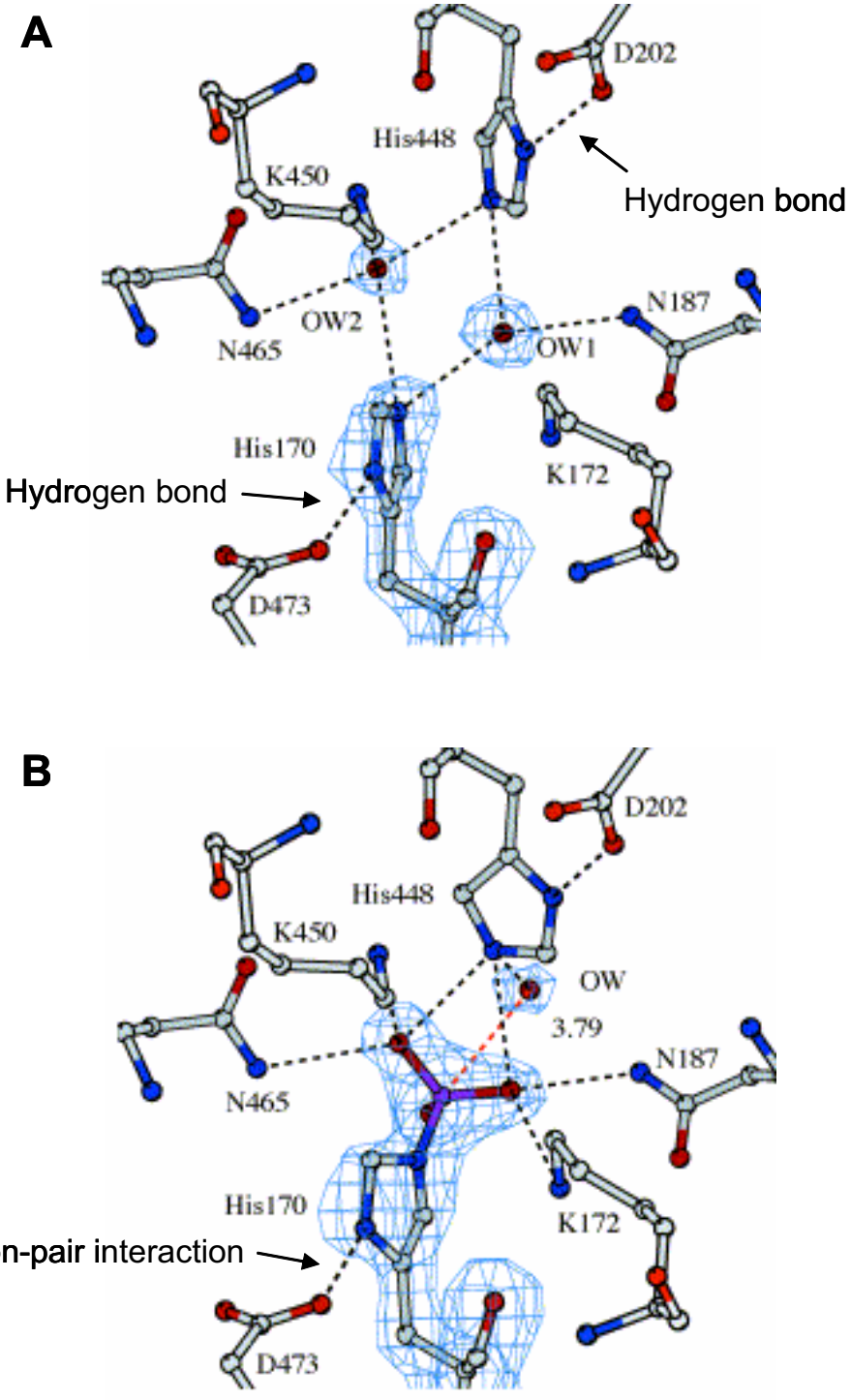

Figure 2. The active site of PMFPLD unliganded (A) and in the presence of diC_4PC (B). These illustrations are cited from Leiros *et al*., J. Mol. Biol., 339, 805-820 (2004).

information in this thesis, high-performance PLDs could be created by substitution of the key amino acid residues relating the activities with other residues. In fact, previous studies showed that the substitution of thermostability-related residues with other residues, such as Phe, Val or Trp, provided dramatic thermostability (Negishi *et al*., 2005; Mori *et al*., 2005). Creation of a high-performance PLD thought to be very useful for synthesizing phospholipid derivatives, such as phosphatidylserine, phosphatidylglycerol, from inexpensive materials such as phosphatidylcholine. For example, production of PS may contribute on the prevention and treatment of nervous diseases, such as senile dementia and Alzheimer's disease.

In this thesis, key amino acid residues, Gly188, Asp191, Ala426 and Lys438 of TH-2PLD, which relate to PLD-catalyzed activities, were identified using RIBS *in vivo* DNA shuffling. Thus, this method has the advantage of the application to cytotoxic proteins, such as PLD, although *in vitro* DNA shuffling method is hard to apply to cytotoxic proteins. In the previous study, several amino acid residues relating thermostability were identified from chimeras between two *Streptomyces* PLDs with similar thermostability by this method (Mori *et al.*, 2005). By this homology–dependent recombination method, recombination is often occurred at highly conserved regions, which are important for function and conformation of protein in the evolutional process. Therefore, differences in properties of two parent proteins tend to be amplified. This finding enables to identify functional regions in parental proteins having similar properties. Furthermore, chimeras could be useful for elucidating function of protein because of less conformational change than deletion mutants. This method may increase the chance of carrying out molecular evolution of proteins that had not been targeted for other DNA shuffling, and supply a useful strategy for analyzing the function of individual amino acid residues or sequences.

REFERENCES

Aikens, C. L., Laederach, A., and Reilly, P. J. Visualizing complexes of phospholipids with Streptomyces phospholipase D by automated docking. (2004) *Proteins* **57**, 27-35

Amaducci, M. D. Phosphatidylserine in the treatment of Alzheimer's disease: results of a multicenter study. (1988) *Psychopharmacol. Bull.***24**, 130-134

Arnold, F. H., and Moore, J. C. Optimizing industrial enzymes by directed evolution. (1997) *Adv. Biochem. Eng. Biotechnol*. **58**, 1-14

Bian, J., and Roberts, M. F. Comparison of surface properties and thermodynamic behavior of lyso- and diacylphosphatidylcholines. (1992) *J. Colloid Interface Sci*. **153**, 420-428

Bigon, E., Boarato, E., Bruni, A., Leon, A., and Toffano, G. Pharmacological effects of phosphatidylserine liposomes: the role of lysophosphatidylserine. (1979) *Br. J. Pharmacol.* **67**, 611-616

Bruzik, K., and Tsai, M.-D. Phospholipids chiral at phosphorus. Synthesis of chiral phosphatidylcholine and stereochemistry of phospholipase D. (1984) *Biochemistry* **23**, 1656-1661

Chae, Y. C., Lee, S., Lee, H. Y., Heo, K., Kim, J. H., Kim, J. H., Suh, P. G., and Ryu, S. H. Inhibition of muscarinic receptor-linked phospholipase D activation by association with tubulin. (2005) *J. Biol. Chem.* **280**, 3723-3730

Chen, K., and Arnold, F. H. Tuning the activity of an enzyme for unusual environments: Sequential random mutagenesis of subtilisin E for catalysis in dimethylformamide. (1993) *Proc. Natl. Acad. Sci.* USA **90**, 5618-5622

Chopra, S., and Ranganathan, A. Protein evolution by 'codon shuffling': a novel method for generating highly variant mutant libraries by assembly of hexamer DNA duplexes. (2003) *Chem. Biol.* **10**, 917-926

Comfurius, P., Bevers, E. M., and Zwaal, R. F. A. Enzymatic synthesis of phosphatidylserine on small scale by use of a one-phase system. (1990) *J. Lipid Res.* **31**, 1719-1721

Crameri, A., Raillard, S.-A., Bermudez, E., and Stemmer, W. P. C. DNA shuffling of a family of genes from diverse species accelerates directed evolution. (1998) *Nature* **391**, 288-291

D'Arrigo, P., Piergianni, V., Scarcelli, D., and Servi, S. A spectrophotometric assay for phospholipase D (1995) *Anal. Chim. Acta* **304**, 249-254

D'Arrigo, P., and Servi, S. Using phospholipases for phospholipid modification. (1997) *Trends Biotechnol.* **15**, 90-96

Dennis, E. A. Phospholipase A2 activity towards phosphatidylcholine in mixed micelles: surface dilution kinetics and the effect of thermotropic phase transitions. (1973) *Arch. Biochem. Biophys*. **158**, 485-493

Dittmer, J. C., and Lester, R. L. A simple, specific spray for the detection of phospholipids on thin-layer chromatograms. *J. Lipid Res*. **5**, 126-127

Exton, J. H. Phospholipase D. (1998) *Biochim. Biophys. Acta* **1436**, 105-115

Exton, J. H. Regulation of phospholipase D. (1999) *Biochim. Biophys. Acta* **1439**, 121-133

Exton, J. H. Regulation of phospholipase D. (2002) *FEBS Lett.* **531**, 58-61

Giver, L., Gershenson, A., Freskgard, P.-O., and Arnold, F. H. Directed evolution of a thermostable esterase. (1998) *Proc. Natl. Acad. Sci.* USA **95**, 12809-12813

Gottlin, E. B., Rudolph, A. E., Zhao, Y., Matthews, H. R., and Dixon, J. E. Catalytic mechanism of the phospholipase D superfamily proceeds via a covalent phosphohistidine intermediate. (1998) *Proc. Natl. Acad. Sci.* USA **95**, 9202-9207

Hagishita, T., Nishikawa, M., and Hatanaka, T. A spectrophotometric assay for the transphosphatidylation activity of phospholipase D enzyme. (1999) *Anal. Biochem.*, **276**,

161-165

Hagishita, T., Nishikawa, M., and Hatanaka, T. Isolation of phospholipase D producing microorganisms with high transphosphatidylation activity. (2000) *Biotechnol. Lett.* **22**, 1587-1590

Hammond, S. M., Altshuller, Y. M., Sung, T.-C., Rudge, S. A., Rose, K., Engebrecht, J., Morris, A. J., and Frohman, M. A. Human ADP-rebosylation factor-activated phosphatidylcholine-specific phospholipase D defines a new and highly conserved gene family. (1995) *J. Biol. Chem*. **270**, 29640-29643

Hatanaka, T., Negishi, T., Kubota-Akizawa, M., and Hagishita, T. Purification, characterization, cloning and sequencing of phospholipase D from *Streptomyces septatus* TH-2. (2002a) *Enzyme Microb. Technol.* **31**, 233-241

Hatanaka, T., Negishi, T., Kubota-Akizawa, M., and Hagishita, T. Study on thermostability of phospholipase D from Streptomyces sp. (2002b) *Biochim. Biophys. Acta* **1598**, 156-164

Hatanaka, T., Negishi, T., and Mori, K. A mutant phospholipase D with enhanced thermostability from Streptomyces sp. (2004) *Biochim. Biophys. Acta* **1696**, 75-82

Hiraga, K., and Arnold, F. H. General method for sequence-independent site-directed chimeragenesis. (2003) *J. Mol. Biol.* **330**, 287-296

Hirche, F., Koch, M. H. J., König, S., Wadewitz, T., and Ulbrich-Hofmann, R. The influence of organic solvents on phospholipid transformations by phospholipase D in emulsion systems. (1997) *Enz. Microb. Technol.* **20**, 453-461

Honda, A., Nogami, M., Yokozeki, T., Yamazaki, M., Nakamura, H., Watanabe, H., Kawamoto, K., Nakayama, K., Morris, A. J., Frohman, M. A., and Kanaho, Y. Phosphatidylinositol 4-phosphate 5-kinase alpha is a downstream effector of the small G protein ARF6 in membrane ruffle formation. (1999) *Cell* **99**, 521-532

Hughes, M. D., Nagel, D. A., Santos, A. F., Sutherland, A. J., Hine, A. V. Removing the

redundancy from randomised gene libraries. (2003) *J. Mol. Biol.* **331**, 973-979

Interthal, H., Pouliot, J. J., and Champoux, J. J. The tyrosyl-DNA phosphodiesterase Tdp1 is a member of the phospholipase D superfamily. (2001) *Proc. Natl. Acad. Sci.* USA **98**, 12009-12014

Iwasaki, Y., Nakano, H., and Yamane, T. Phospholipase D from *Streptomyces antibioticus*: cloning, sequencing, expression, and relationship to other phospholipases. (1994) *Appl. Microbiol*. *Biotechnol*. **42**, 290-299

Iwasaki, Y., Horiike, S., Matsushima, K., and Yamane, T. Location of the catalytic nucleophile of phospholipase D of *Streptomyces antibioticus* in the C-terminal half domain. (1999) *Eur. J. Biochem*. **264**, 577-581

Juneja, L. R., Hibi, T., Yamane, T., and Shimizu, S. Repeated batch and continuous operations for phosphatidylglycerol synthesis from phosphatidylcholine with immobilized phospholipase D. (1987) *Appl. Microbiol. Biotechnol.* **27**, 146-151

Juneja, L. R., Kazuoka, T., Goto, T., Yamane, T., and Shimizu, S. Kinetic evaluation of phosphatidylcholine to phosphatidylethanolamine by phospholipase D from different sources. (1988) *Biochim. Biophys. Acta* **960**, 334-341

Juneja, L. R., Kazuoka, T., Goto, T., Yamane, T., and Shimizu, S. Conversion of phosphatidylcholine to phosphatidylserine by various phospholipase D in the presence of L- or D- serine. (1989) *Biochim. Biophys. Acta* **1003**, 277-283

Kim, J.-Y., and Deverotes, P. N. Random chimeragenesis of G-protein-coupled receptors. Mapping the affinity of the cAMP chemoattractant receptors in *Dictyostelium*. (1994) *J. Biol. Chem.* **269**, 28724-28731

Laemmli, U. K. Cleavage of structural proteins during assembly of the head of bacteriophage T4. (1970) *Nature* **227**, 680-685

Leiros, I., Secundo, F., Zambonelli, C., Servi, S., and Hough, E. The first crystal structure of a

phospholipase D. (2000) *Structure* **8**, 655-667

Leiros, I., McSweeney, S., and Hough, E. The reaction mechanism of phospholipase D from Streptomyces sp. strain PMF. Snapshots along the reaction pathway reveal a pentacoordinate reaction intermediate and an unexpected final product. (2004) *J. Mol. Biol.* **339**, 805-820

Lichtenberg, D., Robson, R. J., and Dennis, E. A. Solubilization of phospholipids by detergents. Structural and kinetic aspects. (1983) *Biochim. Biophys. Acta* **737**, 285-304

Lutz, S., Ostermeier, M., and Benkovic, S. J. Rapid generation of incremental truncation libraries for protein engineering using α-phosphothioate nucleotides. (2001) *Nucleic Acids Res*. **29**, e16

MacDonald, R. C., MacDonald, R. I., Menco, B. P., Takeshita, K., Subbarao, N. K., and Hu L. R. Small-volume extrusion apparatus for preparation of large, unilamellar vesicles. (1991) *Biochim. Biophys. Acta* **1061**, 297-303

Mishima, N., Mizumoto, K., Iwasaki, Y., Nakano, H., and Yamane, T. Insertion of stabilizing loci in vectors of T7 RNA polymerase-mediated Escherichia coli expression systems: a case study on the plasmids involving foreign phospholipase D gene. (1997) *Biotechnol. Prog.* **13**, 864-868

Mori, K., Mukaihara, T., Uesugi, Y., Iwabuchi, M., and Hatanaka, T. Repeat-length-independent broad-spectrum shuffling, a novel method of generating a random chimera library *in vivo*. (2005) *Appl. Environ. Microbiol.* **71**,754-760

Morris, A. J., Engebrecht, J., and Frohman, M. A. Structure and regulation of phospholipase D. (1996) *Trends Pharmacol. Sci*. **17**, 182-185

Mukaihara, T., and Enomoto, M. Deletion formation between the two *salmonella typhimurium* flagellin genes encoded on the mini F plasmid: Escherichia coli ssb alleles enhance deletion rates and change hot-spot preference for deletion endpoints. (1997) *Genetics.* **145**, 563-572

Negishi, T. R., Mukaihara, T., Mori, K., Nishikido, H., Kawasaki, Y., Aoki, H., Kodama, M.,

Uedaira, H., Uesugi, Y., Iwabuchi, M., and Hatanaka, T. Identification of a key amino acid residue of *Streptomyces* phospholipase D for thermostability by *in vivo* DNA shuffling. (2005) *Biochim. Biophys. Acta* **1722**, 331-342

O'Maille, P. E., Bakhtina, M., and Tsai, M. D. Structure-based combinatorial protein engineering (SCOPE). (2002) *J. Mol. Biol.* **321**, 677-691

Ostermeier, M., Shim, J. H., and Benkovic, S. J. A combinatorial approach to hybrid enzymes independent of DNA homology. (1999) *Nat. Biotechnol*. **17**, 1205-1209

Ponting, C. P., and Kerr, I. D. A novel family of phospholipase D homologues that includes phospholipids synthases and putative endonucleases: Identification of duplicated repeats and potential active site residues. (1996) *Protein Sci.* **5**, 914-922

Raetz, C. R., Carman, W., Dowhan, R. T., Jiang, R. T., Waszkuc, W.,Loffredo, W. and Tsai, M. D. Phospholipids chiral at phosphorus. Steric course of the reactions catalyzed by phosphatidylserine synthase from *Escherichia coli* and yeast. (1987) *Biochemistry* **26**, 4022-4027

Raymond, A. C., Rideout, M. C., Staker, B., Hjerrild, K., and Burgin, A. B. Jr. Analysis of human tyrosyl-DNA phosphodiesterase I catalytic residues. (2004) *J. Mol. Biol.* **338**, 895-906

Reynolds, L. J., Washburn, W. N., Deems, R. A., and Dennis, E. A. Assay Strategies and methods for phospholipases. (1991) *Methods in enzymology* **197**, 3-23

Rizzo, M. A., Shome, K., Vasudevan, C., Stolz, D. B., Sung, T. C., Frohman, M. A., Watkins, S. C., and Romero, G. Phospholipase D and its product, phosphatidic acid, mediate agonist-dependent raf-1 translocation to the plasma membrane and the activation of the mitogen-activated protein kinase pathway. (1999) *J. Biol. Chem.* **274**, 1131-1139

Rudolph, A. E., Stuckey, J. A., Zhao, Y., Matthews, H. R., Patton, W. A., Moss, J. and Dixon, J. E. Expression, characterization, and mutagenesis of the *Yersinia pestis* murine toxin, a phospholipase D superfamily member. (1999) *J. Biol. Chem.* 274, 11824-11831.

Sato, R., Itabashi, Y., Hatanaka, T., and Kuksis, A. Asymmetric *in vitro* synthesis of diastereomeric phosphatidylglycerols from phosphatidylcholine and glycerol by bacterial phospholipase D. (2004) *Lipids* **39**, 1013-1018

Satoh, T., Takahashi, Y., Oshida, N., Shimizu, A., Shinoda, M., Watanabe, T., and Samejima, T. A chimeric inorganic pyrophosphatase derived from *Escherichia coli* and *Thermus thermophilus* has an increased thermostability. (1999) *Biochemistry* **38**, 1531-1536

Secundo, F., Carrea, G., D'Arrigo, P., and Servi, S. Evidence for an essential lysyl residue in phospholipase D from *Streptomyces* sp. by modification with diethyl pyrocarbonate and pyridoxal 5-phosphate. (1996) *Biochemistry* **35**, 9631-9636.

Shimbo, K., Yano, H., and Miyamoto, Y. Two *Streptomyces* strains that produce phospholipase D with high transphosphatidylation activity. (1989) *Agric. Biol. Chem*. **53**, 3083-3085

Sieber, V., Martinez, C. A., and Arnold, F. H. Libraries of hybrid proteins from distantly related sequences. (2001) *Nat. Biotechnol*. **19**, 456-460

Stanacev, N. Z., and Stuhne-Sekalec, L. On the mechanism of enzymatic phosphatidylation. Biosynthesis of cardiolipin catalyzed by phospholipase D. (1970) *Biochim. Biophys. Acta* **210**, 350-352

Stemmer, W. P. C. Rapid evolution of a protein *in vitro* by DNA shuffling. (1994) *Nature* **370**, 389-391

Stuckey, J. A., and Dixon, J. E. Crystal structure of a phospholipase D family member. (1999) *Nat. Struct. Biol.* **6**, 278-284

Sung, T.C., Roper, R. L., Zhang, Y., Rudge, S. A., Temel, R., Hammond, S. M., Morris, A. J., Moss, B., Engebrecht, J., and Frohman, M.A. Mutagenesis of phospholipase D defines a

superfamily including a trans-Golgi viral protein required for poxvirus pathogenicity. (1997) *EMBO J.* **16**, 4519-4530

Takahara, M., Houriyou, K. and Imamura, S. (1993) Japanese patent, JP1993252935-A/1

Takami, M., Hidaka, N., Miki, S., and Suzuki, Y. Phospholipase D-catalyzed synthesis of phosphatidyl aromatic compounds. (1994) *Biosci. Biotechnol. Biochem.* **58**, 2140-2144

Turner, D. L., Silver, M. J., Baczynski, E., Holburn, R. R., Herb, S. F., and Luddy, F. E. The synthesis of phosphatidylethanolamine and phosphatidylserine containing acetylenic or cyclopropane fatty acids and the activity of these phosphatides in blood coagulation. (1970) *Lipids*, **5**, 650-657

Waite, M. The PLD superfamily: insights into catalysis. (1999) *Biochim. Biophys. Acta* **1439**, 187-197

Waksman, M., Eli, Y., Liscovitch, M., and Gerst, J. E. Identification and characterization of a gene encoding phospholipase D activity in yeast. (1996) *J. Biol. Chem.* **271**, 2361-2364

Wong, T. S., Tee, K. L., Hauer, B., and Schwaneberg, U. Sequence saturation mutagenesis (SeSaM): a novel method for directed evolution. (2004) *Nucleic Acids Res*. **32**, e26

Xie, Z., Ho, W. T., and Exton, J. H. Association of the N- and C-terminal domains of phospholipase D. Contribution of the conserved HKD motifs to the interaction and the requirement of the association for Ser/Thr phosphorylation of the enzyme. (2000) *J. Biol. Chem.* **275**, 24962-24969

Yang, H., and Roberts, M. F. Cloning, overexpression, and characterization of a bacterial Ca^{2+}-dependent phospholipase D. (2002) *Protein Sci.* **11**, 2958-2968

Yang, H., and Roberts, M. F. Phosphohydrolase and transphosphatidylation reactions of two Streptomyces phospholipase D enzymes: covalent versus noncovalent catalysis. (2003) *Protein Sci.* **12**, 2087-2098

You, L., and Arnold, F. H. Directed evolution of subtilisin E in Bacillus subtilis to enhance total activity in aqueous dimethylformamide. (1996) *Protein Eng*. **9**, 77-83

Zambonelli, C., Casali, M., and Roberts, M. F. Mutagenesis of putative catalytic and regulatory residues of Streptomyces chromofuscus phospholipase D differentially modifies phosphatase and phosphodiesterase activities. (2003) *J. Biol. Chem.* **278**, 52282-52289

Zhang, J.-H., Dawes, G., and Stemmer, W. P. C. Directed evolution of a fucosidase from a galactosidase by DNA shuffling and screening. (1997) *Proc. Natl. Acad. Sci.* USA **94**, 4504-4509

LIST OF PUBLICATIONS

The present thesis, **"Studies on the catalytic reaction of *Streptomyces* phospholipase D"**, is based on the following publications.

CHAPTER 1

"Binding analysis of *Streptomyces* phospholipase D protein toward phospholipids by surface plasmone resonance" Uesugi, Y., Arima, J., Iwabuchi, M., and Hatanaka,T. *in preparation*

CHAPTER 2

"Recognition of phospholipids in *Streptomyces* phospholipase D"
Uesugi, Y., Mori, K., Arima, J., Iwabuchi, M., and Hatanaka,T. (2005) *J. Biol. Chem.* **280**, 26143-26151

"Repeat-length-independent broad-spectrum shuffling, a novel method of generating a random chimera library *in vivo*"
Mori, K., Mukaihara, T., Uesugi, Y., Iwabuchi, M., and Hatanaka, T. (2005) *Appl. Environ. Microbiol.* **71**, 754-760

CHAPTER 3

"Recognition of phospholipids in *Streptomyces* phospholipase D"
Uesugi, Y., Mori, K., Arima, J., Iwabuchi, M., and Hatanaka,T. (2005) *J. Biol. Chem.* **280**, 26143-26151

"Role of key residues related to catalytic reactions of *Streptomyces* phospholipase D"
Uesugi, Y., Mori, K., Arima, J., Iwabuchi, M., and Hatanaka,T *in preparation*

RELATED PUBLICATIONS

Arima, J., Uesugi, Y., Iwabuchi, M., and Hatanaka,T., Alteration of leucine aminopeptidase from *Streptomyces septatus* TH-2 to phenylalanine aminopeptidase by site-directed mutagenesis. (2005) *Appl. Environ. Microbiol.* **71**, 7229-7235

Arima, J., Uesugi, Y., Iwabuchi, M., and Hatanaka,T., Study on peptides hydrolysis by bacterial leucine aminopeptidase. *Appl. Microbiol. Biotechnol.* in press

Negishi, T., Mukaihara, T., Mori, K., Nishikido, H., Kawasaki, Y., Aoki, H., Kodama, M., Uedaira, H., Uesugi, Y., Iwabuchi, M., and Hatanaka, T., Identification of key amino acid residue of Streptomyces phospholipase D for thermostability by *in vivo* DNA shuffling. (2005) *Biochim. Biophys. Acta* **1722**, 331-342

Hatanaka,T., Arima, J., Uesugi, Y., and Iwabuchi, M., Purification, characterization cloning, and sequencing of metalloendopeptidase from *Streptomyces septatus* TH-2. (2005) *Arch. Biochem. Biophys.* **434**, 289-298

Uesugi, Y., Mori, K., Iwabuchi, M., and Hatanaka,T., Improvement of in vivo DNA shuffling system. *in: Proceeding of the 1st Pacific-Rim International Conference on Protein Science* (2004) pp. 111

OTHER PUBLICATIONS NOT INCLUDED IN THIS THESIS

Uesugi, Y., Ogata , S., and Tanihara, M., DNA delivery with a DNA-binding peptide derived from Fos-Jun complex linked to the covalently crosslinked alginate gel. (2002) *Tissue Eng*. **8**, 1150-1151

Uesugi, Y., Ogata , S., and Tanihara, M., Binding and protection of DNA by a novel peptide derived from the DNA-binding region of the Fos-Jun complex. C.G. Pitt and W.M. Saltzman, ed., *in: Proceeding of 28th International Symposium on Controlled Release of Bioactive Materials* (2001) ***Vol.2***, Controlled Release Society, pp. 1123-1124

ACKNOWLEDGMENTS

The studies in the present thesis were carried out under the direction of Dr. Tadashi Hatanaka at Research Institute for Biological Sciences (RIBS), Okayama, Japan. I wish to express my sincere gratitude to Dr. Tadashi Hatanaka for his direction, valuable advice, discussion, and continuous encouragement all through these studies.

My sincere gratitude goes to Professor Masao Tanihara, Nara Institute of Science and Technology, for his supervising throughout my graduate school course, cordial advice and warm encouragement to complete this thesis.

I am sincerely grateful to Center President Masaki Iwabuchi at RIBS and Emeritus Professor Yukio Imanishi, Nara Institute of Science and Technology, for their continuous encouragement and warm help.

I am also sincerely grateful to Associate Professor Chikara Ohtsuki and Assistant Professors Shin-ichi Ogata and Masanobu Kamitakahara, Nara Institute of Science and Technology, and Assistant Professor Toshiki Miyazaki, Kyushu Institute of Technology, for their encouragement and helpful suggestions.

My heartfelt acknowledgments go to Assistant Professor Koichi Mori, Okayama University, for his technical advice, helpful discussion and encouragement.

My gratefully acknowledgments should also go to Professor Mikio Kataoka, Professor Jun-ichi Kikuchi and Associate Professor Shin-ichi Kugimiya, Nara Institute of Science and Technology, for their cordial comments and improvement of this thesis.

It is a pleasure to acknowledge to the technical advice on SPR analysis, Researcher Madoka Taniai at Hayashibara Biochemical Laboratories.

I would like to thank all researchers at RIBS and graduated students of Biocompatible Materials Science Laboratory at Nara Institute of Science and Technology for their helpful discussion and supports.

Finally I express my hearty gratitude to my parents, Mr. Yoshiaki Uesugi and Mrs. Eriko Uesugi, my sisters, Mrs. Naoko Nagashima and Miss Noriko Uesugi, and My grand mother, Mrs. Mitsuhe Uesugi for their warm understanding and continuous encouragement.

December 2005

Yoshiko Uesugi